Polymer Rheology:
Principles, Techniques and Applications

G. C. Berry
Carnegie Mellon University

Contents

Example Problem

A research laboratory has generated data on the dynamic moduli G'(ω) and G"(ω) over a range of temperatures for an aqueous solution of a certain polymer, with the volume fraction of polymer $\varphi \approx 0.05$. Data on the dependence of the viscosity $\eta(\dot{\gamma})$ as a function of the shear rate $\dot{\gamma}$ are also available at a single temperature. It is suspected that the polymer might associate in solution, and the question is whether the data can be used to assess that possibility.

The dynamic data obtained at temperatures of 25, 35, 50 and 60°C are shown in Figure I in a reduced plot, with a reference temperature of 25°C, prepared under the assumption that the "vertical shift factor" for the modulus b(T) = 1. The various "shift factors" used in this example are defined in the text and Table 5. The values of the "horizontal shift factor" for the frequency log[a(T)] were found to be -0.32, -0.60 and -0.80 for T equal to 35, 50 and 60°C, respectively. It would have been appropriate to subtract $\omega\eta_{solv}$ from G"(ω) , but the difference would be too small to be important in the conclusions reached at this point. In the analyses in this example, the use of a spread sheet with calculation and graphical capabilities provided a convenient method to estimate the parameters a(T), b(T) and h(T). The sheet can be setup so that changes in these parameters are effected globally, with results shown in bilogarithmic plots of the data. Inspection of Figure I shows that the reduction is imperfect, with some suggestion of systematic deviations in the fit. Since it is assumed that b(T) = 1, the frequency shift factor a(T) is equal to the viscosity shift factor h(T), and for a solution as dilute as this, one might expect h(T) to be approximately equal to $h_{solv}(T)$, the ratio of the solvent viscosity at temperature T to that at the reference temperature of 25°C, given by -0.09, -0.21 and -0.28 for T equal to 35, 50 and 60°C, respectively. The substantial deviation between h(T) and $h_{solv}(T)$, and the apparent systematic deviations in the reduced plot both suggest a further analysis.

Following the suggestions in the text re the implementation of time-temperature reduction, the data on G'(ω) and G"(ω) were transformed to give $\eta'(\omega) = G''(\omega)/\omega$ and $J'(\omega) = G'(\omega)/\{G'(\omega)^2 + G''(\omega)^2\}^{1/2}$. Reduced bilogarithmic plots of $[\eta'(\omega) - \eta_{solv}]/a(T)$ and J'(ω) vs ωa(T) prepared with the assumed b(T) = 1, and consequently a(T) = h(T), are shown in Figure II, along with a data on $[\eta(\dot{\gamma}) - \eta_{solv}]$ vs $\dot{\gamma}$. Though subtraction of η_{solv} has little effect in this case owing to the magnitude of η'(ω) and $\eta(\dot{\gamma})$, it is included for completeness; with this inclusion, h(T) is the ratio of $\eta - \eta_{solv}$ at temperatures T and T_{REF}. It is clear that systematic deviations obtain in both plots of $[\eta'(\omega) - \eta_{solv}]/a(T)$ and J'(ω) vs ωa(T), suggesting that the assumption b(T) = 1 is inadequate.

Removal of the constraint on b(T) results in the superposed plots shown in Figure III. In this case, the superposition of $[\eta'(\omega) - \eta_{solv}]/h(T)$ and J'(ω)/b(T) vs $\omega a(T) = \omega h(T)b(T)$ is much improved, and the data on $[\eta'(\omega) - \eta_{solv}]/h(T)$ vs ωa(T) are seen to correspond closely to those on $[\eta(\dot{\gamma}) - \eta_{solv}]$ vs $\dot{\gamma}$ at the reference temperature of 25°C, as expected with the Cox-Merz relation discussed in the text. The values of h(T) and b(T) obtained in this way are given in Figure IV, along with $h_{solv}(T)$. Inspection of Figure D shows that both b(T) and h(T) increases with decreasing temperature, with the change in h(T) far greater than that for $h_{solv}(T)$. Both of these results suggest that association does occur with these aqueous solutions, with the degree of association increasing with decreasing temperature. In addition to an enhanced viscosity, the association increases the

distribution of species present, with the consequence that J_s, and hence b(T) increases markedly with decreasing temperature.

The presumption that superposition should obtain for data over a range of T with a changing extent of association with T is certainly open to question. Such a superposition implies that the functional dependence of $[\eta'(\omega) - \eta_{solv}]/[\eta - \eta_{solv}]$ and $J'(\omega)/J_s$ on $\omega\eta J_s$ is not significantly altered by the formation of associated species, even though η and J_s might individually be strongly altered. The observed reasonable applicability of the Cox-Merz relation supports this assumption, but does not provide definitive proof of its validity. Further assessment would have been possible if data on the recoverable compliance R(t) had been obtained at 25°C for comparison with the corresponding estimate based on the approximation $R(t) \approx \{J'(\omega)^2 + [J''(\omega) - (\omega\eta)^{-1}]^2\}^{1/2}$ discussed in the text. If accepted as meaningful, further interpretation of the imputed changes in η and J_s based on h(T) and b(T) would required a model for the association process. For example, it might be assumed that the association creates a randomly branched structure, with the modified Fox parameter $\tilde{\tilde{X}}$ discussed in the text proportional to the ratio g of the mean square radii of branched and linear chains of the same molecular weight. Then, if it can be assumed that $\eta^{(c)}_{LOC} \approx \eta_{solv}$, the ratio $h(T)/ h_{solv}(T)$ would be about proportional to $(gM)^a$ with $a \approx 3.4$ if $\tilde{\tilde{X}} > \tilde{\tilde{X}}_c$, or $a \approx 1$ otherwise. Use of g for a randomly branched polymer could then give the change in the association with T.

Example Problem Figure Captions

Figure I $G'(\omega)$ and $G''(\omega)$ as functions of $\omega a(T)$ for a polymer solution at the indicated temperatures, with a(T) chosen to give the best superposition possible; $T_{REF} = 25°C$.

Figure II $[\eta'(\omega) - \eta_{solv}]/a(T)$ and $J'(\omega)$ as functions of $\omega a(T)$ for a polymer solution at the indicated temperatures (see Fig. I), and $[\eta(\dot{\gamma}) - \eta_{solv}]$ vs $\dot{\gamma}$ at 25°C (solid line). Values of a(T) chosen to give the best superposition possible; $T_{REF} = 25°C$.

Figure III $[\eta'(\omega) - \eta_{solv}]/h(T)$ and $J'(\omega)/b(T)$ as functions of $\omega a(T) = \omega h(T)b(T)$ for a polymer solution at the indicated temperatures (see Fig. I), and $[\eta(\dot{\gamma}) - \eta_{solv}]$ vs $\dot{\gamma}$ at 25°C (solid line). Values of h(T) and b(T) chosen to give the best superposition possible; $T_{REF} = 25°C$.

Figure IV The functions h(T) and b(T) from the analysis in Fig. III as functions of temperature, and $h_{solv}(T)$ for the solvent (water).

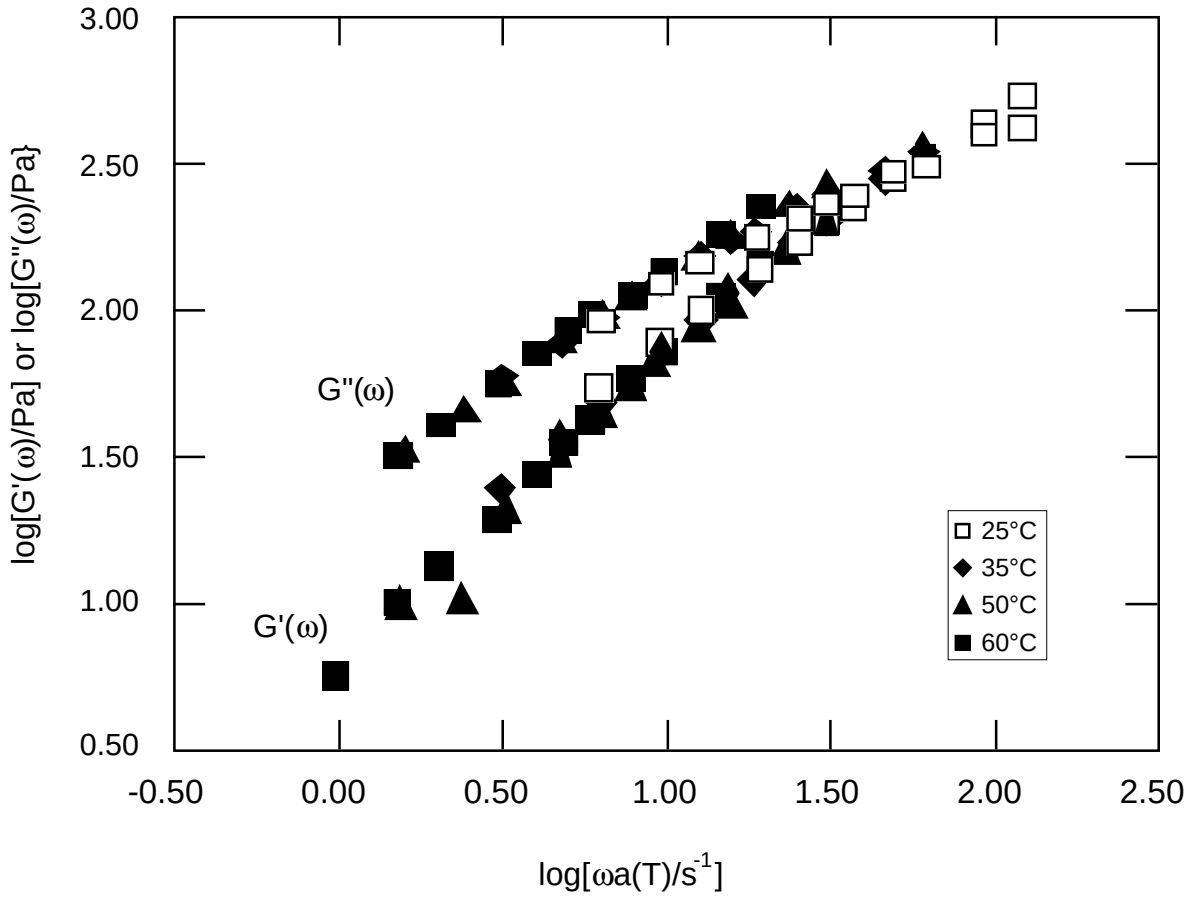
3.00
2.50
2.00
1.50
1.00
0.50
-0.50
0.00
0.50
1.00
1.50
2.00
2.50
log[G'(ω)/Pa] or log[G"(ω)/Pa}
log[ωa(T)/s-1]
G"(ω)
G'(ω)
25°C
35°C
50°C
60°C

Figure I

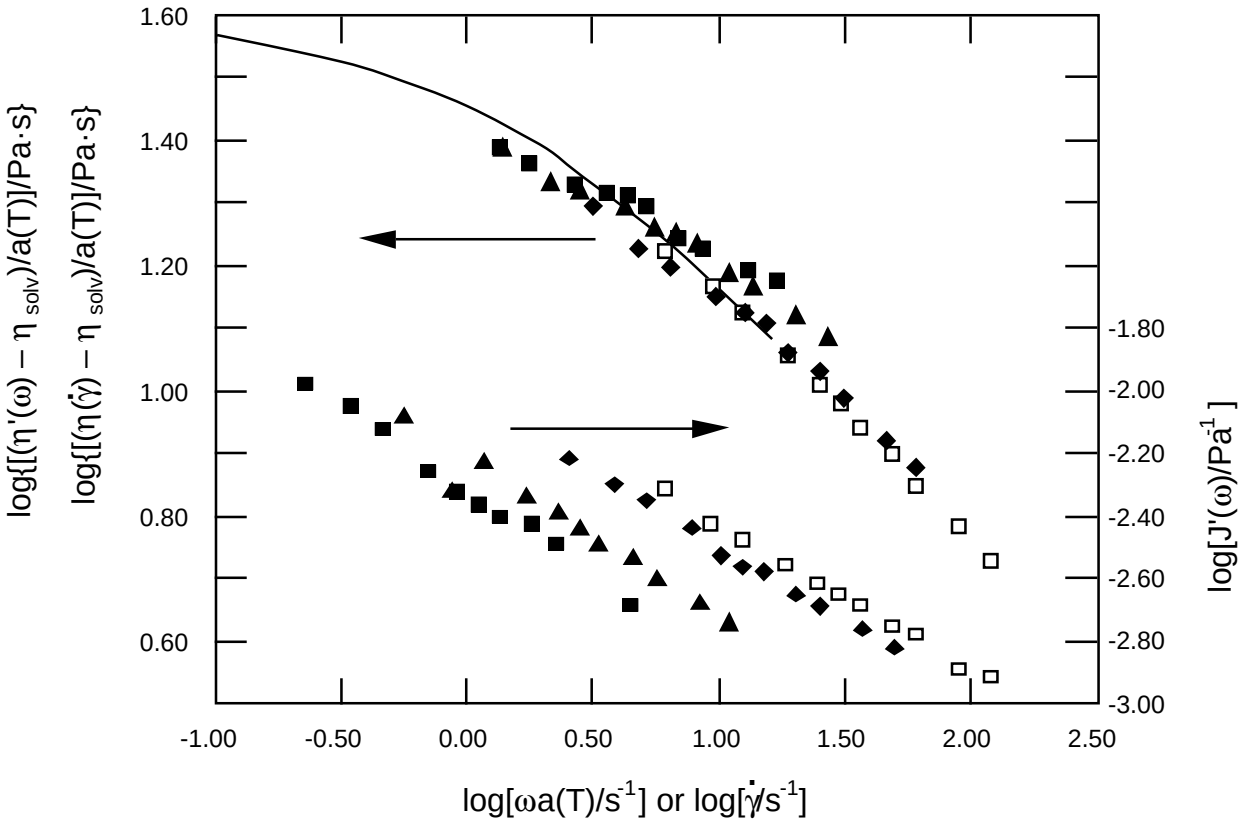
1.60
1.40
1.20
1.00
0.80
0.60
-1.00
-0.50
0.00
0.50
1.00
1.50
2.00
2.50
-1.80
-2.00
-2.20
-2.40
-2.60
-2.80
-3.00
log{[(η'(ω) – η solv)/a(T)]/Pa·s}
log{[(η(γ̇) – η solv)/a(T)]/Pa·s}
log[J'(ω)/Pa-1]
log[ωa(T)/s-1] or log[γ̇/s-1]

Figure II

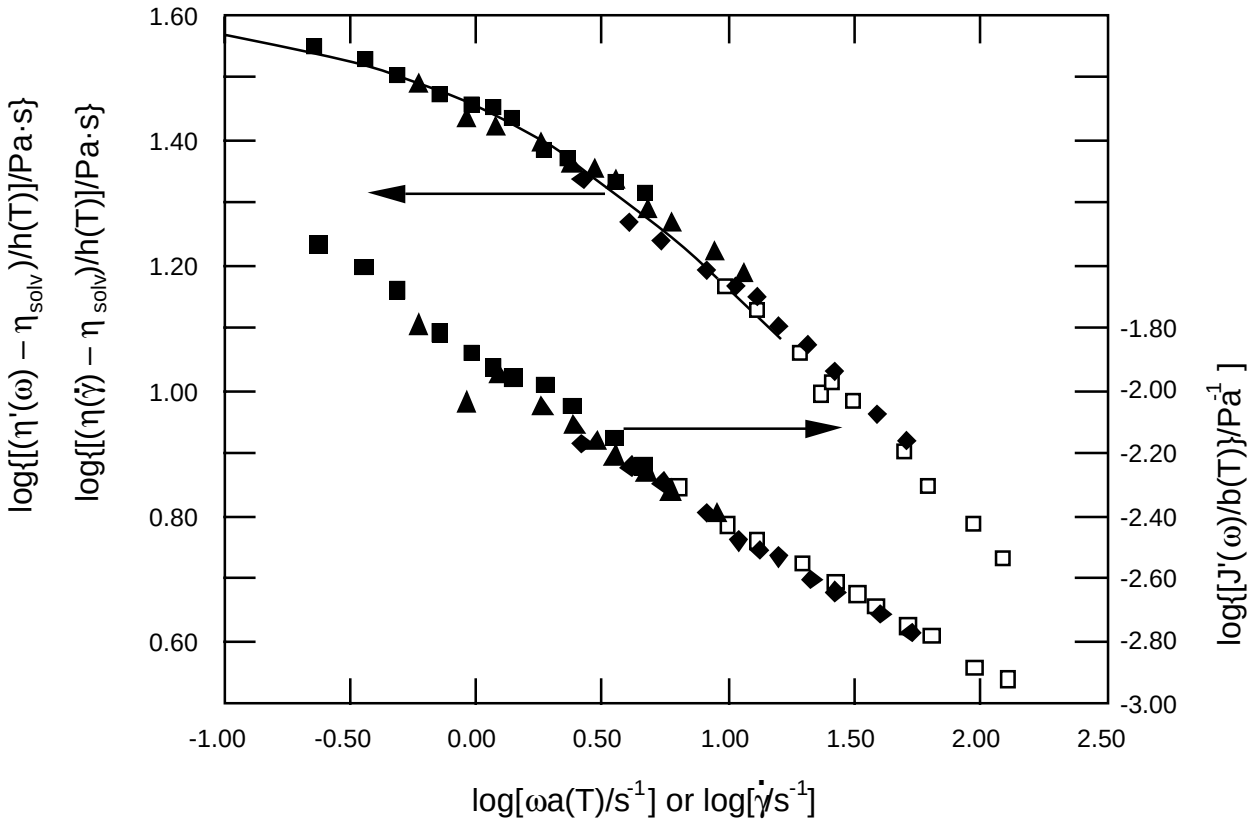
1.60
1.40
1.20
1.00
0.80
0.60
-1.00
-0.50
0.00
0.50
1.00
1.50
2.00
2.50
-1.80
-2.00
-2.20
-2.40
-2.60
-2.80
-3.00
log{[(η'(ω) – η_solv)/h(T)]/Pa·s}
log{[(η(γ̇) – η_solv)/h(T)]/Pa·s}
log{[J'(ω)/b(T)]/Pa^-1]
log[ωa(T)/s^-1] or log[γ̇/s^-1]

Figure III

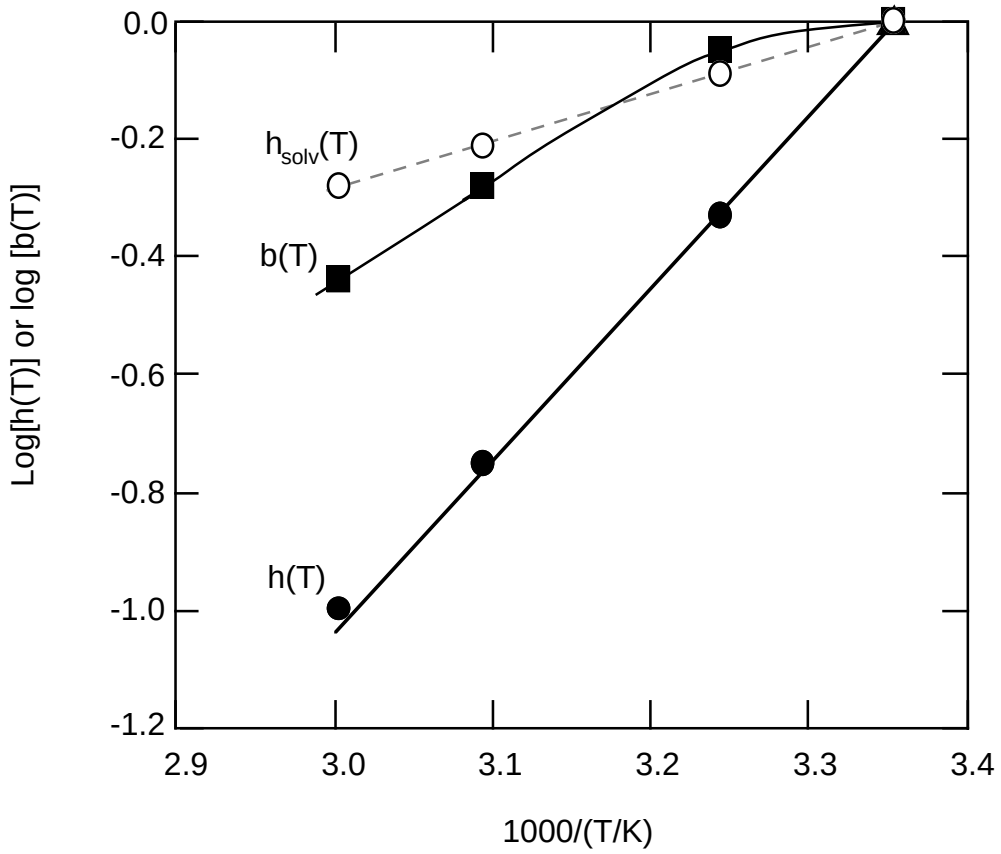
0.0
-0.2
-0.4
-0.6
-0.8
-1.0
-1.2
Log[h(T)] or log [b(T)]
h_solv(T)
b(T)
h(T)
2.9
3.0
3.1
3.2
3.3
3.4
1000/(T/K)

Figure IV

1. Introduction

The definition of *rheology* provided by the Society of Rheology (U.S.) describes it as the science of the deformation and flow of matter (e.g., see the web site for the Society[1]). The importance and vitality of the subject is demonstrated by the many reviews and monographs available, some of which are cited in references [2-27], as well as the original literature from laboratories around the world devoted to scientific and technological issues in rheology. Clearly, the topics covered in a single chapter must be circumscribed, and cannot present the entire field. The subjects selected here include the following:

1. The general principles of rheometry, focusing on requirements for instrumentation.
2. The principal methods of rheometry, with emphasis on the functions determined.
3. The elements of linear viscoelasticity, including creep, recovery, stress growth and relaxation, and dynamic properties.
4. Approximations used in linear viscoelasticity, including time-temperature superposition.
5. The viscosity of dilute solutions of polymers and colloids.
6. Linear viscoelastic of concentrated and undiluted polymeric fluids.
7. Nonlinear viscoelastic behavior of concentrated and undiluted polymeric fluids.
8. Strain-induced birefringence for concentrated and undiluted polymeric fluids.
9. Linear and nonlinear viscoelastic behavior of colloidal dispersions.

Although the general expressions for the linear viscoelastic behavior will be presented, most of the discussion will incorporate so-called incompressible behavior, for which the volume change is negligible. Many of the formulae presented below are presented in a succinct form in reference [9].

The separation into linear and nonlinear viscoelastic behavior, though very useful, and employed in the following, is somewhat arbitrary. As discussed below, a material that approximates linear viscoelastic behavior under conditions of a recently small deformation may exhibit a nonlinear response if that condition is not met.[17a; 18; 22a; 28] In general, the constitutive equation describing the nonlinear behavior should reduce to the linear response under appropriate conditions, often met if the deformation has been recently small. In most of the examples discussed here, the material response may be cleanly separated into two regimes: fluid and solid behavior. These may be distinguished by their response at long time (or small frequency), with a solid exhibiting an equilibrium modulus, whereas a fluid presents steady-state flow. An interesting material that may not be cleanly incorporated into these two limits is the incipient, or critical, gel, see below. Materials that show solid behavior if the deformation is small, but fluid behavior if the deformation exceeds some critical value, exhibiting yield at that deformation, are also discussed below.

In studying these materials, the investigator may impose forces (or torques) and follow the resultant deformation, or vice versa. As discussed below, under suitable conditions, analytical expressions, dependent on the test geometry may be used to express the forces as stresses, and the deformation as strains. A central tenant of a linear response is that these may be used to define compliances, given by a ratio of strain divided by stress, or moduli, given by a ratio of stress divided by strain. For a viscoelastic material, the functions so defined will depend on the time t for which the stress or strain is imposed. Functions appearing in linear viscoelasticity are given in Table 1; some corresponding functions for nonlinear behavior are discussed below. It is frequently useful to express two of these, J(t) and G(t), in terms of related functions and parameters:[2; 9; 10; 11a; 16a; 18; 23a]

$$R(t) = J(t) - t/\eta = J_\infty - [J_\infty - J_o]\alpha(t) \quad (1)$$

$$G(t) = G_e + [G_o - G_e]\varphi(t) \quad (2)$$

Here,

η is the (linear) viscosity, with $1/\eta = 0$ for a fluid,

G_e is the equilibrium modulus, with $G_e = 0$ for a solid,

G_o is the "instantaneous" modulus, with $J_oG_o = 1$, and

J_∞ is the limit of R(t) for large t, with values discussed below .

For both a linear elastic solid ($1/\eta = 0$ and $J_\infty = J_e = 1/G_e$) and a linear viscous fluid ($1/\eta > 0$ and $G_e = 0$), $\alpha(t) = \varphi(t) = \delta(t)$, with $\delta(t)$ the Dirac delta function (e.g., see references [13a; 23b]). Consequently, $G(t) = G_o$ and $J(t) = J_o$, as expected for a linear elastic solid, or $J(t) = t/\eta$ and $G(t) = 0$ for $t > 0$ for a linear viscous fluid. For a more general linear viscoelastic material, $\alpha(t)$ and $\varphi(t)$ are each unity for $t = 0$ and zero for large t, with $\alpha(t) < \varphi(t)$ for $0 < t < \infty$, and in this case, $J_\infty \geq J_o$ is equal to the equilibrium compliance $J_e = 1/G_e$ for a solid or to the steady-state recoverable compliance J_s for a fluid (J_s was formerly denoted J_e^o [11a]). The evaluation of η and J_s from G(t) for a fluid is discussed below.

The significance of the parameter J_o (or $G_o = 1/J_o$) in the preceding is a bit murky in practice, and in fact is operationally defined in terms of the time scale of interest as a practical matter. Effectively, it can be considered that J_o is the value of J(t) for t such that $\alpha(t) \approx 1$ on the experimental time scale, or equivalently, G_o is the value of G(t) for t such that $\varphi(t) \approx 1$ on the experimental time scale. Since these conditions are frequently reached as T approaches the glass

temperature T_g for noncrystalline polymers, J_o and G_o are sometimes denoted J_g and G_g, respectively,[11a,b] but it must be appreciated that in fact, small contributions to J(t) and G(t) obtain for $T < T_g$, and may be directly the subject of study, and importance in some applications.[5; 12] Occasionally, the expression for G(t) is characterized by a response at very small t, followed by a range of time for which time for which $\varphi(t)$ is essentially constant, before decreasing again for larger time. In such cases, the G(t) may be represented by limiting the function $\varphi(t)$ to the behavior for the regime of larger t, and adding a term $\delta(t)(G_o - G_1)$ to G(t), and normalizing $\varphi(t)$ to reflect the remaining contributions $G_1 - G_e$ that relax on the longer time scale; an example of this is given in the section on the rheology of colloidal suspensions below. Similar expressions may be introduced for the other functions in Table 1. For example, for the bulk properties,[11c; 23a]

$$B(t) = B_e - [B_e - B_o]\beta(t) \quad (3)$$

$$K(t) = K_e + [K_o - K_e]\kappa(t) \quad (4)$$

where $\beta(t)$ and $\kappa(t)$ correspond to the functions $\alpha(t)$ and $\varphi(t)$, respectively, in the shear functions, with the same general characteristics.

The often assumed limit of incompressibility implies that volume changes in the deformation are negligible. For a linear elastic solid, this condition is met if $K >> G \approx E/3$ or, equivalently, $B << J \approx 3D$. The general relations among these functions for linear viscoelastic behavior are discussed below. The time-dependent functions may be used to compute dynamic moduli or compliances for the response under a steady sinusoidal deformation at constant a frequency, see below.

Finally, a number of the symbols used, and the units for the quantities represented, are given in Table 2 for easy reference.

2. Principles of Rheometry

As emphasized above, the experimenter cannot measure stresses or strains, but merely forces (torques) and deformations that may be reduced to these under appropriate circumstances. The discipline of rheometry seeks to define practical instrumentation to provide experimental data under this constraint. Thus, some general requirements include the ability to:[10; 11d,e,f; 14a; 21]

1. Measure the torque (force) as a function of time, and have a method to compute the stress from the measured values.

2. Measure the deformation as a function of time, and have a method to compute the strain from the measured values.
3. Precisely define the sample geometry (e.g., sample radius and height for parallel plates, sample radius and cone angle for cone & plate, and sample radii and height for concentric cylinders, etc.).
4. Minimize the influence of extraneous torques (forces) on the sample (e.g., ball bearing friction, gravitational forces, …).
5. Provide for measurement over as wide a span in time (frequency) as possible, consistent with the sample behavior.
6. Control the temperature and, if necessary, the sample environment; sample geometry may require adjustment as the temperature is changed owing to sample volumetric expansion (contraction).

Increasingly, computer aided data acquisition and instrumentation control is used in rheometry. Indeed, it is indispensable in some cases, especially in experiments involving a steady sinusoidal deformation. The general features of the interactions that may be monitored by a computer system are illustrated in Figure 1, and simplified generalized examples of some of the instrumentation used in rheometry to study behavior in elongation or in shear follow in Figures 2-4. The simplest of these, shown schematically in Figure 2, is clearly limited in application to solids (or fluids with a very large viscosity), and may suffer from nonuniformity of the deformation, limiting the ability to convert forces and deformations to stresses and strains, respectively. Further, even if applicable, the method has inherent limitations in the magnitude of the deformation that may be realized. Deformation of a sample confined between parallel plates (not illustrated) carries the same limitation of deformation magnitude. As discussed below, oscillatory deformations with a small deformation amplitude are frequently used to study the rheological properties of solids and fluids in shear, in which case the limitation to small deformation is usually not a problem. Similar methods may be applied to the elongational deformation of a solid.[29] The expressions in Table 4 give the shear stress σ in terms of the force $\mathfrak{F}$, and the shear strain γ in terms of the displacement D for two geometries;[8a; 10; 11g] the displacement of coaxial cylinders usually is limited to studies of the viscosity of a fluid, or the modulus of a confined solid.

Torsional deformation, using instrumentation shown schematically in Figures 3-4 has wide-spread use precisely because it is not afflicted by some of the limitations encountered in planar deformations, especially the limitation to a small deformation, though torsional geometries may introduce other limitations. The torsional geometries illustrated in Figure 5 lend themselves to analysis under idealized conditions,[4a; 8a; 10; 11d; 14b; 19a] including the assumptions of perfect

alignment of the fixtures, the suppression of end effects, uniform temperature in the sample, and the condition of no slip of the sample at the fixture surfaces. The expressions in Table 4 give the shear stress σ in terms of the torque $\mathfrak{M}$, and the shear strain γ in terms of the angular deformation φ for several torsional geometries.[8a; 10; 11g; 14b] Similar expressions are available for other arrangements, and expressions are available to determine the first normal stress difference N_1 from the total normal force required to maintain a set distance between the cone and plate fixtures.[4b; 8b; 14c]

Application of the scheme in Figure 2 to determine the elongational properties of solids may suffer from nonuniformity of the deformation along the length of the sample in applications to solids, but it is even more problematic when applied to fluids, unless the viscosity of the fluid is extremely high. Although such measurements would be of interest, particularly with reference to nonlinear rheological behavior (see section 7), methods to study the rheological properties of fluids in elongational deformations have been difficult to implement and will not be discussed here for reasons of space and the overall limitations of the available specialized methods that have been utilized.[14d; 29; 30]

The use of a controlled angular deformation, as in Figure 4, was historically the preferred mode for a long period, since the resultant torque could be determined, for example, using the deflection of a calibrated torsion bar supporting the 'fixed' platen opposite that being driven by the controlled deformation. The ability to provide a controlled deformation was advanced by the use of motors under the control of a computer to impose a controlled angular rotation (e.g., a step, a ramp or an oscillatory rotation) on one of the fixtures in the apparatus, and the sophisticated use of a beam-supported structure for the other fixture, to allow determination of the torque and normal force imposed on that fixture by analysis of the (small) deflection of those beams in response to the deformation imposed on the sample.[31] An important consideration is the design of a transducer to cover the wide range of torques of interest experimentally, limiting, for example, the smallest torque that could be determined in a stress relaxation experiment, in which the torque is studied following a step in the strain. Since this method may be used to determine G(t) (see the next section), inaccuracy in the measurement of a small torque will compromise the estimate of G(t) for large t. The use of a controlled torque, as in Figure 3, was advanced by the ability to apply a controlled torque (e.g., a step, a ramp or an oscillatory torque) over an arbitrarily large angular deformation by the use of an eddy-current torque motor, with a suitable position transducer to detect the angular deformation of that fixture.[32; 33] In most cases, the second fixture is held fixed in the use of a controlled torque, but in some cases, it is rotated at a controlled (usually steady) rate. A major advantage of this design

is the ability to determine the recoil following cessation of steady flow, from which R(t) may be computed (see the next section). Any extraneous torques will seriously compromise the determination of R(t) at large t. For example, the use of ball-bearings in the suspension of the rotating fixture is unacceptable, owing to unavoidable friction at some level. The use of a gas-bearing reduces friction effects, but introduces a turbine torque, which may be largely suppressed by imposition of a counter torque from the eddy-current torque motor.[33] Further reduction of the residual torque may be achieved with a magnetic suspension of the rotating member, reducing the residual torque to a contribution related to geometric asymmetry in the suspended member--the effects of this may be suppressed by aligning the instrument so that the center of gravity of the suspended member is on the axis of rotation.[32]

Inspection of the expressions in Table 4 shows that the shear strain is independent of position only in the cone and plate geometry, though it becomes nearly so in the concentric cylinder geometry if $\Delta/R << 1$. The uniform shear strain is important in studies of nonlinear rheological behavior, making these two geometries especially useful in that regard. However, corrections may be applied to the steady-state data on the torque $\mathfrak{M}$ as a function of the rotational velocity Ω to give the shear stress σ_R at the periphery of the parallel plates (radius R):[4c; 8c; 19a]

$$\sigma_R = \frac{\mathfrak{M}}{2\pi R^3}\left(3 + \frac{\partial \ln \mathfrak{M}}{\partial \ln \Omega}\right) \tag{5}$$

Thus, the steady-state viscosity $\eta(\dot{\gamma}_R)$ at rate of strain $\dot{\gamma}_R = R\dot{\phi}/h$ at the same position may be calculated as $\eta(\dot{\gamma}_R) = \sigma_R/\dot{\gamma}_R$ For a linear response, $\partial \ln \mathfrak{M}/\partial \ln \Omega = 1$, and the relation in Table 4 is recovered.

A similar situation arises in capillary rheometry, in which the shear rate in steady flow is a strong function of the radius.[8d] Thus, for the flow of a linear viscous fluid through a cylindrical tube of radius R, the shear stress and shear rate $\dot{\gamma}_R$ at the capillary wall are given by[4d; 8d; 10; 14e]

$$\sigma_R = -(R/2)(\Delta P/L) \tag{6a}$$

$$\dot{\gamma}_R = 4Q_{vol}/\pi R^3 \tag{6b}$$

were $\Delta P/L$ is the pressure drop per unit capillary length and Q_{vol} is the volume flow rate. In this case, the viscosity is simply calculated as $\eta = \sigma_R/\dot{\gamma}_R$. Similar expressions are available for flow in tubes with other cross-sectional geometries.[8e] As is well known, the velocity profile is parabolic in capillary flow with a linear viscous fluid, but this profile is altered in nonlinear flow, requiring a correction to the expression for $\dot{\gamma}_R$ to permit calculation of η:[4d; 8f; 10; 19a; 34]

$$\dot{\gamma}_R = \frac{Q_{vol}}{\pi R^3}\left(3 + \frac{\partial \ln Q_{vol}}{\partial \ln \sigma_R}\right) \tag{7}$$

Thus, the steady-state viscosity $\eta(\dot{\gamma}_R)$ at rate of strain $\dot{\gamma}_R$ may be calculated as $\eta(\dot{\gamma}_R) = \sigma_R/\dot{\gamma}_R$. Additional important issues involving end-effects are not discussed here, though they are important, and may provide additional rheological information.[8d; 10; 14e] A variety of other methods to determine the viscosity are available, many of which are discussed in reference [35].

The control of temperature is almost always important in rheological studies, and can be a critical consideration under some conditions, e.g., as the temperature approaches the glass transition temperature, or some equilibrium phase transition. Since the deformation should be laminar for suitable analysis, effective heat transfer to maintain isothermal conditions in the sample may be an issue, especially at high deformation rates, or with nonmetallic surfaces and large thicker samples.[14f]

Measurement of the bulk properties tends to involve customized equipment, often involving an arrangement in which an inert fluid is displaced by the volume change of the sample, with the displacement monitored by the level of the inert fluid in an attached capillary tube.[11h]

3. Linear viscoelastic phenomenology

Although limited to deformations that have been recently small, the linear viscoelastic constitutive relation provides the basis for unambiguous characterization of most materials within that constraint.[11i; 13b; 23a] In addition to their use in material characterization, the functions and parameters determined in the linear response provide the basis for some constitutive relations designed to describe nonlinear rheological behavior, as might often be of interest in material processing. Linear viscoelastic behavior may be approached phenomenologically, on the basis of a linear response theory with analogs in many areas of science (optical dispersion, dielectric dispersion, electric circuit theory, etc.).[23c; 36] The subject may also be approached through

statistical mechanics, using renormalized models of the real chain.[11j,k; 17a; 22b] The phenomenological treatment is the subject of this section; several experimentally important deformation histories are considered using the phenomenological constitutive equation. Limited aspects of theoretical treatments are discussed in a subsequent section.

The elements of the principal assumptions in linear viscoelasticity of isotropic materials can be stated in terms of experiments under a controlled strain or a controlled stress history. Thus, for a shear deformation in the linear viscoelastic regime, these may be expressed in the forms, respectively:[2; 9; 11m; 13b; 18; 23d]

$$\sigma(t) = \sum_{i=1}^{N} G(t - t_i)\,\Delta\gamma_i = \int_0^{\gamma(t)} d[\gamma(u)]\,G(t - u) \tag{8}$$

for the response in the shear stress $\sigma(t)$ to a series of step shear strains $\Delta\gamma_i$ at times $t_1, t_2, \ldots, t_i, \ldots, t_N$, and

$$\gamma(t) = \sum_{i=1}^{N} J(t - t_i)\,\Delta\sigma_i = \int_0^{\sigma(t)} d[\sigma(u)]\,J(t - u) \tag{9}$$

for the response in the shear strain $\gamma(t)$ to a series of step shear stresses $\Delta\sigma_i$ at times $t_1, t_2, \ldots, t_i, \ldots, t_N$. The additive processes in these expressions are illustrated in Figure 6. The Stieltjes integrals in these expressions may be converted to give the generally more useful forms

$$\sigma(t) = \int_{-\infty}^{t} du\,G(t - u)\,\frac{\partial\gamma(u)}{\partial u} = G_o\gamma(t) + \int_0^{\infty} du\,\gamma(t - u)\,\frac{\partial G(u)}{\partial u} \tag{10}$$

$$\gamma(t) = \int_{-\infty}^{t} du\,J(t - u)\,\frac{\partial\sigma(u)}{\partial u} = J_o\sigma(t) + \int_0^{\infty} du\,\sigma(t - u)\,\frac{\partial J(u)}{\partial u} \tag{11}$$

where in each case, the second form follows from the first by integration by parts. Steps in the imposed strain or stress may be incorporated by use of a Dirac delta function.[13a; 23b] Thus, if $\gamma(t)$ is a step shear strain γ_o imposed at time t_1, then $\partial\gamma(t)/\partial t = \gamma_o\delta(t - t_1)$ for this piece of the strain history, with a contribution $\gamma_o G(t - t_1)$ to the total shear stress for times $t > t_1$. A similar expression applies for a step shear stress, etc. For a linear elastic material, $\partial G(t)/\partial t = \partial J(t)/\partial t = 0$, so that $\gamma(t) =$

$J_o\sigma(t) = (1/G_o)\sigma(t)$, as expected in this case. Both J(t) and G(t) are found to be nonnegative for all t, and further it is usually found that $\partial J(t)/\partial t \geq 0$ and $\partial G(t)/\partial t \leq 0$. Given the functions J(t) or G(t) (see below for the relation between these), these expressions are sufficient to define the response to arbitrarily complex strain or stress histories in shear in the linear viscoelastic response approximation.

A similar set of expressions may be obtained for normal forces and the corresponding deformations. The combination of normal and shear deformations may be expressed in terms of the strain and stress tensors, with components $\varepsilon_{ij}(t)$ and $S_{ij}(t)$, respectively in Cartesian coordinates (i,j = 1-3). Thus, using the Einstein notation for summation over repeated indices on a tensor component:[2; 9; 11n; 13b; 16b; 18; 23a]

$$\varepsilon_{ij} = \frac{1}{2}\left(\frac{\partial u_i}{\partial x_j} + \frac{\partial u_j}{\partial x_i}\right) \tag{12}$$

$$2\varepsilon_{ij}(t) = \int_{-\infty}^{t} ds\left\{J(t-s)\left[\frac{\partial S_{ij}(s)}{\partial s} - \frac{1}{3}\delta_{ij}\frac{\partial S_{\alpha\alpha}(s)}{\partial s}\right] + (2/9)\delta_{ij}\,B(t-s)\frac{\partial S_{\alpha\alpha}(s)}{\partial s}\right\} \tag{13}$$

$$S_{ij}(t) = \int_{-\infty}^{t} ds\left\{2G(t-s)\left[\frac{\partial \varepsilon_{ij}(s)}{\partial s} - \frac{1}{3}\delta_{ij}\frac{\partial \varepsilon_{\alpha\alpha}(s)}{\partial s}\right] + \delta_{ij}\,K(t-s)\frac{\partial \varepsilon_{\alpha\alpha}(s)}{\partial s}\right\} \tag{14}$$

Here, **u** is the displacement vector. For example, in terms of the preceding, $\gamma(t) = 2\,\varepsilon_{12}(t)$ and $\sigma(t) = S_{12}(t)$ for shear deformation with a shear strain gradient along x_2 and deformation along x_1. It may be noted that some authors use an alternative definition of the strain tensor, differing by a factor of two.[11p] The first and second terms in the stress and strain tensors are sometimes referred to as the deviatoric and volume components, respectively. The term involving K(t) reduces to $-\delta_{ij}P$, with P a pressure, in the limit of incompressible behavior (negligible change in the volume); the term involving B(t) may be neglected in that same limit. A similar, but more complex, set of equations may be obtained in the more general case with the assumption of material isotropy relaxed.[13c; 37]

It can be shown that the functions J(t) and G(t) are related through a convolution integral:[2; 9; 11q; 13d; 16a; 18; 23d]

$$\frac{1}{t}\int_0^t du\, G(t-u)\, J(u) \;=\; 1 \qquad (15)$$

with Laplace transform:

$$s^2\hat{G}(s)\hat{J}(s) \;=\; 1 \qquad (16)$$

Similar relations obtain between B(t) and K(t), as well as D(t) and E(t), the latter two, of course being related to the other four, see Table 1. Although the Laplace transform appears simple, its analytic use is usually not possible, however, see Table 1 and reference [23e]. Since these relations may be used to compute one function from its paired member (e.g., J(t) given G(t), etc.), it is seen that in principle an experimenter need only arrange to determine two functions, say J(t) and B(t), to fully characterize the material. Nevertheless, for various reasons, some elaborated in the following, it is frequently desirable to carry out more than one type of experiment.[10; 11r]

As mentioned above, the assumption of material isotropy may be relaxed in the linear viscoelastic response regime, with corresponding increase in the complexity of the expressions.[13c; 37] For example, for a nematic fluid exhibiting only Frank curvature elasticity and Leslie viscosity coefficients, with no true viscoelastic behavior, the minimal representation contains nine coefficients.[17b; 22c; 38] A discussion of the tensor character of the response function for materials of various symmetries is given in reference [37].

It should be emphasized that the general theory of linear viscoelasticity presented above does not stipulate the dependence of the functions J(t), etc., on temperature, important as that may be in the response obtained. Methods to incorporate the effect of temperature in the analysis of experimental data are discussed below.

The preceding simplifies considerably if the functions G(t), K(t), etc., reduce to constants G, K, etc., as for a linear elastic material.[2; 9; 23f] For example, in this limit, the compliances and moduli are simply related: JG = BK = DE = 1, with relations among the moduli given in Table 3. The additional constant Poisson's ratio ν introduced in Table 3 is particularly useful in considering the volume change ΔV of a linear elastic material under an elongational deformation. For example, for a uniaxial elongation with strain ε, $\Delta V/V = \varepsilon(1 - 2\nu)$, showing that ΔV tends to zero as ν goes to 1/2. Reference to Table 3 shows that ν tends to 1/2 for K >> G. In addition, the components of the strain for a deformation with normal stresses may be expressed as $\varepsilon_{11} = D[S_{11} - \nu(S_{22} + S_{33})]$, etc. The

relations given above with time-dependent moduli and compliances may be recast in terms of a time-dependent Poisson ratio $\nu(t)$, but that will not be done here.[23g]

Examples of the application of the linear viscoelastic response are given in the following for illustrative purposes and to develop certain important expressions for frequently used histories:

i. Creep and recovery with a step shear stress;
ii. Stress relaxation with a step shear strain;
iii. Stress relaxation after a ramp shear strain;
iv. Recovery after a ramp shear strain;
v. Oscillation with a sinusoid shear stress;
vi. Oscillation with a sinusoid shear strain;
vii. Volume and elongational deformations.

(i). Creep and recovery with a step shear stress, see Figure 7a:

Stress history:

$$\sigma(t) = 0 \qquad t < 0$$
$$\sigma(t) = \sigma_o \qquad 0 \le t \le T_e$$
$$\sigma(t) = 0 \qquad t > T_e$$

The strain in creep for $t \le T_e$ is given by:

$$\gamma(t) = \sigma_o \int_0^t du\, J(t-u)\, \delta(u-0) \tag{17a}$$
$$= \sigma_o J(t) = \sigma_o [R(t) + t/\eta] \tag{17b}$$

Thus, for a fluid, a bilogarithmic plot of $\gamma(t)$ vs t approaches unit slope if T_e is large enough that $R(T_e) \approx J_s$; inspection of linear plots of $\gamma(t)$ vs t are not recommended for this analysis as deviation from linearity of J(t) with t may be difficult to discern in such a representation. In principle, R(t) may be computed from this response as $\gamma(t)/\sigma_o - t/\eta$ for a fluid, but this method will generally not give accurate results unless $t << \tau_c = J_s\eta$ since otherwise the method requires the difference between two large numbers for large t.[10; 11s]

The strain for $t > T_e$ is given as a function of the time $\vartheta = t - T_e$ in recovery by:

$$\gamma(t) = \sigma_o \int_0^{T_e} du\, J(t-u)\, \delta(u-0) - \sigma_o \int_{T_e}^{t} du\, J(t-u)\, \delta(u-T_e) \qquad (18a)$$

$$\gamma(\vartheta) = \sigma_o [J(\vartheta + T_e) - J(\vartheta)] = \sigma_o [R(\vartheta + T_e) - R(\vartheta) + T_e/\eta] \qquad (18b)$$

Consequently, the permanent set, or nonrecoverable strain is given by $\gamma_{NR} = \gamma(\infty) = \sigma_o T_e/\eta$, providing a means to estimate η for a fluid, even if T_e is not large enough to reach steady-state flow in creep. Of course, accurate measurement of $\gamma(t)$ in recovery requires the elimination of extraneous torques, as from ball bearing suspensions, etc.[10]

The recoverable strain $\gamma_R(\vartheta) = \gamma(T_e) - \gamma(t)$ for $t > T_e$ is given by

$$\gamma_R(\vartheta) = \sigma_o \{J(T_e) - [J(\vartheta + T_e) - J(\vartheta)]\} = \sigma_o \{R(\vartheta) + R(T_e) - R(\vartheta + T_e)\} \qquad (19)$$

for either a solid or a fluid, with $R(\infty) = J_\infty$. Inspection shows that that $\gamma_R(\vartheta) = \sigma_o R(\vartheta)$ for $\vartheta << T_e$, $\gamma_R(\vartheta) = \sigma_o R(T_e)$ if $\vartheta >> T_e$, and $\gamma_R(\vartheta) = \sigma_o R(\vartheta)$ for any ϑ if T_e is large enough that $R(T_e) \approx J_\infty$. In the latter case, the function R(t) may be determined directly from the recoil. A priori estimation of T_e large enough that $\gamma_R(\vartheta) = \sigma_o R(\vartheta)$ for any ϑ for an unknown fluid sample is not generally possible, but as a guide, T_e should be several-fold larger than (say, ten-fold) the time required to obtain $\partial \ln J(t)/\partial \ln t \approx 1$ during creep; an apparent constant slope $\partial J(t)/\partial t$ is usually not a sufficiently critical criterion. The function $\gamma_R(\vartheta)$ defined above should more precisely be called the constrained recoverable strain, since the experiment envisioned does not provide for relaxation of any stress normal to the shear stress. The distinction is moot for the linear viscoelastic response since normal stresses are nil in that model, but can become important in nonlinear behavior discussed below.

It may be noted that with use of the preceding relation for the strain $\gamma(t)$ in recovery, the running sum of N successive strains for $t = nT_e$ (n = 1, 2, …, N) is given by

$$\sum_{n=1}^{N} \gamma(nT_e) = \sigma_o J(NT_e) = \sigma_o R(NT_e) + N\gamma_{NR} \qquad (20)$$

Since γ_{NR} is known, in principle this expression permits assessment of R(t) for $t = NT_e$, and that method has been proposed for use with T_e small enough that $R(T_e) < J_\infty$, to avoid the necessity of

long times in creep.[39] In practice, the inaccuracies in determining the difference between the sum of successive strains and $N\gamma_{NR}$ will render this estimate inaccurate with increasing N, similar to the inaccuracy that develops in attempts to estimate R(t) as $J(t) - t/\eta$ from data in creep.

For use below, it may be noted that for recovery initiated at time T_e following an arbitrary stress history up to T_e, the recoverable strain is given by

$$\gamma_R(\vartheta) = \sigma(T_e)R(\vartheta) - \int_0^{T_e} du\, [R(\vartheta + T_e - u) - R(T_e - u)] \frac{\partial\sigma(u)}{\partial u} \qquad (21)$$

With this expression the total recoverable strain $\hat{\gamma}_R(T_e)$ obtained as ϑ becomes very large after the stress is reduced to zero at time T_e following an arbitrary strain history up to T_e is given by

$$\hat{\gamma}_R(T_e) = \int_0^{T_e} du\, R(T_e - u) \frac{\partial\sigma(u)}{\partial u} \qquad (22)$$

Inspection will show that these reduce to the preceding for the special stress history used above; the expression for $\hat{\gamma}_R(T_e)$ will find use below in the discussion of strain-induced birefringence.

(ii). Stress relaxation after a step shear strain, see Figure 7b:

Strain history: $\gamma(t) = 0 \qquad t < 0$

$\gamma(t) = \gamma_o \qquad t \geq 0$

The stress response for $t > 0$ is given by

$$\sigma(t) = \gamma_o \int_0^t du\, G(t - u)\, \delta(u - 0) = \gamma_o G(t) \qquad (23)$$

Consequently, this experiment provides direct information on G(t), limited by the sensitivity of the transducer to determine the torque as it decreases to its value at long time.[10]

(iii). Stress Relaxation after a ramp shear strain:

Strain history: $\gamma(t) = 0 \qquad t < 0$

$\gamma(t) = \dot{\gamma}t \qquad 0 \leq t \leq T_e$

$$\gamma(t) = \dot{\gamma} T_e \qquad t > T_e$$

The stress response for $t \le T_e$ is given by

$$\sigma(t) = \dot{\gamma} \int_0^t du\, G(t-u) = \dot{\gamma}\,[G_e t + (G_o - G_e) \int_0^t ds\, \varphi(s)] \tag{24}$$

With this expression, $\partial\sigma(t)/\partial t = \dot{\gamma} G(t)$, providing an alternative, though usually less precise, means to estimate G(t) than that from a step-strain. The integral over $\varphi(t)$ is bounded for either a fluid or a solid, and for a fluid must equal the steady-state viscosity as t becomes large, since in that limit of steady-state flow $\sigma = \dot{\gamma}\eta$, so that:

$$\eta = G_o \int_0^\infty ds\, \varphi(s) \tag{25}$$

providing a means to determine η from G(t) for a fluid. In addition, as illustrated in an example given below, for a fluid

$$J_s = G_o \int_0^\infty ds\, s\varphi(s)/\eta^2 \tag{26}$$

For this strain-defined history with $\gamma(t) = \dot{\gamma} t$, use of the expression

$$\gamma(t) = \int_{-\infty}^t du\, J(t-u) \frac{\partial \sigma(u)}{\partial u} \tag{27}$$

provides an illustration of the convolution integral cited above relating G(t) and J(t). Thus, from above, $\partial\sigma(t)/\partial t = \dot{\gamma} G(t)$, giving

$$\gamma(t) = \dot{\gamma} \int_0^t du\, J(t-u)\, G(u) = \dot{\gamma} t \tag{28}$$

reproducing the convolution integral. For a fluid, the strain for $t > T_e$ is given by

$$\sigma(t) = \dot{\gamma} \int_0^{T_e} du\, G(t-u) = \dot{\gamma} \int_\vartheta^{\vartheta + T_e} ds\, G(s) \tag{29}$$

with $\vartheta = t - T_e$. Consequently, since in steady flow T_e is large compared with the time to give $G(t) \approx 0$, the final integral gives $\partial\sigma(\vartheta)/\partial\vartheta = -\dot{\gamma}G(\vartheta)$ during stress relaxation following steady flow.

Although not included in the deformation history specified above, it may be noted that the total recoverable strain $\hat{\gamma}_R(T_e)$ on reduction of the stress to zero at time T_e during the stress relaxation may be computed with the expression in the preceding section for a stress history comprising a jump $\gamma_o G_o$ followed by $\sigma(t) = \gamma_o G(t)$ for $0 < t < T_e$, to give $\hat{\gamma}_R(T_e) = \gamma_o[1 - \eta^{-1}\int_0^{T_e} du\, G(u)]$; this expression will find use below in the section on strain-induced birefringence.

(iv). Recovery after a ramp shear strain, see Figure 7c:

Strain history:	$\gamma(t)$	= 0	$t < 0$
	$\gamma(t)$	= $\dot{\gamma}t$	$0 \le t \le T_e$
Stress history:	$\sigma(t)$	= 0	$t > T_e$

The stress response for $t \le T_e$ follows that in the preceding example. The strain for $t > T_e$ is given by

$$\sigma(t) = 0 = \dot{\gamma}\int_0^{T_e} du\, G(t-u) + \int_{T_e}^{t} du\, G(t-u)\,\frac{\partial\gamma(u)}{\partial u} \qquad (30)$$

In general, a numerical iteration would be required to obtain $\gamma(t)$ in recovery, and hence the recoverable strain $\gamma_R(t)$, but the total recoverable strain γ_R following steady-state flow (large T_e) for a fluid may be calculated in terms of integrals involving G(t), permitting calculation of $\gamma_R/\dot{\gamma}\eta = J_s$ for a fluid from integrals over G(t), as mentioned above:[19b]

$$\tau_c = \eta J_s = \int_0^{\infty} ds\, s\varphi(s) \Big/ \int_0^{\infty} ds\, \varphi(s) \qquad (31)$$

The parameter τ_c is seen to be a certain average time constant of the relaxation modulus. It should be noted that whereas the parameters J_s and η appear directly in J(t) for a fluid, their determination from G(t) requires the evaluation of integrals over G(t). Conversely, complete knowledge of R(t) does not provide an estimate for η.

(v). Oscillation with a sinusoid shear stress, see Figure 7d:

Stress history: $\sigma(t) = 0 \qquad t < 0$

$\sigma(t) = \sigma_o \sin(\omega t) \qquad t \geq 0$

The strain response for $t > 0$ is given by

$$\gamma(t) = \omega\sigma_o \int_0^t du\, J(t-u)\cos(\omega u) \tag{32}$$

After a transformation of variable with $s = t - u$, the use of trigonometric identities, and passage to the steady-state limit with large t,

$$\gamma(t) = \sigma_o\{J'(\omega)\sin(\omega t) - J''(\omega)\cos(\omega t)\} \tag{33}$$

$$J'(\omega) = J_\infty - \omega[J_\infty - J_o]\int_0^\infty ds\, \alpha(s)\sin(\omega s) \tag{34}$$

$$J''(\omega) = (1/\omega\eta) + \omega[J_\infty - J_o]\int_0^\infty ds\, \alpha(s)\cos(\omega s) \tag{35}$$

where $J'(\omega)$ and $J''(\omega)$ are the in-phase (or real or storage) and out-of-phase (or imaginary or loss) dynamic compliances, respectively, and $\alpha(t)$ is defined above. Inspection of these expressions shows that $J'(\omega) \approx J_\infty$, $J''(\omega) \approx 1/\omega\eta$, and $J''(\omega) - 1/\omega\eta \approx \omega$ at low frequency. In an alternative representation of the response,

$$\gamma(t) = \sigma_o\, |J^*(\omega)| \sin\,[\omega t - \delta(\omega)] \tag{36}$$

where $|J^*(\omega)|^2 = [J'(\omega)]^2 + [J''(\omega)]^2$ and the phase angle $\delta(\omega)$ is given by $\tan\,\delta(\omega) = J''(\omega)/J'(\omega)$. For a linear viscoelastic material, the relation between the stress and the strain may be expressed in compact form in complex notation: $\gamma^* = \sigma^* J^*$; for example, $\sigma(t) = \mathrm{Im}\{\sigma^*\} = \mathrm{Im}\{\sigma_o \exp(i\omega t)\}$, $\gamma(t) = \mathrm{Im}\{\gamma^*\} = \mathrm{Im}\{\gamma_o \exp[i(\omega t - \delta)]\}$, and $J^* = |J^*|\exp(-i\delta)$, with $J^* = J' - iJ''$ equal to the complex compliance. Given their status as sine or cosine Fourier transforms, the functions given above may be used to obtain the following relations that permit conversion of the dynamic functions to the time-dependent compliances:[2; 9; 11q; 23h]

$$R(t) = J(t) - t/\eta = J_o + \frac{2}{\pi}\int_0^\infty d\omega \frac{J'(\omega) - J_o}{\omega} \sin(\omega t) \quad (37)$$

$$R(t) = J(t) - t/\eta = J_o + \frac{2}{\pi}\int_0^\infty d\omega \frac{J''(\omega) - (\omega\eta)^{-1}}{\omega} [1 - \cos(\omega t)] \quad (38)$$

As would be anticipated, Kramers–Kronig relations may be used to relate J'(ω) and J''(ω):[2; 9; 11t; 23h]

$$J'(\omega) - J_o = \frac{2}{\pi}\int_0^\infty d\alpha\, \alpha \frac{J''(\alpha) - (\alpha\eta)^{-1}}{\alpha^2 - \omega^2} \quad (39)$$

$$J''(\omega) - (\omega\eta)^{-1} = \omega \frac{2}{\pi}\int_0^\infty d\alpha \frac{J'(\alpha) - J_o}{\omega^2 - \alpha^2} \quad (40)$$

The Cauchy principal value of the integral is taken to resolve the apparent singularity when $\alpha = \omega$; the calculations required are readily implemented using a desktop computer.

(vi). Oscillation with a sinusoid shear strain, see Figure 7d:

Strain history: $\gamma(t) = 0 \qquad t < 0$

$\gamma(t) = \gamma_o \sin(\omega t) \qquad t \geq 0$

The stress response for $t > 0$ is given by

$$\sigma(t) = \omega\gamma_o \int_0^t du\, G(t-u)\cos(\omega u) \quad (41)$$

Again, after a transformation of variable with $s = t - u$, the use of trigonometric identities, and passage to the steady-state limit with large t,

$$\sigma(t) = \gamma_o\{G'(\omega)\sin(\omega t) + G''(\omega)\cos(\omega t)\} \quad (42)$$

$$G'(\omega) = G_e + \omega[G_o - G_e]\int_0^\infty ds\, \varphi(s)\sin(\omega s) \quad (43)$$

$$G''(\omega) = \omega[G_o - G_e]\int_0^\infty ds\, \varphi(s)\cos(\omega s) \quad (44)$$

where G'(ω) and G"(ω) are the in-phase (or real or storage) and out-of-phase (or imaginary or loss) dynamic compliances, respectively. In an alternative representation of the response,

$$\sigma(t) = \gamma_o |G^*(\omega)| \sin [\omega t + \delta(\omega)] \quad (45)$$

where $|G^*(\omega)|^2 = [G'(\omega)]^2 + [G''(\omega)]^2$ and the phase angle $\delta(\omega)$ is given by $\tan \delta(\omega) = G''(\omega)/G'(\omega)$. In complex notation, $\sigma^* = \gamma^* G^*$ with $\gamma(t) = \text{Im}\{\gamma^*\} = \text{Im}\{\gamma_o \exp(i\omega t)\}$, $\sigma(t) = \text{Im}\{\sigma^*\} = \text{Im}\{\sigma_o \exp[i(\omega t + \delta)]\}$, and $G^* = |G^*|\exp(i\delta)$, with $G^* = G' + iG''$ equal to the complex modulus. Comparison with the expression given in the previous example shows that $G^*J^* = 1$, which provides the very useful algebraic relation $|G^*(\omega)||J^*(\omega)| = 1$, and expressions that permit algebraic conversion of the dynamic functions to the time-dependent compliances or moduli:[2; 9; 11u; 16; 23h]

$$J'(\omega) = G'(\omega)/|G^*(\omega)|^2 \quad (46)$$

$$J''(\omega) = G''(\omega)/|G^*(\omega)|^2 \quad (47)$$

$$G'(\omega) = J'(\omega)/|J^*(\omega)|^2 \quad (48)$$

$$G''(\omega) = J''(\omega)/|J^*(\omega)|^2 \quad (49)$$

$$\tan \delta(\omega) = J''(\omega)/J'(\omega) = G''(\omega)/G'(\omega) \quad (50)$$

These algebraic expressions contrast with the convolution integral relating J(t) and G(t); it may be noted, however, that the Laplace transforms of J(t) and G(t) are algebraically related,[23i] just as are these Fourier transforms of J(t) and G(t). As above, the properties of sine and cosine Fourier transforms lead to useful relations:[2; 9; 11u; 16d; 23j]

$$G(t) = G_e + \frac{2}{\pi}\int_0^\infty d\omega \frac{G'(\omega) - G_e}{\omega} \sin(\omega t) \quad (51)$$

$$G(t) = G_e + \frac{2}{\pi}\int_0^\infty d\omega \frac{G''(\omega)}{\omega} \cos(\omega t) \quad (52)$$

It is often useful to define a complex viscosity $\eta^* = \sigma^*/\dot{\gamma}^* = (1/i\omega)\sigma^*/\gamma^* = G^*/i\omega$; the $\pi/2$ phase shift represents the dependence of the viscosity on deformation rate. Thus, $\eta^*(\omega) = \eta'(\omega) - i\eta''(\omega)$, where $\eta'(\omega) = G''(\omega)/\omega$ and $\eta''(\omega) = G'(\omega)/\omega$ are the components $\eta^*(\omega)$ that are in phase and out of phase with the shear rate, respectivel. Inspection of these expressions shows that at low frequency

$G'(\omega) \approx G_e$ for a solid or $(\omega\tau_c)^2/ J_s$ for a fluid, and $G''(\omega) \approx \omega\eta'(0)$ for either solid or fluid. The low frequency limiting value $\eta'(0)$ of $\eta'(\omega)$ is given by $\eta'(0) = [G_o - G_e]\int ds\, \varphi(s)$, so that $\eta'(0)$ is equal to the viscosity η for a fluid ($G_e = 0$) or a constant for a solid; $\eta''(\omega) = J_s\eta^2\omega$ for a fluid at low ω. For high frequencies $\eta'(\omega)$ and $\eta''(\omega)$ are proportional to ω^{-2} and ω^{-1}, respectively. In some cases, the decline of $\eta'(\omega)$ to zero with decreasing ω is interrupted by a high frequency response causing $\eta'(\omega)$ to exhibit a plateau; examples of this are discussed below.

Inspection of the relations given above shows that $J'(\omega) \le [R(t)]_{\omega t=1} < 1/G'(\omega) < [1/G(t)]_{\omega t=1}$, see below. As would be anticipated, Kramers–Kronig relations may be used to relate $G'(\omega)$ and $G''(\omega)$:[2; 9; 16d; 19c; 23k]

$$G'(\omega) - G_e = \omega^2 \frac{2}{\pi}\int_0^\infty d\alpha \frac{G''(\alpha)}{\alpha[\omega^2 - \alpha^2]} \tag{53}$$

$$G''(\omega) = \omega \frac{2}{\pi}\int_0^\infty d\alpha \frac{G'(\alpha) - G_e}{\alpha^2 - \omega^2} \tag{54}$$

As above, the Cauchy principal value of the integral is taken to resolve the apparent singularity when $\alpha = \omega$.

(vii). Volume and elongational deformations

Although the preceding has been cast in terms of shear deformation, similar expressions apply in terms of the other functions, with reference to the stress and strain tensors given above. For example, the relations in the first example apply to elongation in response to a step by redefinition of symbols. Thus, for a force along x_1, $\gamma(t)$ is replaced by the elongational strain $\varepsilon(t) = \varepsilon_{11}(t)$, σ_o is replaced by the tensile stress component $S_{11}(t)$ and $J(t)$ is replaced by $D(t)$. For material behavior in the incompressible approximation (negligible volume change), $D(t) \approx J(t)/3$, giving, for example, an elongational viscosity $\eta_{elg} = 3\eta$, with η the viscosity in shear. The relations may be applied to bulk deformation under an applied pressure P, with $\gamma(t)$ replaced by the volume change $\Delta V(t)$, equal to $\varepsilon_{11}(t) + \varepsilon_{22}(t) + \varepsilon_{33}(t)$, σ_o replaced by the –P, and $J(t)$ replaced by $B(t)$. Similarly, for the dynamic functions, $J^*G^* = B^*K^* = D^*E^* = 1$, and the functions $B'(\omega)$, etc., may be expressed in obvious ways. It may be noted that for an isotropic linear viscoelastic material, $D^*(\omega) = J^*(\omega)/3 + B^*(\omega)/9$, analogous to the expression for $D(t)$ in Table 1; however, the expression for $E^*(\omega)$

becomes equally simple, in contrast with the relation for E(t).[2; 9] A principal difference between the shear and volume deformations is the ratio of parameters such as J_∞/J_o and B_e/B_o, etc. Thus, whereas these ratios may easily reach 10^6 or higher for shear deformation, they are seldom larger than 2-3 for a volume deformation.

4. Approximations used in linear viscoelasticity

The information in J(t) and G(t) involves both parameters and functions, e.g., η, J_∞, J_o and $\alpha(t)$ in J(t) or G_o, G_e and $\varphi(t)$ in G(t). Although it is not a necessary attribute for linear viscoelastic behavior, the functions $\alpha(t)$ and $\varphi(t)$ are sometimes represented in terms of weighted distributions of exponential functions involving retardation times λ or relaxation times τ, respectively:[11v; 18; 23m]

$$\alpha(t) = \frac{1}{J_\infty - J_o}\int_{-\infty}^{\infty} d(\ln \lambda)\, L(\lambda)\exp(-t/\lambda) \approx \sum_{m}^{N-1}\alpha_i \exp(-t/\lambda_i) \qquad (55)$$

$$\varphi(t) = \frac{1}{G_o - G_e}\int_{-\infty}^{\infty} d(\ln \tau)\, H(\tau)\exp(-t/\tau) \approx \sum_{1}^{N}\varphi_i \exp(-t/\tau_i) \qquad (56)$$

where $\Sigma\alpha_i = \Sigma\varphi_i = 1$, and m is equal to 0 or 1 for a solid and fluid, respectively (the nomenclature $L(\lambda)$ and $H(\tau)$ preserves that commonly used[11v]). The discrete forms, which are frequently sufficient to represent data within experimental error, may be obtained from the continuous functions, e.g., $\lambda^{-1}L(\lambda)/[J_\infty - J_o] \approx \Sigma\alpha_i\delta(\lambda - \lambda_i)$. With the discrete distribution , for example, $\eta = G_o\Sigma\varphi_i\tau_i$, $\eta^2 J_s = G_o\Sigma\varphi_i\tau_i^2$ and $\tau_c = \Sigma\varphi_i\tau_i^2/\Sigma\varphi_i\tau_i$ for a fluid, the latter revealing τ_c as a certain average relaxation time. For the discrete representation the times alternate regularly in magnitude (with λ_0 absent for a fluid): $\lambda_0 > \tau_1 > \lambda_1 > \ \ldots > \lambda_i > \tau_i > \lambda_{i+1} > \ldots > \lambda_{N-1} > \tau_N$.

The determination of $L(\lambda)$ or $H(\tau)$, or the corresponding α_i:λ_i or φ_i:τ_i sets, from experimental data requires an iterative process. In some methods this is assisted by the use of approximations to provide the initial guess of the desired function. A number of these have been developed,[23m] including one found to be particularly useful for computation of $L(\lambda)$:[11w]

$$L_2(\lambda) \approx \{[\partial J(t)/\partial \ln t] - [\partial^2 J(t)/\partial(\ln t)^2]\}_{\lambda=t/2} \qquad (57)$$

Since the differentiation removes the influence of the term t/η, the same relation applies with J(t) replaced by R(t). In a scheme utilized to estimate $L(\lambda)$, the residuals between the measured and calculated J(t) using the estimate for $L(\lambda)$ begins with $L(\lambda) = L_2(\lambda)$, with sequential improvements in the estimate for $L(\lambda)$ to minimize the residuals between the calculated and observed R(t) to the level of experimental uncertainty; $L(\lambda)$ leading to nonphysical behavior, such as oscillations in R(t) are rejected in this process. Other methods utilize inverse transforms in iterative calculations, such as the well-known CONTIN often applied to dynamic light scattering analysis,[40] or methods devised especially for use with rheological data.[41] Some commercial rheometers provide software for this purpose. Typically, these methods are designed to provide discrete weighting functions for a set of times selected to span the experimental range, with the number of times chosen to provide an acceptable representation of the data within experimental error, without introducing fictitious oscillations in the transform. Examples of $L(\lambda)$ are given in subsequent sections.

Although analytical computation of $\varphi_i:\tau_i$ sets from $\alpha_i:\lambda_i$ sets, and vice versa, is possible for small N, iterative methods or required for N normally of interest.[23n; 42; 43] Similarly, iterative methods are required to compute $H(\tau)$ from $L(\lambda)$, and vice versa.[11x; 23m] Thus, for example, the so-called Maxwell model with N = 1 for a fluid is characterized by a single relaxation time τ, and no retardation times ($\alpha(t) = \delta(t)$ and $\varphi(t) = \exp(-t/\tau)$). For a Maxwell solid with N = 1, $\varphi(t)$ is unchanged, but $\alpha(t) = \exp(-t/\lambda)$, with $\lambda = (G_o/G_e)\tau$. Although algebraic methods may be conveniently applied for N up to about three, in general, iterative calculations are necessary to interconvert $\varphi_i:\tau_i$ and $\alpha_i:\lambda_i$ sets for larger N; the latter are readily implemented on desktop computers.[43]

The so-called stretched exponential form $\exp[-(at)^n]$ has been used to represent $\alpha(t)$ or $\varphi(t)$.[44] The relation between $\alpha(t)$ and $\varphi(t)$ when one or the other is represented by a stretched exponential function has been considered in detail, showing that both cannot be stretched exponential functions for a given material.[44]

The dynamic mechanical functions take on a simple form for the special case with $\alpha(t)$ and $\varphi(t)$ expressed in terms of retardation or relaxation times:[11v; 18; 23p]

$$J_\infty - J'(\omega) = \int_{-\infty}^{\infty} d(\ln \lambda)\, L(\lambda) \frac{(\omega\lambda)^2}{1 + (\omega\lambda)^2} = [J_\infty - J_o] \sum_{m}^{N-1} \alpha_i \frac{(\omega\lambda_i)^2}{1 + (\omega\lambda_i)^2} \quad (58)$$

$$J''(\omega) - (1/\omega\eta) = \int_{-\infty}^{\infty} d(\ln \lambda)\, L(\lambda) \frac{\omega\lambda}{1 + (\omega\lambda)^2} = [J_\infty - J_o] \sum_{m}^{N-1} \alpha_i \frac{\omega\lambda_i}{1 + (\omega\lambda_i)^2} \quad (59)$$

$$G'(\omega) - G_e = \int_{-\infty}^{\infty} d(\ln \tau)\, H(\tau) \frac{(\omega\tau)^2}{1 + (\omega\tau)^2} = [G_o - G_e] \sum_{1}^{N} \varphi_i \frac{(\omega\tau_i)^2}{1 + (\omega\tau_i)^2} \quad (60)$$

$$G''(\omega) = \int_{-\infty}^{\infty} d(\ln \tau)\, H(\tau) \frac{\omega\tau}{1 + (\omega\tau)^2} = [G_o - G_e] \sum_{1}^{N} \varphi_i \frac{\omega\tau_i}{1 + (\omega\tau_i)^2} \quad (61)$$

These expressions give the expected limits, e.g., $G''(\omega) = \omega\eta'(0)$ for small ω, etc. For the special case of a fluid with only one relaxation time τ_1, it can be seen that the maximum in $G''(\omega)$ occurs for $\omega\tau_1 = 1$, at which point $G'(\omega) = G''(\omega) = G_o/2$. This feature is sometimes generalized to assert that $\omega\tau_1 = 1$ for $G'(\omega) = G''(\omega)$ and the maximum in $G''(\omega)$ for the more general case with a number of relaxation times. Although that will not usually be correct, with the maximum in $G''(\omega)$ occurring for a larger value ω_{max} than the value of ω_x for which $G'(\omega_x) = G''(\omega_x)$. Thus, for a fluid,

$$\omega_a = (1/\tau_c) \frac{\int_0^{\infty} ds\, \cos(\omega_a s)\varphi(s) / \int_0^{\infty} ds\, \varphi(s)}{\int_0^{\infty} ds\, [\sin(\omega_a s)/(\omega_a s)^a] s\varphi(s) / \int_0^{\infty} ds\, s\varphi(s)} \quad (62)$$

with a = 0 for ω_{max} or a = 1 for ω_x. Consequently, $\omega_x \le \omega_{max} \le 1/\tau_c$ in general, with equality only if $\varphi(t)$ has decreased substantially for t such that the functions $\sin(\omega_a t)/(\omega_a t)^a$ and $\cos(\omega_a t)$ begin to deviate from their limiting values of unity for small $\omega_a t$.

As will be seen in a subsequent section, the time spanned by the functions $\alpha(t)$ and $\varphi(t)$ as they decay from unity to zero may easily encompass 12-15 decades, almost always too much to be covered by a single instrument at a given temperature (and pressure). In some cases, it is possible to extend the time by combination of steady-state dynamic mechanical experiments with time-dependent measurements. This is useful since dynamic experiments may be carried out for a range

of ω corresponding to shorter t (≈ 1/ω) than may be convenient in the time domain, and vice versa, permitting an effective extension of the time span probed. For example, the relation

$$R(t) \approx \{J'(\omega)^2 + [J''(\omega) - (\omega\eta)^{-1}]^2\}^{1/2}_{\omega t=1} \quad (63)$$

provides a useful approximation, which could be improved by use of the appropriate exact integral relations given above; this expression is a variant of the approximation $J(t) \approx |J^*(\omega)|_{\omega t=1}$.[45] Conversely, the relations

$$J'(\omega) \approx \{[1 - m(2t)]^{0.8} R(t)\}_{\omega t=1} \quad (64a)$$

$$J''(\omega) - (\omega\eta)^{-1} \approx \{[m(2t/3)]^{0.8} R(t)\}_{\omega t=1} \quad (64b)$$

have been found to be accurate representations, where $m(t) = \partial \ln R(t)/\partial \ln t$ (note typographical errors with 2t/3 given as 2/3t in some references).[11y; 23q; 46]

A less rigorous attempt to expand the effective time (or frequency) range for which linear viscoelastic functions may be estimated beyond that available experimentally relies on the so-called "time-temperature equivalence" approximation employing reduced variables. In essence, the approximation assumes that properly reduced compliances or moduli as functions of reduced time or frequency could be independent of temperature. Consideration of the behavior at intermediate and long times shows that if it obtains, such invariance should be based on the use of the dimensionless time t/τ_c and frequency $\omega\tau_c$, with the definition of τ_c generalized to read $\tau_c = \eta'(0)J_\infty$, dimensionless shear compliances by division of J(t), J'(ω) or J''(ω) by J_∞, and dimensionless shear moduli by multiplication of G(t), G'(ω) or G''(ω) by J_∞.[47; 48] Similar expressions may be written for the other compliances and moduli. For example, for a fluid,

$$J(t/\tau_c)/J_s = 1 - [1 - J_o/J_s]\alpha(t/\tau_c) + t/\tau_c \quad (65)$$

Since normally (except for small molecules) $J_o/J_s << 1$, it can be seen that the time-temperature approximation in which $J(t/\tau_c)/J_s$ is considered to be a function of t/τ_c, and not otherwise dependent on temperature, will hold if $\alpha(t/\tau_c)$ proves to be independent of temperature. Examples of other reduced functions are given in Table 5.

Although J_∞ is frequently only slightly dependent on temperature,[18] the viscosity will generally depend markedly on temperature, with this dependence increasing markedly for T near the glass transition temperature T_g.[11z; 18] In the latter case, it is useful to correlate the temperature dependence of η (or $\eta'(0)$) with the simple relation[11z; 49; 50]

$$\eta(T)/\eta(T_{REF}) = \exp[C/(T - T_o) - C/(T_{REF} - T_o)] \quad (66a)$$

$$= \exp\left(-\frac{C(T - T_{REF})}{\Delta_{REF}(T - T_{REF} + \Delta_{REF})}\right) \quad (66b)$$

with C and T_o being constants, and $\Delta_{REF} = T_{REF} - T_o$. Thus, with this representation, $\eta(T)/\eta(T_{REF})$ becomes a function of $T - T_{REF}$, with a constant Δ_{REF} that depends on the arbitrarily chosen reference temperature T_{REF}. Fitting this relation to experimental data permits estimation of C and T_o.[11z; 18; 49] If T_{REF} is put equal to T_g then

$$\eta(T)/\eta(T_g) = \exp\left(-\frac{\mathfrak{K}(T - T_g)}{T - T_g + \Delta}\right) \quad (67)$$

where $\Delta = T_g - T_o$ and $\mathfrak{K} = C/\Delta$. The latter form emphasizes the role of T_g in the temperature dependence, and is especially useful since the parameters $\mathfrak{K}$ and Δ are often found to be nearly equal to "universal" values of $\mathfrak{K} = 2300$ K and $\Delta = 57.5$ K for polymeric materials.[11z; 18; 49] This form takes account of the anticipated dependence of T_g on the number average molecular weight M_n for low molecular weight polymers,[11a'; 49] as well as the dependence of T_g on the volume fraction of polymer in a solution. Since $T_m/T_g \approx 1.4\text{-}2$[51] for crystallizable polymers above their melting temperature T_m, if $T > T_m$, then T is far enough above T_o to permit simplification of this expression to the Arrhenius relation $\eta(t) \propto \exp(W/T)$, with W a constant; similarly, the Arrhenius relation applies if T is greater than about $(1.4\text{-}2)T_g$ for noncrystallizable polymers.

Since J_s and η may not be known as functions of T, the time-temperature approximation is usually implemented in terms of reference variables $b(T,T_{REF}) = J_\infty(T)/J_\infty(T_{REF})$, $h(T,T_{REF}) = \eta(T)/\eta(T_{REF})$ and $a(T,T_{REF}) = b(T,T_{REF})h(T,T_{REF})$ called "shift factors", see Table 4.[11b'; 48] The

notation for T_{REF} is usually suppressed, i.e., $a(T,T_{REF})$ is usually written a_T or occasionally a(T), etc.[11b'] Implementation of this approximation is usually accomplished by finding the values of the reference variables that will superpose bilogarithmic plots of data at temperature T as a function of time or frequency onto data at some convenient T_{REF}. For example, as illustrated in Figure 8, data on log[J(t)] as a function of log(t) at temperature T are "shifted" horizontally to coincide with data at T_{REF} to estimate $\log[a(T,T_{REF})]$; $b(T,T_{REF})$ is often small or negligible, and is taken to be unity for these data, but otherwise, a vertical shift needed to superpose the data would give $\log[b(T,T_{REF})]$ in this case. The shift factors for other functions are given in Table 4. Implementation of this procedure with dynamic mechanical data is facilitated by examination of $J'(\omega)$ and $\eta'(\omega)$ since in each case, these approach a constant value at low ω, making it simple to assess the shift factors $b(T,T_{REF})$ and $h(T,T_{REF})$, respectively, from the "vertical shift" for those portions of the data for which ω is small enough to approximate constancy in $J'(\omega)$ and $\eta'(\omega)$. Then, a degree of consistency is imposed by the requirement that $a(T,T_{REF}) = b(T,T_{REF})h(T,T_{REF})$ for the shift factor to be applied to the frequency.

In some cases experimenters carry out dynamic experiments as a function of temperature at a fixed frequency (so-called isochronal experiments). This practice arose in an age when it was not easy to do measurements as a function of ω, and has become embedded in certain fields. In-so-far as the time-temperature equivalence behavior is a reasonable approximation, there is a simple mapping between the time and frequency domains. An example based on the used of the empirical temperature dependence discussed below is given in Figure 9 for a viscoelastic solid.

5. The viscosity of dilute of polymer solutions and colloidal dispersions

Although viscoelastic measurements can be carried out on dilute solutions of polymers, that requires specialized equipment, and is not normally of interest; however see below for a brief discussion of such measurements. The viscosity, however, is widely used to characterize macromolecules or colloidal particles in dilute solution, and capillary viscometry is by far the most widely used method for that purpose. The parameters of usual interest arise in a series expansion of the viscosity in terms of the polymer concentration c (wt/vol):

$$\eta = \eta^{(c)}_{LOC}\{1 + [\eta]c + k'([\eta]c)^2 + k''([\eta]c)^3 + \ldots\} \qquad (68)$$

with the local viscosity $\eta^{(c)}_{LOC}$ usually assumed to be approximated by the solvent viscosity η_{solv} in a dilute solution (however, see below) and k' a parameter of order unity.[15a] Although the use of this

virial expansion is usually appropriate for a dilute solution ($[\eta]c < 1$), it may not apply to all systems, with solutions of charged species in a solvent of low dielectric strength providing one example where it may fail.[15b] The expression for the relative viscosity $\eta_{rel} = \eta/\eta_{solv}$ may be transformed into several useful forms for analysis (assuming that $\eta^{(c)}_{LOC} \approx \eta_{solv}$) to determine $[\eta]$ and k', including

$$\eta_{sp}/c = (\eta_{rel} - 1)/c = [\eta] + k'[\eta]^2c + k''[\eta]^3c^2 + \ldots \quad (69a)$$

$$\ln(\eta_{rel})/c = [\eta] - (1/2 - k')[\eta]^2c + (1/3 - k' + k'')[\eta]^3c^2 + \ldots \quad (69b)$$

$$\{2[\eta_{sp} - \ln(\eta_{rel})]\}^{1/2}/c = [\eta] - (1/3 - k')[\eta]^2c + \ldots \quad (69c)$$

all to the same order in c, with η_{sp} the specific viscosity. Additional transformations of the basic series expansion have sometimes been used to aid analysis to determine $[\eta]$ and k',[15a] but these are the forms most commonly encountered. Simultaneous analysis with these three forms should yield common values for $[\eta]$ and k', and failure to do so should be taken as evidence of inaccuracy in the data, or data confined to c too large to permit a reliable extrapolation to infinite dilution. In particular, if $k' \approx 1/2$, then the curvature in η_{sp}/c will be enhanced, whereas the initial tangent for $\ln(\eta_{rel})/c$ will be zero, making it easy to underestimate $[\eta]$ and overestimate k' by assuming linearity in both of these functions over the measured range of c.[52] The third form is particularly useful if $k' \approx 1/3$, as is often the case for flexible chain polymers in so-called good solvents (see below),[15a] and can be recommended for use in the analysis of viscometric data obtained for the effluent in a chromatographic analysis.

Capillary viscometry using a suspended-level Ubbelohde capillary viscometers to permit successive dilutions in the viscometer is the usual method to obtain η_{rel} as a function of c for analysis with the preceding relations. Viscometers are available that suppress end-effects, so that the efflux time for a calibrated volume is accurately proportional to the viscosity, permitting evaluation of η_{rel} as the ratio of the efflux times for solution and solvent; consideration of the analysis to determine $[\eta]$ and k' will show that η_{rel} should be determined to ± 0.0005 to obtain the desired precision in $[\eta]c$. A viscometer with an efflux time of about 100 s should normally be used, with means to determine the efflux time to ± 0.03 s applied to obtain the necessary precision in the analysis. The viscometer must be held to ± 0.02°C to obtain this precision in the efflux times. It is essential that solution and solvent be filtered to remove extraneous matter that might lodge in the capillary or otherwise alter the efflux time, and that η_{rel} not exceed about 1.8 for the most

concentrated solution, and preferably be less than 1.5 if k' ≈ 1/2; typically, the solution is diluted until $\eta_{rel} \approx 1.1$. Application of a vacuum to force the solution from the dilution bulb of the viscometer into the capillary should be avoided, especially with volatile organic reagents; the application of a pressure being preferred. Specialized sealed capillary viscometers are available for work above the normal boiling temperature of the solvent. Studies on very high molecular weight polymers can introduce two special problems: (1) degradation of the polymer in solution in the filtration process or in the capillary in flow, and (2) nonlinear behavior such that $[\eta]$ becomes a function of the rate of shear in the capillary flow, e.g., the rate of strain at the wall of a capillary viscometer will typically be in the range 10^2 to 10^3 s^{-1}. Both of these difficulties may be suppressed by use of specialized concentric cylinder viscometers designed to operate at a low rate of strain (< 1 s^{-1}), with a gap between the cylinders large enough to suppress the effects of a few "dust" particles, and sufficiently precise to give the necessary precision in η_{rel}.[52]

Consideration of the preceding shows that for a heterodisperse sample, the observed $[\eta]$ is an average over the $[\eta]_i$ for the components with weight fraction $w_i = c_i/c$ given by

$$[\eta] = \Sigma[\eta]_i w_i \tag{70}$$

Thus, if $[\eta] = KM^{\mu}$ for each of the components, the average molecular weight corresponding to the observed $[\eta]$ is given by $M_{(\mu)} = (\Sigma M_i^{\mu} w_i)^{1/\mu}$. For example, a Shulz-Zimm (two-parameter exponential) distribution of molecular weight with $Z^{-1} = (M_w/M_n - 1)$ gives $M_{(\mu)} = [M_w/(Z + 1)]\{\Gamma(Z + 1 + \mu)/\Gamma(Z + 1)\}^{1/\mu}$ so that $M_{(\mu)}$ lies intermediate to M_n and M_w for μ in the range 0.5 to 1.0;[53] see reference [53] for additional examples.

The intrinsic viscosity $[\eta]$ has a simple interpretation for rigid spherical particles of molecular weight M and radius R since the product $[\eta]c$ is equal to $5\varphi/2$,[54a] with $\varphi = cN_A(4\pi R^3/3) / M$ the volume fraction of the spheres: $[\eta] = 5\varphi/2c = 10\pi N_A R^3/3M$. More generally, it is convenient to express the $[\eta]$ in the form[55]

$$[\eta] = \pi N_A K_{\eta} R_G^2 R_H / M \tag{71}$$

where R_G is the root-mean-square-radius of gyration, R_H is the hydrodynamic radius, equal to $kT/6\pi\eta_{solv}D_T$, with D_T the translational diffusion constant, and the dimensionless parameter K_{η}

depends on the solute shape and other characteristics, with K_η in the range 1 to 10/3 for polymeric solute, and ranging up to 50/9 for spherical particles (for which $R_G^2 R_H = 3R^3/5$).

For high molecular weight flexible chain polymers, $R_H \approx 2R_G/3$ and $K_\eta \approx 10/3$ in the so-called nondraining hydrodynamic limit,[55; 56a] leading to the well-known Flory-Fox relation $[\eta]M = \Phi' R_G^3$, with $\Phi' = \pi N_A K_\eta R_H/R_G$, or $\Phi' \approx 20\pi N_A/9$ for linear flexible chain polymers. The proportionality $[\eta]M \propto R_G^3$ was originally suggested by analogy with the behavior of hard spheres.[57; 58] In this form, the molecular weight dependence of $[\eta]M$ is attributed to that of R_G^3, which in turn is given by the relation $R_G^2 = \hat{a}L\alpha^2/3 \propto M^\varepsilon$, where α is the excluded volume expansion factor, $\hat{a}$ is the persistence length of the chain and L its contour length ($L = M/M_L$ with M_L the mass per unit length of the chain).[59] Under Flory Theta conditions, defined by the condition that the second virial coefficient A_2 is zero, $\alpha = 1$ and $R_G^2 = \hat{a}L/3 \propto M$. In the opposite extreme, repulsive interactions among the chain segments saturate to give $A_2M^2 \propto R_G^3 \propto [\eta]$ and $\alpha \propto z^{1/5}$, where the interaction parameter $z \propto (L/\hat{a})^{1/2}$, so that ε varies from unity at the Theta temperature to 6/5 in a so-called good solvent. Correspondingly, $\mu = \partial \ln [\eta]/\partial \ln M = (3\varepsilon/2) - 1$ varies from 1/2 to 4/5. Values of the so-called Mark-Houwink-Sakarada parameters μ and $K = [\eta]/M^\mu$ are listed in handbooks for the range of M for which these are essentially constant for a given polymer/solvent pair.[60]

The presence of branching can alter the analysis of $[\eta]$. The effects of short branches placed randomly, or uniformly along a much longer backbone of an otherwise linear chain, are readily accommodated by assuming that K_η and R_G/R_H will be unaltered, and that R_G^2 will be essentially the value for the linear backbone in the absence of the short branches.[61] In this case, the ratio $g' = [\eta]/[\eta]_{LIN}$ of the intrinsic viscosities of chains with common M is given by $g' \approx g^{3/2}$, with $g = R_G^2/(R_G^2)_{LIN}$ the ratio of the mean-square-radii of gyration of chains with common M. The introduction of long-chain branching, as with randomly branched or comb-shaped branched chains, or star-branched chains, introduces additional complications, as then both K_η and R_G/R_H may be altered. Thus, the ratio $h = R_H/(R_H)_{LIN}$ of the hydrodynamic radii of chains with common M is in the range $1 \le hg^{-1/2} \le 1.4$ for Gaussian comb- or star-branched chains, and for those same models, K_η increases with decreasing g for the same model.[55] These effects can be expressed in the form $g' \approx g^{m(\lambda)}$, with λ the fraction of the repeating units in the longest linear segment of the branched structure; $m(\lambda) \approx 0.44 + \lambda^{10/3}$ and $g \approx \lambda + [(3p - 2)/p^2](1 - \lambda)^{7/3}$ for comb- or star-branched molecules with p branches per molecule.[55] Consequently, $m(\lambda)$ varies from about 1/2 for regular star-branched chains to 3/2 for comb-branched chains with short branches (as in the preceding

discussion). This same form may approximate g' for a randomly branched chain based on the statistically longest linear segment in those structures.

With decreasing L/â for flexible chain polymers, α tends to unity, even in systems with large A_2, and R_H/L and K_η tend to unity, giving $[\eta] \approx \pi N_A R_G^2/M_L \propto M$ in the free draining hydrodynamic limit.[55; 56a] This regime is not usually encountered except for low M, but may be observed with semiflexible chains for which â is large enough that L/â is in the range for this behavior even for chains with relatively high molecular weight, e.g., with cellulosic polymers and certain other chains with relatively large â.[55] Expressions are available for a variety of other solute shapes, such as rods, semiflexible wormlike chains and ellipsoids of revolution. For rods with diameter $d << L$, $K_\eta = 1$, $R_G^2 = L^2/12$ and $R_H \approx L/2\ln(3L/2d)$. Relations for the wormlike chain and prolate and oblate ellipsoids of revolution are given in reference [55].

For very small M, the observed $(\partial \ln \eta/\partial c)_{c=0}$, interpreted as $[\eta]$ by the preceding, may be negative. This effect is attributed to a failure of the assumption $\eta_{LOC}^{(c)} = \eta_{solv}$ for non zero c if η is to be interpreted by the preceding relations or more sophisticated variations on them.[62] For example, in a dilute solution, $\eta_{LOC}^{(c)}$ might be expressed as a Taylor series in c with $(\eta_{LOC}^{(c)})_{c=0} = \eta_{solv}$, but with $|\partial \eta_{LOC}^{(c)}/\partial c|$ not negligible in comparison with $[\eta]$, as is usually assumed for dilute solutions. In this case, the series expansion for η given above must be modified, so that $(\partial \ln \eta/\partial c)_{c=0} = [\eta] + (\partial \ln \eta_{LOC}^{(c)}/\partial c)_{c=0}$, requiring an estimate of $\partial \ln \eta_{LOC}^{(c)}/\partial c$ to evaluate the desired parameter $[\eta]$ from the dependence of η on c. This correction would be expected to be negligible for high molecular weight solute, since then $[\eta] >> |\partial \ln \eta_{LOC}^{(c)}/\partial c|_{c=0}$, but could become important for oligomeric polymers, and in some cases it appears that $(\partial \ln \eta_{LOC}^{(c)}/\partial c)_{c=0} < 0$, leading to negative $(\partial \ln \eta/\partial c)_{c=0}$.[62-66] Non zero $\partial \ln \eta_{LOC}^{(c)}/\partial c$ for a dilute solution might reflect a number of effects, including the situation in which a solvent with a high glass temperature T_g is mixed with a polymer with a low T_g, so that $\partial \ln \eta_{LOC}^{(c)}/\partial c < 0$, although this mechanism has been challenged.[67]

The Huggins constant k' appearing in the virial expansion is expected to depend on both hydrodynamic and thermodynamic effects, and for flexible chain polymers may usually be approximated by the relation

$$k' = c_1 + c_2 A_2 M/[\eta] \qquad (72)$$

For example, for linear flexible chain polymers, $c_1 \approx 1/2$ and $c_2 \approx -1/6$,[15c; 56b; 68] in reasonable agreement with the experimental observations that $k' \approx 1/2$ under Flory Theta conditions ($A_2 = 0$) and $k' \approx 1/3$ as $A_2M/[\eta]$ approaches its asymptotic value of approximately unity in a so-called good solvent. For rigid spheres interacting through a hard-core potential the dependence on $A_2M/[\eta]$ is moot, since $A_2M/[\eta] = 8/5$. Numerous estimates of k' for rigid spheres have appeared, but the accepted theoretical and experimental estimates give $k' \approx 1.0$.[54a; 69; 70]

Most of the linear viscoelastic studies on dilute polymer solutions have involved either dynamic mechanical or dynamic birefringence measurements. The stress-optic approximation discussed in the final section has been invoked in the latter. These studies often have the objective of comparison of the reduced responses $[\eta]'(\omega) = \{\eta'(\omega)/\eta^{(c)}_{LOC}c\}_{c=0}$ and $[\eta]''(\omega) = \{[\eta''(\omega) - \eta^{(c)}_{LOC}]/\eta^{(c)}_{LOC}c\}_{c=0}$ with theoretical estimates of the same functions, where it is usual to assume that $\eta^{(c)}_{LOC} \approx \eta_{solv}$.[11j; 64] An anomaly at high frequency[62; 65; 66] suggests that $\eta^{(c)}_{LOC} \neq \eta_{solv}$, similar to the behavior discussed above in which $(\partial \ln\eta/\partial c)_{c=0}$ may be negative for solutions of oligomeric polymers, and understood in the same general way, though care must be taken to account for any viscoelastic character of the solvent, which could make $\eta'(\omega) \neq 0$ and $\eta''(\omega) < \eta_{solv}$ for the solvent even if $\eta^{(c)}_{LOC} \approx \eta_{solv}$.

With increasing c, in the range of moderately concentrated (or semi-dilute) solutions, the virial expansion of η given above fails. This regime is marked approximately by the condition that R_G is about equal to the mean separation $\Lambda = (M/cN_A)^{1/3}$ of molecular centers. The behavior in this regime is conveniently represented by the expression

$$\eta = \eta^{(c)}_{LOC}\{1 + [\eta]^{(c)}c\} \tag{73}$$

For dilute solutions, $[\eta]^{(c)} \approx [\eta]\{1 + [\eta]c\}^{k'}$ to approximate the virial expression to order c^2. With increasing c, both $K_\eta R_H$ and α reduce to unity through screening of hydrodynamic and thermodynamic interactions, respectively, and $[\eta]^{(c)}c \approx \tilde{X} = [\pi N_A \hat{a}(\alpha^{(c)})^2/3M_L^2]cM$, provided cM is small enough to suppress intermolecular entanglement interactions discussed in the next section.[50] Here, $\alpha^{(c)}$ is expansion factor for the root-mean-square radius of gyration of the chain at polymer volume fraction φ, and other parameters are introduced above. A semi-empirical cross-over expression to span these two extremes has been presented in reference [50]; a schematic representation of the range of the concentration for the successive screening of thermodynamic and

hydrodynamic interactions and the development of entanglement effects is given in Figure 10. The dependence of $\eta^{(c)}_{LOC}$ on c may be important in this regime, even if $\eta^{(c)}_{LOC} \approx \eta_{solv}$ for dilute solutions. In some cases, $\eta^{(c)}_{LOC} \approx \eta_{solv}\exp(b_T\varphi)$, with b_T a temperature dependent parameter,[71] before reaching the behavior described in the preceding with $\eta^{(c)}_{LOC}$ a function of the glass transition temperature.

6. Linear viscoelastic behavior of concentrated and undiluted polymeric fluids

According to the preceding, linear viscoelastic behavior may be represented through several parameters and functions. For example, in shear deformation the parameters $J_o = 1/G_o$, J_∞ (equal either to $J_e = 1/G_e$ for a solid or J_s for a fluid), η for a fluid, and the functions $\alpha(t)$ or $\varphi(t)$, with the latter related through a convolution integral. Similar representations may be written for the volume functions B(t) and K(t), and for the elongational functions D(t) and E(t), with the latter approximated by $D(t) \approx J(t)/3$ and $E(t) \approx 3G(t)$ in the incompressible approximation (negligible volume change).

It is convenient to discuss η before turning to J_s and the time-dependent functions G(t) and J(t). Empirically, the viscosity of polymers and their concentrated solutions may be represented for linear polymer by the simple expression[50]

$$\eta = \eta^{(c)}_{LOC} H^{(c)} \tilde{X}[1 + (\tilde{X}/\tilde{X}_c)^{4.8}]^{1/2} \qquad (74a)$$

$$\tilde{X} = [\pi N_A \rho \hat{a} (\alpha^{(c)})^2/3M_L^2]\varphi M \qquad (74b)$$

where â is the persistence length, $\alpha^{(c)}$ is expansion factor at polymer volume fraction φ, ρ is the polymer density, $M_L = M/L$ with L the contour length of the chain, N_A is the Avogadro number, $\eta^{(c)}_{LOC}$ is a "local" viscosity, $H^{(c)} \approx \varphi^{1/2}$ and $\tilde{X}_c \approx 100$ for a variety of chains. For Gaussian chain statistics, as would occur in the absence of excluded volume effects, the mean square radius of gyration $R_G^2 = \hat{a}L/3 \propto M$.[59] Since $\alpha^{(c)} \approx 1$ for concentrated solutions and undiluted polymer,[49; 50; 59; 72] $\tilde{X} \propto \varphi M$ for such, in which case $\eta \propto \varphi M$ for $\tilde{X} \le \tilde{X}_c$ or $\eta \propto (\varphi M)^{3.4}$ for $\tilde{X} > \tilde{X}_c$. The molecular weight M_c corresponding to this condition for undiluted polymer is seen to be given by $M_c \approx 100/[\pi N_A \rho \hat{a}/3M_L^2]$ in-so-far as $\tilde{X}_c \approx 100$. An illustration of this behavior is given in Figure 11, which shows $\eta/\eta^{(c)}_{LOC}$ vs a parameter $X = \tilde{X}/\pi N_A m_a/M_L$, with m_a the molar mass per repeat atom of the chain;[49] m_a/M_L is essentially a constant for the examples shown. The division by $\eta^{(c)}_{LOC}$ corrects for the variation of $\eta^{(c)}_{LOC}$ with M_n at low molecular weight owing to the variation of T_g with M_n. The

general features of this behavior may be understood in terms of models based on Rouse-like dynamics for $\tilde{X} \le \tilde{X}_c$, modified by entanglement effects, perhaps represented by some model involving reptation concepts, for $\tilde{X} > \tilde{X}_c$.[17c]

The local viscosity $\eta^{(c)}_{LOC}$ is not precisely defined, but $\eta^{(c)}_{LOC}(T)/\eta^{(c)}_{LOC}(T_g)$ can be represented by the expression used above for $\eta(T)/\eta(T_g)$. An additional, usually very much smaller, temperature dependence to the viscosity is possible through the dependence of the parameters ρ, â and $\alpha^{(c)}$ on temperature.[50] Without further information, the approximation $\log\{\eta^{(c)}_{LOC}(T_g)/Pa{\cdot}s\} \approx 10\text{-}12$ can sometimes provide an adequate approximation.[73; 74] For more precise work, $\eta^{(c)}_{LOC}(T_g)$ should be evaluated from experimental data on the system of interest. In this representation, the dependence of $\eta^{(c)}_{LOC}$ on polymer concentration through the dependence of T_g on concentration may be much larger than that from the variation of $\tilde{X}$ with concentration.[50] In most cases, the effect of molecular weight heterodispersity on the viscosity may be represented by the use of the weight average molecular weight M_w in the calculation of $\tilde{X}$, and the use of the number average molecular weight to obtain T_g appearing in $\eta^{(c)}_{LOC}$;[49] the simple dependence on M_w may be inadequate for especially broad or strongly binodal distributions.[49; 75] Some of these effects are illustrated in Figure 12 for data on the viscosity of fractions of a polymer as a function of φM_w for five series at fixed φ over a range of M_w.[76] The deviation of the data from the dashed lines at lower φM_w for the samples with larger φ is caused by the variation of T_g with molecular weight, and the corresponding effect on $\eta^{(c)}_{LOC}$.[49; 50] Other than this effect, $\eta^{(c)}_{LOC}$ is constant at fixed φ, and the data for $\log(\eta)$ vs $\log(\varphi M_w)$ are parallel, but offset by the variation of $\eta^{(c)}_{LOC}$ with φ owing to the variation of T_g with φ,[49; 50] since $\alpha^{(c)} \approx 1$ for the range of φ encompassed by the data.[76] In some cases, attempts are made to estimate the critical value of φM_w for the onset of entanglement effects without consideration of the variation of $\eta^{(c)}_{LOC}$ with φ, leading to erroneous results.

Schematic illustrations of the behavior for the shear compliances and moduli, along with the corresponding distribution of retardation or relaxation times for glass forming polymeric fluids over a range of molecular weight are shown in Figure 13. The schematic illustrations in Figure 13 show essential features observed for fluids as the molecular weight increases from the oligomeric range through values with $M < M_e$ and $M > M_e$, where M_e is the mean molecular weight between entanglement loci; typically, $M_e \approx M_c/2$. The gradual expansion of the time scale required for G(t)

to relax to zero, and J(t) to approach linearity in t, is seen to increase with increasing M, with corresponding effects on H(τ) and L(λ), respectively. The figures for with $M < M_e$ and $M > M_e$ illustrate behavior for Rouse-like response and a fluid with entanglements, respectively, as discussed below. A more detailed example for a high molecular weight polymer is given in Figure 14, showing a comparison of various functions for the same material. As may be seen, J(t) differs from R(t) only for larger t, wherein the term t/η becomes dominant. As expected, 1/G(t) is generally larger than J(t), with the two being about equal in regions of intermediate t for which $\partial J(t)/\partial t \approx 0$, e.g., in the first plateau, for which $J(t) \approx R(t) \approx J_N$. Further, $J'(\omega) \leq [R(t)]_{\omega t=1}$, with equality occurring only in the plateau regions, and $G'(\omega) \geq [G(t)]_{\omega t=1}$, with the latter pair being very close except for large t, for which $G'(\omega) \propto (\omega\tau_c)^2/J_s$, but G(t) decreases exponentially with t. These functions demonstrate the inequalities $J'(\omega) \leq [R(t)]_{\omega t=1} < 1/G'(\omega) < [1/G(t)]_{\omega t=1}$ expected for any linear viscoelastic material. As mentioned above, a close approximation to $[R(t)]_{\omega t=1}$ is given by $\{[J'(\omega)]^2 + [J''(\omega) - (\omega\eta)^{-1}]^2\}^{1/2}$ over a wide range of ω.

A schematic illustration for R(t) and L(λ) for a high molecular weight monodisperse polymeric fluid is given in Figure 15.[9; 18] In the latter case, the functions R(t) and L(λ) reveal several distinctive and characteristic features for a monodisperse high molecular weight polymer in the entanglement regime, arbitrarily arranged here in order of their importance with increasing t:[11c'; 18]

1. A response at small t with R(t) linear in $t^{1/3}$, following the initial "instantaneous" J_o;
2. A range of t with R(t) increasing more sharply, but with $\partial R(t)/\partial t < 1$, to reach a "plateau" for which $\partial R(t)/\partial t \approx 0$ and $R(t) \approx J_N$;
3. A second increase in R(t) to a final plateau, for which $R(t) = J_s$.

As may be seen, J(t) differs from R(t) only for larger t, wherein the term t/η becomes dominant. As expected, 1/G(t) is generally larger than J(t), with the two being about equal in regions of intermediate t for which $\partial J(t)/\partial t \approx 0$, e.g., in the first plateau, for which $J(t) \approx R(t) \approx J_N$.

The regimes described above in R(t) are mirrored in the function L(λ) by several peaks that appear successively with increasing λ, so that, respectively:[11c'; 18]

1. Peak I with L(λ) linear in $\lambda^{1/3}$ before the peak decreases sharply to zero (the decrease is obscured by overlap with peak II in the example);
2. Peak II that increases in peak area with increasing M until reaching a certain level, beyond which the peak is invariant with increasing M, both in area and position in λ;

3. Peak III that develops as peak II area ceases to increase with increasing φM, with peak III developing an area invariant with φM, and a maximum at λ_{MAX} that moves to larger λ as $\lambda_{MAX} \propto (\varphi M/M_c)^{3.4}$ for $\varphi M > M_c$.

Peaks II and III lead to the first and second plateaus in R(t) seen in Figure 15. Of course, these effects are also reflected in H(τ), but the dominant role of the longer relaxation times on H(τ) for larger τ, largely reflecting viscous deformation, tends to obscure the additive features seen in L(λ). Peak III does not develop for chains with $\varphi M < M_c$.

The behavior ascribed to peak I, first reported by Andrade,[77] is seen in a variety of materials, such as metals, ceramics, crystalline and glassy polymers and small organic molecules;[78] the decrease of L(λ) to zero being evident in examples of the latter.[79] The area under peak I provides the contribution $J_A - J_o$ to the total recoverable compliance J_s. It seems likely that the mechanism giving rise to peak I may be distinctly different from the largely entropic origins of peaks II and III described in the following.

Peak II is ascribed to Rouse-like modes of motion, either fluid-like for low molecular weight in the range for which the area increases with M, or pseudo-solid like (on the relevant time scale) in the range of M after peak III develops.[11c'; 17d; 18; 22d] For low molecular weight, the Rouse model gives the area of peak II as $J_s - (J_A + J_o) = (2M/5\varphi RT)$. For the pseudo-solid like behavior, obtaining when peak III has developed, reflecting the effects of intermolecular entanglement, the area of peak II becomes $J_N - (J_A + J_o) = (M_e/\varphi RT)$, invariant with M, whereas the area under peak III, also invariant with M, ascribed to the effects of chain entanglements,[17e; 18] is given by $J_s - (J_N + J_A + J_o) = (kM_e/\varphi^{2+s}RT)$, where k is in the range 6-8 in most cases, and $s \approx 2(\varepsilon - 1)/(3\varepsilon - 2)$ with $\varepsilon = \partial \ln R_G^2/\partial \ln M$.[18; 75] Overall,

$$J_s - (J_A + J_o) = (2M/5\varphi RT)[1 + (\varphi^{1+s}M/kM_c)^{\varepsilon}]^{-1/\varepsilon} \qquad (75)$$

where the sharpness of the "transition" may be represented by adjustment of ε.[18] The term in square brackets accounts for effects due to entanglements, making J_s independent of M for φM greater than kM_c.[18; 72; 75] A reptation model, developed to give G(t) as a discrete sum of weighted exponentials for φ(t) may be used to compute both η and R(t) as a discrete sum of weighted exponentials for α(t).[80]

Increasing molecular weight heterodispersity affects R(t) in various ways, conveniently discussed in terms of the effects on $L(\lambda)$. The effects of molecular weight heterogeneity are marked for J_s in both the Rouse and entanglement regimes.[11d'; 18] Calculation with the Rouse model gives the average $M_z M_{z+1}/M_w$ for the molecular weight average in that regime, reflecting a broadening of peak II.[11e'] Experience in the entanglement regime reveals an equally strong dependence of J_s on the molecular weight distribution, reflecting a broadening of peak III, with effects on peak II being nil if the molecular weights of all components exceeds M_e.[81-88] Thus, the dominant effect for high molecular weight polymer in the entanglement regime is to broaden the final peak III, causing it to encompass a larger range in λ, as shown schematically in Figure 15, reflecting enhancement of J_s, with little influence on J_N, e.g., with $J_s \propto (M_z/M_w)^{2.5}$ in some experiments for all $M > M_c$.[11f'; 81-88] For a distribution containing both low and high molecular weight components, one can expect effects on both peaks II and III, as well as η. Available theoretical treatments available are not too well suited to reveal this, as they focus on consideration of G(t), and must include the (approximate) correlation of η on M_w, as well as the dependence of J_s on molecular weight heterogeneity. A number of treatments of this type that have been proposed for fluids may be cast in the form[11g'; 81-88]

$$G(t) = \{\sum_i w_i G_i(t)^\nu\}^{1/\nu} \qquad (76)$$

A recent treatment for mixtures of chains with all components having molecular weights in excess of M_c gives an result of this from with $\nu = 1/2$, and an expression for G(t);[85; 86] by comparison, in the original reptation model, $\nu = 1$.[17f] Other variations have been proposed to deal with mixtures of chains of molecular weights $M_2 > M_c$ and $M_1 < M_c$.[79; 82; 87] The short chains essentially act as a diluent for the longer chains, such that J_s increases about as the inverse of the square of the volume fraction φ_2 of the longer chains. A single peak I is observed, but two peak II's are observed, one for each component, with the separation between peak II for the higher molecular weight component and peak III given by $M_2\varphi_2$.[79] Thus, the effect of molecular weight heterodispersity can be simply represented in terms of $L(\lambda)$ (or R(t)):

1. Peak I is essentially unaffected by molecular weight dispersion;
2. Peak II gives an area proportional to $\varphi_L M_z M_{z+1}/M_w$, with the averages calculated for chains at volume fraction φ_L with $M < M_c$, and a separate peak for chains with area proportional to $(1 - \varphi_L)M_c$ for chains at volume fraction $1 - \varphi_L$ with $M > M_c$;

3. Peak III with an area that varies about as $(1 - \varphi_L)^{-2}(M_z/M_w)^{2.5}$, with the averages calculated for chains with $M > M_c$; the maxima for peaks II and III separate in λ as $(1 - \varphi_L)M_w$.

In addition to these effects, the reduced parameters λ/τ_c and t/τ_c will both depend on M_n for low M_n through the variation of T_g with M_n, and the consequent effect on $\eta^{(c)}_{LOC}(T)/\eta^{(c)}_{LOC}(T_g)$, see above. The complex behavior characterized here would be difficult to represent by the expression given above for G(t).

The effect of a distribution of species shows up especially strongly in a material undergoing crosslinking to form a network. For example, for a linear polymer undergoing random crosslinking, say by radiation chemistry, $L(\lambda)$ first extends to longer λ, as with heterogeneity in molecular weight, corresponding to increased J_s for the pre-network fluid.[11h'; 89] At a certain level of crosslink density at incipient network formation R(t) extends to such long times that the long time limiting behavior cannot be experimentally assessed. In the post-network solid the contributions with longer λ are successively suppressed as the crosslink density increases, until the retardation exhibits only peaks I and II for networks with a molecular weight M_{XL} between crosslinks less than M_c, with the area of peak II proportional to M_{XL}. These effects are shown schematically in Figure 15. Similar behavior is observed on forming a network through the polymerization of a mixture of difunctional monomer containing some trifunctional monomer. The behavior for the incipient network formation frequently approximates a power-law with $R(t) \approx J(t) = J_o[1 + (t/\lambda_p)^{\alpha}]$, with λ_p and α constants. In this power-law regime, $\tan \delta(\omega) \approx \tan[\sin(\alpha\pi/2)]$, so that $J'(\omega) \propto J''(\omega)$ and $G'(\omega) \propto G''(\omega)$, and for the special case $\alpha = 0.5$, $J'(\omega) \approx J''(\omega)$ and $G'(\omega) \approx G''(\omega)$.[90] It may be noted that behavior with $\alpha \approx 0.5$ would obtain for a wide range in ω with the Rouse model with a proliferation of relaxation times, particularly long relaxation times corresponding to larger species, as might result from the wide range of molecular structures present at incipient network formation. In such a case, the anticipated behavior at low ω for either a fluid or a solidmight be suppressed to such low ω as to be experimentally unattainable.

As might be anticipated, the "time-temperature equivalence" approximation discussed above is not truly adequate over the full range of material response embodied in J(t) or G(t).[91] For example, the Andrade creep reflected in peak I in $L(\lambda)$ appears to have a different dependence on temperature than that for other contributions to $L(\lambda)$, as might be expected given its rather different origin.[74; 91-93] Additional departures from the approximation have also been reported for behavior in connection with peaks II and III.[91]

The behavior for the linear viscoelastic volume properties B(t) or K(t), or their dynamic counterparts, has not been explored in as much detail as that for the shear functions J(t), etc.[74; 94] It has been reported that the distribution of retardation times λ_{vol} found in $\beta(t)$ is similar to that the retardation times λ in $\alpha(t)$ for shear deformation, except that they terminate at much smaller λ_{vol}, corresponding to the initial parts of peak I.[95]

Some of the early development of linear viscoelasticity was cast in terms of mechanical models of arrays of springs and dashpots, by virtue of the mathematical homology of the linear response theory for familiar models with that for the retarded response and relaxation behavior of linear viscoelasticity. A thorough discussion of these models and their relation to linear viscoelastic behavior may be found in reference [23c].

7. Nonlinear viscoelastic behavior of concentrated and undiluted polymeric fluids

All polymers and their solutions will exhibit nonlinear viscoelastic behavior if the strain is not recently small, where the specifics of that criterion depend on the linear viscoelastic functions, e.g., G(t) or J(t) in shear deformation. Nonlinear behavior can take many forms, and it is possible to consider only a very limited range of those here. The well-studied behavior of nonlinear elastic materials provides the motivation for a constitutive equation often used to approximate the properties of nonlinear viscoelastic materials, in the incompressible limit (negligible volume change). For example, the Mooney-Rivlin theory gives a widely used relation for an incompressible nonlinear elastic solid[3a; 9]

$$\tau(\lambda) = 2(\lambda^2 - \lambda^{-1})(C_1 + C_2\lambda^{-1}) \qquad (77)$$

where $\tau = S_{11} - S_{22}$ is a tensile stress, $\lambda = 1 + \varepsilon_{11}$, for an elongational deformation along x_1, and the parameters C_1 and C_2 are called the Mooney-Rivlin constants; this expression is also seen in the form using the apparent stress $\tau_{APP}(\lambda) = \tau(\lambda)/\lambda$ based on the original cross-sectional area. Inspection for small strain shows that $2(C_1 + C_2) = G_e$. The expression for an ideal network results with $C_2 = 0$.[3b] The Mooney-Rivlin model also gives the shear stress $\sigma = S_{12}$, and first and second normal stresses $N_1 = S_{11} - S_{22}$ and $N_2 = S_{22} - S_{33}$, respectively, for a shear deformation with shear strain γ along x_1, and gradient along x_2:[3c; 9]

$$\sigma(\gamma) = G_e\gamma \qquad (78a)$$

$$N_1(\gamma) = G_e\gamma^2 \tag{78b}$$

$$N_2(\gamma) = -2C_2\gamma^2 \tag{78c}$$

The third normal stress difference is given by $N_3 = N_1 + N_2 = S_{11} - S_{33}$, or $N_3 = 2C_1\gamma^2$ for this model; the result $N_1(\gamma)/\sigma(\gamma) = \gamma$ obtained for this model will reappear for fluids in the following. These results are used below in the section on birefringence.

Certain of these features are carried over in theories of the nonlinear deformation of viscoelastic materials. Thus, a number of models constructed to account for nonlinear dependence on the strain for an incompressible fluid may be expressed in the form[17g]

$$S_{\alpha\beta}(t) = -\int_0^\infty du\, Q_{\alpha\beta}(t,u)\,\frac{\partial G(t-u)}{\partial u} - \delta_{\alpha\beta}P \tag{79a}$$

$$\mathbf{Q} = \mathbf{Q^o}\cdot\mathbf{F} \tag{79b}$$

where the tensor $\mathbf{Q^o}$ represents the response under a certain deformation range discussed below for which $\mathbf{F}$ may be approximated by the unitary tensor, and the tensor $\mathbf{F}$ accounts for nonlinear departures from that response. Not all models are cast in the form of integral expressions; a number of forms are discussed in reference [22e], many of these having the form of differential equations. In Cartesian coordinates for shear deformation along x_1 and shear gradient along x_2, and uniaxial elongational deformation with deformation along x_1:

$$\mathbf{Q^o_{sh}} = \begin{pmatrix} 1+\gamma(t,u)^2 & \gamma(t,u) & 0 \\ \gamma(t,u) & 1 & 0 \\ 0 & 0 & 1 \end{pmatrix}; \qquad \gamma(t,u) = \int_u^t ds\,\dot\gamma(s) \tag{80a}$$

$$\mathbf{Q^o_{el}} = \begin{pmatrix} \lambda(t,u)^2 & 0 & 0 \\ 0 & \lambda(t,u)^{-1} & 0 \\ 0 & 0 & \lambda(t,u)^{-1} \end{pmatrix}; \qquad \ln[\lambda(t,u)] = \int_u^t ds\,\dot\lambda(s) \tag{80b}$$

Several applications employing $\mathbf{Q^o}$ to compute the shear stress $\sigma(t) = S_{12}(t)$ and the first normal stress difference $N_1(t) = S_{11}(t) - S_{22}(t)$ are of interest, as these represent the second-order approximation, with the first appearance of normal stresses in shear deformation of an

incompressible fluid. The stress relaxation of steady-state shearing flow after a small step strain of γ is found to be[96; 97]

$$N_1(t, \gamma) \approx \gamma\sigma(t, \gamma) = \gamma^2 G(t) \tag{81}$$

similar to the result noted above for an elastic solid. This result is discussed below in the section on birefringence. The stresses following imposition of a constant shear rate $\dot{\gamma}$ are given by[97]

$$N_1(t, \dot{\gamma}) \approx 2\dot{\gamma}^2 \int_0^t du\, uG(u) \tag{82a}$$

$$\sigma(t, \dot{\gamma}) \approx \dot{\gamma} \int_0^t du\, G(u) \tag{82b}$$

whereas during relaxation following steady-state flow,[97]

$$\partial N_1(t, \dot{\gamma})/\partial t \approx -2\dot{\gamma}\sigma(t, \dot{\gamma}) = -2\dot{\gamma} \int_0^t du\, G(u) \tag{83}$$

For steady shear flow, the first two reduce to the important result[98]

$$N_1(\dot{\gamma})/2\sigma(\dot{\gamma})^2 = J_s \tag{84}$$

that will find use in the following. Finally, for a steady-state oscillation induced by a strain $\gamma(t) = \gamma_o \sin(\omega t)$, with a small strain amplitude γ_o, use of the strain tensor $\mathbf{Q^o}$ gives[97; 99]

$$N_1(t) = S_{11}(t) - S_{22}(t) = \gamma_o^2\{G'(\omega) + [G''(\omega) - G''(2\omega)/2]\sin(2\omega t) - [G'(\omega) - G'(2\omega)/2]\cos(2\omega t)\} \tag{85a}$$

$$N_3(t) = S_{11}(t) - S_{33}(t) = (1 - \hat{\beta})[S_{11}(t) - S_{22}(t)] \tag{85b}$$

in the Cartesian coordinate system introduced above, where $\hat{\beta} = -N_2/N_1$, with $N_2 = N_3 - N_1$. Theoretical and experimental estimates give $\hat{\beta} \approx 0.1$-0.3.[100] The normal stresses oscillates at frequency 2ω for the deformation at frequency ω, reflecting symmetry requirements; the response is

offset by a time independent term involving G'(ω), so that $S_{11}(t) - S_{22}(t) > 0$ in this approximation.

These approximations fail for larger deformations that have not been recently small, and a form for the nonlinear response tensor **F** is required. A particular formulation for **F** given by theoretical considerations for entangled flexible chain polymers gives the following forms for shear and elongation, respectively,[17g]

$$\mathbf{F_{sh}} = \begin{pmatrix} F_1[\gamma(t,u)] & 0 & 0 \\ 0 & F_1[\gamma(t,u)] & 0 \\ 0 & 0 & F_2[\gamma(t,u)] \end{pmatrix} \tag{86a}$$

$$\mathbf{F_{el}} = \begin{pmatrix} F_3[\lambda(t,u)] & 0 & 0 \\ 0 & F_3[\lambda(t,u)] & 0 \\ 0 & 0 & F_3[\lambda(t,u)] \end{pmatrix} \tag{86b}$$

A model based on reptational diffusion in the entanglement regime gives results that may be expressed in the forms

$$F_1[\gamma] \approx [1 + (|\gamma|/\gamma'')^2]^{-1} \tag{87a}$$

$$F_2[\gamma] - F_1[\gamma] \approx (2/7\gamma^2)[1 + k(|\gamma|/\gamma'')^2]^{-3/2} \tag{87b}$$

$$F_3[\lambda] \approx \left[1 + \left(\frac{\lambda^3 - 1}{\lambda''^3 - 1}\right)^{2/3}\right]^{-1} \tag{87c}$$

where k, γ'' and λ'' are expected to be universal constants.(ref) ADDIN ENRfu [17g] Thus, for the shear deformation,

$$\_(t) = \text{eq } \int\backslash o(0, t)\ du\ \ EQ\ \backslash F(\partial G(u),\partial u)\ \_(t - u)F1\_\_(t - u)\_ \tag{88a}$$

$$N_1(t) = \int_0^t du\, \frac{\partial G(u)}{\partial u}\, \gamma(t - u)^2 F_1[\gamma(t - u)] \tag{88b}$$

with $F_1[\gamma(t)] \approx 1$ in limit discussed above. A principal feature of this form is the factorization of effects due to time and strain, a form often referred to as a BKZ form after investigators who exploited it on a phenomenological basis.[101] For a strain-defined history with a step γ_o in the

strain at time zero, the stress relaxation is found to be simply $\sigma(t, \gamma_o) = \gamma_o F_1(\gamma_o)G(t)$ and $N_1(t, \gamma_o) = \gamma_o^2 F_1(\gamma_o)G(t)$, so that $N_1(t, \gamma_o)/\sigma(t, \gamma_o) = \gamma_o$, independent of t, in reasonable accord with data in the so-called terminal time response of interest here;[17g] this result gives the same behavior $N_1(t)/\sigma(t) \approx \gamma$ noted above for smaller γ. Restricting attention to deformation at constant strain rate ($\gamma(t) = \dot{\gamma}t$ in shear, or $\lambda(t) = \dot{\lambda}t = 1 + \dot{\varepsilon}t$ in elongation), nonlinear models of this type have been developed for a number of deformations, including the shear stress $\sigma(t,\dot{\gamma}) = S_{12}(t,\dot{\gamma})$ and the first-normal stress difference $N_1(t,\dot{\gamma}) = S_{11}(t,\dot{\gamma}) - S_{22}(t,\dot{\gamma})$ as functions of the time and shear strain γ in shear deformations at constant rate $\dot{\gamma}$, and the tensile stress $\tau(t,\dot{\varepsilon}) = S_{11}(t,\dot{\varepsilon}) - S_{22}(t,\dot{\varepsilon})$ as a function of the time and elongational strain ε in uniaxial elongation at constant rate $\dot{\varepsilon}$:

$$\sigma(t,\dot{\gamma}) = -\int_0^t du\, \Delta\gamma(t,u)F_1[\Delta\gamma(t,u)] \frac{\partial G(u)}{\partial u} \tag{89}$$

$$N_1(t,\dot{\gamma}) = -\int_0^t du\, [\Delta\gamma(t,u)]^2F_1[\Delta\gamma(t,u)] \frac{\partial G(u)}{\partial u} \tag{90}$$

$$\tau(t,\dot{\varepsilon}) = -\int_0^t du\, \Delta\varepsilon(t,u)F_3[\Delta\varepsilon(t,u)] \frac{\partial E(u)}{\partial u} \tag{91}$$

for incompressible fluids, where $\Delta\gamma(t,u) = (t - u)\dot{\gamma}$, etc. Although the theoretical and expressions given above for F_1 and F_3 may be used, it is convenient to adopt simpler forms more amenable to integration for some purposes. For example, the simple expression

$$F_1(\gamma) = 1 \quad \text{for } |\gamma| \le \gamma' \tag{92a}$$

$$= \exp(-[|\gamma| - \gamma']/\gamma'') \quad \text{for } |\gamma| > \gamma' \tag{92b}$$

based on the proposition that a linear response obtains for $|\gamma| \le \gamma'$ for any deformation rate, provides a useful approximation to both the theoretical expression given above and experimental data, but facilitates analytical integration if G(t) is expressed as a sum of exponential functions of time;[18; 43] more complex forms involving sums of exponential functions have also been used.[102; 103] This simple single-exponential form gives a maxima in $\sigma(t,\dot{\gamma})$ and $N_1(t,\dot{\gamma})$ for $\dot{\gamma}t$ equal to γ'' and $2\gamma''$, respectively, in qualitative accord with experiment.[17g; 22e] The simple form may be also be used to obtain observable shear-rate dependent functions in steady-state flow given information on the linear viscoelastic shear relaxation modulus G(t):[18; 43]

$$\eta(\dot\gamma) = \eta H(\tilde\beta\tau_c\dot\gamma) \quad (93)$$

$$S^{(1)}(\dot\gamma) = J_s S(\tilde\beta\tau_c\dot\gamma) \quad (94)$$

$$J_s(\dot\gamma) = J_s P(\tilde\beta\tau_c\dot\gamma) \quad (95)$$

where η, J_s and τ_c are the linear viscoelastic parameters, $\tilde\beta$ is a weak function of γ'/γ'', often about 0.3-0.5, and $H(0) = S(0) = P(0) = 1$. Here, $S^{(1)}(\dot\gamma) = N_1(\dot\gamma)/2[\dot\gamma\eta(\dot\gamma)]^2$, and $J_s(\dot\gamma) = \gamma_R(\dot\gamma)/\dot\gamma\eta(\dot\gamma)$, with $\gamma_R(\dot\gamma)$ the total constrained recoverable strain following steady-state flow at shear rate $\dot\gamma$; as noted above, the equality $S^{(1)}(\dot\gamma) = J_s$ for small $\tau_c\dot\gamma$ is found in a more general continuum mechanical treatment.[98] It should be remembered that the constrained recoverable strain is determined following reduction of the shear stress to zero, but that the normal stress is allowed to relax during the recovery process. Although the parameters γ' and γ'' are expected to be universal constants according to a theoretical model in which $F_{sh}(\gamma)$ and $F_{el}(\lambda)$ are universal functions,[17g] in practice they both depend weakly on the molecular weight distribution and on the polymer concentration in polymer solutions.[18; 43] The functions $H(\tilde\beta\tau_c\dot\gamma)$, $S(\tilde\beta\tau_c\dot\gamma)$ and $P(\tilde\beta\tau_c\dot\gamma)$ all depend markedly on the molecular weight distribution through its effect on G(t), see below. A comparison of experimental data on $\eta(\dot\gamma)/\eta$, $J_s(\dot\gamma)/J_s$ and $S^{(1)}(\dot\gamma)/J_s$ vs $\tau_c\dot\gamma$ for a high molecular weight polyethylene[102; 103] with calculated curves determined with $\varphi(t)$ represented by the discrete form $\varphi(t) = \Sigma\varphi_i\exp(-t/\tau_i)$ to reproduce the linear viscoelastic response, and $F_1(\gamma)$ given above is shown in Figure 16;[43] calculation of $J_s(\dot\gamma)$ requires an iterative calculation. Additional examples for a range of polymers are given in reference [43]. As demonstrated in this example, the function $H(\tilde\beta\tau_c\dot\gamma)$ is essentially unity for $\tilde\beta\tau_c\dot\gamma < 1$, and decreases for larger $\tilde\beta\tau_c\dot\gamma$, perhaps reaching a constant value again for $\tau_c\dot\gamma$ too large for the behavior to be represented by this simple model. Similarly, for a sample with a broad distribution of molecular weight, both $S(\tilde\beta\tau_c\dot\gamma)$ and $P(\tilde\beta\tau_c\dot\gamma)$ are predicted to decrease with increasing $\dot\gamma$ for polymers with $P(\tilde\beta\tau_c\dot\gamma) \geq S(\tilde\beta\tau_c\dot\gamma)$, in accord with experiment. By contrast, both $S(\tilde\beta\tau_c\dot\gamma)$ and $P(\tilde\beta\tau_c\dot\gamma)$ are predicted to increase with increasing $\dot\gamma$ for polymers with a narrow distribution of relaxation times, as would be expected with a narrow distribution of molecular weight. An example of data on $\eta(\dot\gamma)/\eta$ and $S^{(1)}(\dot\gamma)/J_s$ vs $\tau_c\dot\gamma$, along with the behavior of $\eta'(\omega)/\eta$ and $J'(\omega)/J_s$ vs $\tau_c\omega$ for solutions of an anionically synthesized polystyrene are shown in Figure 17,[104] showing the increase in $S^{(1)}(\dot\gamma)$ with increasing $\tau_c\dot\gamma$, by contrast with the behavior for a sample with a broad distribution of molecular

weight, and examples for $P(\tilde{\beta}\tau_c\dot{\gamma})$ show qualitatively similar behavior.[43] It should be noted that the general form of these relations is the same for polymers and their concentrated solutions, albeit that the value of τ_c and to a lesser extent $\tilde{\beta}$, will depend on the polymer concentration. In some cases, for polymer solutions of polymera narrow molecular weight τ_c may be small enough that both $H(\tilde{\beta}\tau_c\dot{\gamma})$, $P(\tilde{\beta}\tau_c\dot{\gamma})$ and $S(\tilde{\beta}\tau_c\dot{\gamma})$ are all essentially unity, even though the sample exhibits measurable $N_1(\dot{\gamma}) \propto \dot{\gamma}^2$, with $S^{(1)}(\dot{\gamma}) \approx J_s(\dot{\gamma})$, both independent of $\dot{\gamma}$ over a substantial range of $\dot{\gamma} < 1/\tau_c$. Such systems are sometimes called "Boger fluids".[22f]

With $\varphi(t)$ expressed in terms of a distribution of relaxation times, a close approximation to $\eta(\dot{\gamma})$ with the preceding is given by[18; 43]

$$\eta(\dot{\gamma}) = G_o\sum_1^N \varphi_i\tau_i \frac{1}{[1 + (\tilde{\beta}\dot{\gamma}\tau_i)^{\varepsilon}]^{2/\varepsilon}} \tag{96}$$

with $\varepsilon \approx 6/5$. By comparison, for a linear viscoelastic response for a fluid, as seen above

$$\eta'(\omega) = G_o\sum_1^N \varphi_i\tau_i \frac{1}{1 + (\omega\tau_i)^2} \tag{97}$$

In effect, the factors in the denominators act as a filter in each case, to delete the contributions of successively smaller relaxation times τ_i as ω or $\dot{\gamma}$ increase, and they do this in more-or-less equivalent ways, leading to the Cox-Merz approximation $\eta(\dot{\gamma}) \approx \eta'(\omega=\dot{\gamma})$ (or perhaps better $\eta(\dot{\gamma}) \approx |\eta^*(\omega=\dot{\gamma})|$) proposed long ago.[105] This approximation is likely to improve as the distribution of relaxation time broadens. Similarly, $J_s(\dot{\gamma}) \approx R(t=\omega^{-1})$ for samples with a reasonably broad distribution of relaxation times; $S^{(1)}(\dot{\gamma})/J_s(\dot{\gamma}) \leq 1$,[18; 43] tending toward a ratio of about 0.5 with increasing $\tau_c\dot{\gamma}$, similar to the value of m noted above for a linear elastic solid.

Nonlinear behavior may also be exhibited in transient behavior. For example, maxima are observed in the shear stress $\sigma(t; \dot{\gamma}) = \eta(t; \dot{\gamma})\dot{\gamma}$ and the first-normal stress difference during stress growth $N_1(t; \dot{\gamma})$ at constant shear rate $\dot{\gamma}$,[22g; 102; 104; 106-110] and the recoverable compliance $R(t; \sigma)$ observed after cessation of nonlinear steady flow depends on the steady state stress $\sigma(\dot{\gamma}) = \dot{\gamma}\eta(\dot{\gamma})$

.[43; 103] The maxima in the stress growth tend to occur at a given strain $\gamma_c = \dot{\gamma} t_c$, independent of $\dot{\gamma}$, with the γ_c for the normal stress about twice that for the shear stress difference, e.g., $\gamma_c \approx 2\gamma''$ and $\gamma_c \approx \gamma''$ for normal and shear stresses, respectively.[108] The function $R(t; \sigma)$ is found to be equal to the linear response $R(t)$ for small t, but tends to a steady state limit $J_s(\dot{\gamma})$ that depends on the steady state shear rate $\dot{\gamma}$.[43; 103] These features may be represented reasonably well by the simple function for $F_1(\gamma)$ given above, or by other similar expressions.[102] Some other stress histories are less satisfactorily represented by this simple expression, especially those with multiple reversing steps in the stress.[22g]

Nonlinear behavior with an entirely different origin occurs in some systems exhibiting a yield stress behavior.[24a; 26a] In these systems, the material behaves as a linear viscoelastic solid provided the strain does not exceed some critical value γ°, but exhibits the nonrecoverable deformation of a fluid if the strain exceeds γ°. It is presumed that the intermolecular (or interparticle) interactions responsible for the solid-like behavior rupture under deformation. The most easily interpreted, but most time-consuming, means to determine γ° is to investigate successive creep and recovery cycles with increasing applied stress σ_o until it a nonrecoverable strain is observed. In some cases, the yield will occur with a clear enhancement of the compliance for $\gamma(t) = \gamma^\circ$ during creep in comparison with the behavior for the linear response for smaller strain. An example of this is given if Figure 18 for a thermally reversible gel of a rodlike polymer.[111] In this case, the deformation of the gel for $\gamma(t) < \gamma^\circ$ follows Andrade creep. Moreover, after deformation with $\gamma(t) > \gamma^\circ$, the recoverable strain is given by the formula for a linear viscoelastic deformation. The latter behavior may not be unusual, provided an example of a quasi-linear behavior within an over-all nonlinear response. In many cases, γ° is essentially independent of the applied stress, such that the stress σ° at yield may vary with the rate of deformation, even though γ° is essentially invariant. For example, under a shear deformation at constant shear rate $\dot{\gamma}$, $\sigma(t) = \dot{\gamma}\int_0^t du\, G(u)$ provided $\dot{\gamma} t < \gamma^\circ$, but $\sigma(t)$ will deviate markedly from this response for larger strain. Clearly, in a steady-state deformation, the strain will always exceed γ°, making it difficult or impossible to obtain a reliable estimate for γ° from such experiments. In some cases, the yielding gives an approximately constant stress in steady-state flow over a range of shear rate, providing an approximate estimate for σ°.[24b; 26b] Moreover, the apparent viscosity determined in such a case will differ markedly form $\eta'(\omega = \dot{\gamma})$ obtained with a strain amplitude less than γ°. A plot of the steady-state stress $[\sigma_{ss}(\dot{\gamma})]^{1/2}$ versus $\dot{\gamma}^{1/2}$ is sometimes used to estimate a yield stress as the intercept of a straight line fitted to the data in a so-called Casson plot.[112] However, evaluation of viscoelastic data at still smaller stress

usually will show that such an estimated yield stress is too large, and may even be entirely fallacious, with the material behaving as a viscoelastic liquid to arbitrarily small stress.

A nonlinear behavior with a different origin occurs in measurements of volume properties. The general principles of linear viscoelasticity may be applied to deduce exact relations among the relative rates of creep and relaxation in shear, elongation and volume. Thus,[113]

$$\frac{\partial \ln J(t)/\partial \ln t}{\partial \ln D(t)/\partial \ln t} = 1 + \frac{B(t)}{3J(t)}\left(1 - \frac{\partial \ln B(t)/\partial \ln t}{\partial \ln J(t)/\partial \ln t}\right) \tag{98}$$

with a similar expression for the moduli with J, D and B replaced by G, E and K, respectively. Consequently, if $0 < [\partial \ln B(t)/\partial \ln t]/[\partial \ln J(t)/\partial \ln t] < 1$, the shear compliance changes faster than the elongational compliance. Opposite behavior has been cited in the literature, suggesting a nonlinear behavior, even though the deformation would appear to be small, even recently small.[74; 94] The behavior, which manifests itself in the so-called aging behavior of glasses, is attributed to a nonlinear behavior reflecting a change in the underlying retardation or relaxation times with the volume of the sample.[11i'; 74; 94; 114] Schemes to represent this behavior in approximate ways have been considered by a number of authors.[11i'; 25; 73; 74; 94] In one approach, it is assumed that the expressions for the linear viscoelastic constitutive equation may be adopted if the shift-factor a_V is allowed to vary as the volume of the sample changes, and a time-averaged shift factor is adopted in describing the behavior. Thus, the function $B(t_2 - t_1)$ appearing in expressions for $\Delta V/V$ in terms of the stress history would become[74; 114]

$$B[(t_2 - t_1)\langle a_V^{-1}(t_2,t_1)\rangle] = B_e - (B_e - B_o)\beta[(t_2 - t_1)\langle a_V^{-1}(t_2,t_1)\rangle] \tag{99a}$$

$$\langle a_V^{-1}(t_2,t_1)\rangle = \frac{1}{t_2 - t_1}\int_{t_1}^{t_2} du\, a_V^{-1}(u) \tag{99b}$$

Of course, the linear behavior is recovered if a_V is a constant. Typically, as stated above, $\beta(t)$ would exhibit Andrade creep behavior, with $\beta(t)$ linear in $t^{1/3}$.[74] This nonlinear form is able to represent many aspects of the behavior, but cannot recover some features.[11i'; 74]

8. Strain-induced birefringence for concentrated and undiluted polymeric fluids.

Rheo-optical measurements have long been used in conjunction with rheological measurements. Examples include strain-induced birefringence, optical dichroism and light scattering.[16; 17h; 24c;

27; 97; 99; 115-120] Here only birefringence measurements will be discussed. The increasing availability of commercially available rheo-optical equipment afford enhanced opportunities for the use of birefringence techniques. For an isotropic material, the principal components (proper vectors) n_1, n_2 and n_3 of the refractive index tensor are equal, but this symmetry is usually lost under deformation. Thus, in the shear and elongational deformations discussed above, with deformation in the 1,3-plane (in Cartesian coordinates), the birefringence $\Delta n = n_1 - n_2$ measured by light propagating along x_3 will generally not be zero, and the angle $\chi_n \leq \pi/4$ between n_1 and x_1 will depend on the deformation. The angle χ_n may be visualized by the orientation of the extinction cross of isocline viewed between crossed polars under appropriate optical arrangements. Several effects may contribute to the strain-induced optical anisotropy, including (i) orientation of optically anisotropic chain elements, and (ii) an internal field effect called "form birefringence" arising from spatial variations of the refractive index, as with the anisotropy in a deformed single chain in a dilute solution, or phase separated regimes in a blend, or a semicrystalline polymer.[17i; 27a] Here, consideration is limited to homogeneous amorphous polymers or their concentrated solutions, for which the form birefringence may be neglected. In the simplest case, of interest here, the optical anisotropy of the chain elements is assumed to have ellipsoidal symmetry, with a major axis along the chain axis, so that the optical anisotropy is directly associated with anisotropy of the chain conformation.[16e; 27b; 120] Clearly, that is a major approximation that may not always be valid, and deviations from the behavior anticipated with the simplification may provide insight on the material,[93; 121; 122] see examples cited below.

Optical arrangements for the measurement of Δn and χ_n are amply discussed in the literature,[16f; 27c; 117; 119; 120] and will not be elaborated here. Discussion here is limited to planar samples, with the sample in the 1,3-plane, and deformation along x_1; in shear, the gradient is along x_2, all in Cartesian coordinates. Measurements may be made with a light beam propagating in the 2,3-plane: a birefringence $\Delta n_{1,2}$ and the extinction angle χ_n are determined with a beam propagating along x_3 (i.e., in the sample plane); a birefringence $\Delta n_{1,3}$, but not χ_n, is determined with a light beam propagating along x_2 (i.e., orthogonal to the sample plane); or components of $\Delta n_{1,2}$ and $\Delta n_{1,3}$ and χ_n may be determined with a light beam oriented between x_2 and x_3.[123; 124] In another arrangement, measurements with a light beam along x_1, as along the axis of flow in a tube, give a birefringence $\Delta n_{2,3}$. In some arrangements an average birefringence is obtained, requiring additional analysis (as with a beam along x_3 in flow in a rectangular channel, or with a beam along x_3 in rotating parallel plates).[16f; 119] In the absence of that complication, $\Delta n_{1,2} = n_{11} - n_{22}$, and $\Delta n_{1,3} = n_{11} - n_{33}$, or

$\Delta n_{1,3} \approx (1 - \hat{\psi})\Delta n_{1,2}$ with $\hat{\psi} = -[n_{22} - n_{33}]/[n_{11} - n_{22}]$. For deformation in the 1,3-plane, the optical extinction angle $\chi_n(t)$ and birefringence $\Delta n(t)$ are given by[16f; 27d; 97; 99; 119]

$$\Delta n(t) = [n_{11}(t) - n_{22}(t)]\cos[\chi_n(t)] + 2n_{12}(t)\sin[\chi_n(t)] \quad (100a)$$

$$\cot[\chi_n(t)] = [n_{11}(t) - n_{22}(t)]/2n_{12}(t) \quad (100b)$$

in terms of the components of the refraction tensor. Consequently, $\Delta n(t)\sin[\chi_n(t)] = 2n_{12}(t)$ for a shear deformation along x_1, with $\pi/4 > \chi_n(t) > 0$, and $\Delta n(t) = n_{11}(t) - n_{22}(t)$ for a uniaxial elongation along x_1, with $\chi_n(t) = 0$.

It has been shown by a continuum mechanical argument that for recently small deformations the components n_{ij} of the refractive index tensor in Cartesian coordinates in the linear viscoelastic regime may be expressed by relations similar to the expressions given above, with mechanical compliances and moduli replaced by similarly defined optical compliances and moduli, respectively, denoted by the subscript "n":[99; 118; 125]

$$n_{ij}(t) = \int_{-\infty}^{t} ds\left\{J_n(t-s)\left[\frac{\partial S_{ij}(s)}{\partial s} - \frac{1}{3}\delta_{ij}\frac{\partial S_{\alpha\alpha}(s)}{\partial s}\right] + \delta_{ij}\left[n_o + (2/9)B_n(t-s)\frac{\partial S_{\alpha\alpha}(s)}{\partial s}\right]\right\} \quad (101)$$

$$n_{ij}(t) = \int_{-\infty}^{t} ds\left\{2G_n(t-s)\left[\frac{\partial \varepsilon_{ij}(s)}{\partial s} - \frac{1}{3}\delta_{ij}\frac{\partial \varepsilon_{\alpha\alpha}(s)}{\partial s}\right] + \delta_{ij}\left[n_o + K_n(t-s)\frac{\partial \varepsilon_{\alpha\alpha}(s)}{\partial s}\right]\right\} \quad (102)$$

for stress- and strain-defined histories, respectively, where n_o is the refractive index of the undistorted isotropic material, and $J_n(t)$ is defined by

$$J_n(t) = G_n(0)J(t) + \int_0^t du\, J(t-u)\frac{\partial G_n(u)}{\partial u} \quad (103)$$

with a similar expression for $B_n(t)$ in terms of $B(t)$ and $K_n(t)$. The second form is obtained from the first using the convolution integrals for $J(t)$ in terms of $G(t)$ and $B(t)$ in terms of $K(t)$ given above. That integral may be transformed by differentiation with respect to t to facilitate comparison with the expression for $J_n(t)$:

$$1 = G(0)J(t) + \int_0^t du\, J(t-u)\frac{\partial G(u)}{\partial u} \tag{104}$$

Comparison of these two relations shows that if $G_n(t)/G(t)$ is independent of t, then $J_n(t)$ is a constant, with consequences discussed below. Through an integration by parts, the expressions for the deviatoric components of $n_{ij}(t)$ may be written in the forms

$$\{n_{12}(t)\}_{\text{Deviatoric}} = G_n(0)\varepsilon_{12}(t) + \int_0^\infty du\, \varepsilon_{12}(t-u)\frac{\partial G_n(u)}{\partial u} \tag{105a}$$

$$\{n_{11}(t) - n_{22}(t)\}_{\text{Deviatoric}} = G_n(0)[\varepsilon_{11}(t) - \varepsilon_{22}(t)] + \int_0^\infty du\, [\varepsilon_{11}(t-u) - \varepsilon_{22}(t-u)]\frac{\partial G_n(u)}{\partial u} \tag{105b}$$

for a strain-defined history, and

$$\{n_{12}(t)\}_{\text{Deviatoric}} = J_n(0)S_{12}(t) + \int_0^\infty du\, S_{12}(t-u)\frac{\partial J_n(u)}{\partial u} \tag{106a}$$

$$\{n_{11}(t) - n_{22}(t)\}_{\text{Deviatoric}} = J_n(0)[S_{11}(t) - S_{22}(t)] + \int_0^\infty du\, [S_{11}(t-u) - S_{22}(t-u)]\frac{\partial J_n(u)}{\partial u} \tag{106b}$$

for a stress-defined history. The normal stresses are zero in a shear deformation in this linear approximation, but modifications to this for nonlinear behavior are included below. With these results, it can be seen that validity of the stress-optic approximation $G_n(t)/G(t) = C$ for all t, which requires that $\partial J_n(t)/\partial t = 0$ for all t, means that there be no change in the birefringence during creep. As discussed below, this does not seem reasonable.

In general, the continuum mechanical model cannot provide the relation between the optical functions and their mechanical analogs, e.g., it cannot specify the nature of $G_n(t)/G(t)$, etc. However, for a linear elastic solid, $\partial G_n(t)/\partial t = \partial J_n(t)/\partial t = 0$, and consequently, the preceding reduces to $n_{12}(t) = G_n(0)\varepsilon_{12}(t)$ for the strain-defined history and $n_{12}(t) = J_n(0)S_{12}(t) = G_n(0)J(t)S_{12}(t) = G_n(0)\varepsilon_{12}(t)$ for the stress-defined history, showing the representations to be equivalent for small

strain of an elastic solid, as expected. Similar expressions may be written for $n_{11}(t) - n_{22}(t)$, so that in either case, for an incompressible material, with $C = G_n(0)/G(0)$,[16g; 116]

$$\Delta n = C\tau(\lambda) = (C/D_e)[D_e/D_e(\lambda)]\hat{\varepsilon}_R(\lambda) \quad (107)$$

for a uniaxial elongation with stretch $\lambda = 1 + \varepsilon_{11}$ along x_1 ($\chi = 0$) under a tensile stress $\tau = S_{11} - S_{22}$, and

$$\Delta n \sin[\chi_n(\gamma)] = 2C\sigma(\gamma) = 2(C/J_e)[J_e/J_e(\gamma)]\hat{\gamma}_R(\gamma) \quad (108a)$$

$$\Delta n \cos[\chi_n(\gamma)] = CN_1(\gamma) \quad (108b)$$

$$\cot[\chi_n(\gamma)] = N_1(\gamma)/2\sigma(\gamma) = m\hat{\gamma}_R(\gamma) \quad (108c)$$

for a shear strain $\gamma = 2\varepsilon_{12}$ with deformation along x_1 under a shear stress $\sigma = S_{12}$, with gradient along x_2. Here $\hat{\gamma}_R(\gamma) = J_e(\gamma)\sigma(\gamma)$ and $\hat{\varepsilon}_R(\lambda) = D_e(\lambda)\tau(\lambda)$, are the strains that would be recovered on removal of the stress, and $mJ_e(\gamma) = N_1(\gamma)/2\sigma(\gamma)^2$. These relations, correspond to the use a generalized constitutive relation incorporating the strain tensor **Q** given above in the section on nonlinear behavior to encompass nonlinear behavior, such as a nonzero $N_1(\gamma)$ in shear. Here, $G_e = G_o$, $J_e = J_o$, $J_e(\gamma)/J_e = D_e(\gamma)/D_e = 1$ and $\sin(2\chi_n) \approx 1$ for the linear elastic response for a small strain, which emphasizing the relation of the birefringence to the recoverable strain in that case. In the final expression for $\cot[\chi_n(\gamma)]$, m and $J_e(\gamma)/J_e$ depend on the constitutive equation for the elastic solid. For example, $J_e(\gamma)/J_e = 1$ and $m = C_1/2(C_1 + C_2)$ for the Mooney-Rivlin network model (see above), and m = 1/2 for an ideal rubber network for which $C_2 = 0$,[3b] showing that the linear elastic expressions may be applied with equivalent results for either a stress- or strain-defined shear deformation for this model. By contrast, since $D_e(\lambda)/D_e = \tau(\lambda)/(\lambda - 1)$ depends on λ for the Mooney-Rivlin model, the linear elastic expression in terms of $\hat{\varepsilon}_R$ would not apply to the nonlinear response using the approximation $D_e(\lambda)/D_e = 1$ obtaining in the linear response. These relations have been applied to interpret the birefringence under nonlinear deformations.[16g]

It has been shown that the steady-state response to a small amplitude oscillatory shear deformation may be expressed in forms similar to those given above for the mechanical response:[99; 125]

$$n_{12}(t) = \gamma_o\{G_n'(\omega)\sin(\omega t) + G_n''(\omega)\cos(\omega t)\} \quad (109)$$

$$n_{12}(t) = \sigma_o\{J_n'(\omega)\sin(\omega t) - J_n''(\omega)\cos(\omega t)\} \quad (110)$$

for the strain- and stress-defined experiments, respectively, where $G_n'(\omega)$ is defined in terms of $G_n(t)$ in a way analogous to the relation between $G'(\omega)$ and $G(t)$, etc. If it is assumed that $G_n(t)/G(t) = C$ for all t, then $G_n'(\omega) = CG'(\omega)$ and $G_n''(\omega) = CG''(\omega)$ for the stress-defined history. Dynamic birefringence measurements in the 1,2-plane with small γ_o appear to be in accord with the stress-optic approximation over limited ranges in ω near the "terminal response" for which $G_n'(\omega) \propto G'(\omega) \propto \omega^2$ and $G_n''(\omega) \propto G''(\omega) \propto \omega$.[100] Dynamic measurements of $\Delta n_{1,3}(t)$ in the 1,3-plane with small γ_o, for which $\Delta n_{1,3}(t) = C(1 - \hat{\psi})N_1(t)$ with $N_1(t)$ given by the expression for nonlinear normal stress in oscillatory shear deformation discussed above using the strain tensor $\mathbf{Q}^{\mathbf{o}}$, have been used to estimate $\hat{\beta}$ on the basis that $\hat{\psi} = \hat{\beta}$, as expected with the stress-optic approximation.[100] Nevertheless, the stress-optic approximation is known to be inadequate in some situations, especially for the response at a temperature close to the glass temperature. For example, in the latter case, the birefringence has been observed to change sign, inconsistent with the approximation $G_n(t)/G(t) = C$ for all t.[93; 126] This behavior may be attributed to the substantially different mechanisms of deformation in the Andrade behavior sampled at higher $\omega\tau_c$, and the Rouse or entanglement behavior that may dominate at lower $\omega\tau_c$.[126; 127] The behavior for a strain-defined history is discussed below, but it should be noted that if $G_n(t)/G(t) = C$ for all t as assumed above, then $J_n(t)$ is a constant, and the birefringence would simply oscillate in phase with the strain. The apparent success of the stress-optic approximation for the response to a oscillatory strain does not necessarily mean that $G_n(t)/G(t)$ is independent of t for all t, or even accurately so for large t, corresponding to the regime for which it appears that $G_n'(\omega) \propto G'(\omega) \propto \omega^2$ and $G_n''(\omega) \propto G''(\omega) \propto \omega$; all that is required is that $t^2G_n(t)$ and $t^2G(t)$ each approach zero with increasing t to obtain the behavior at small ω.[99]

Transient strain-induced birefringence has received less attention. As mentioned above, neither of the extreme requirements for a stress-optic approximation with $G_n(t)/G(t)$ a constant in a strain-defined history, or a strain-optic approximation with $J_n(t)/J(t)$ a constant in a stress-defined history appear to be reasonable. Further, as remarked above, it would not be surprising to find different optical response in the different regimes of the retardation spectrum for the mechanical response,

even if the birefringence from a particular regime could be simply treated. Nevertheless, in the following some consequences of the assumption that $G_n(t)/G(t)$ for all t in strain-defined experiments are surveyed, along with a suggested approximation for stress-defined histories.

Turning first to strain-defined histories under the approximation $G_n(t)/G(t) = C$ for all t for recently small deformations, the expression for the deviatoric components of the refractive index tensor given above reads,

$$\{n_{ij}(t)\}_{\text{Deviatoric}} = 2C\int_0^t ds G(t-s)\left[\frac{\partial \varepsilon_{ij}(s)}{\partial s} - \frac{1}{3}\delta_{ij}\frac{\partial \varepsilon_{\alpha\alpha}(s)}{\partial s}\right] \tag{111}$$

for a sample relaxed for $t < 0$. Thus, for an elongational deformation ($\chi_n = 0$) of an incompressible viscoelastic solid under a strain-defined history resulting in a transient stress $\tau(t) = S_{11}(t) - S_{22}(t)$ and transient strain $\varepsilon(t) = \varepsilon_{11}(t)$ for deformation along x_1,

$$\Delta n(t) = C\tau(t) = 3C\int_0^t du\, G(t-u)\frac{\partial \varepsilon(u)}{\partial u} \tag{112}$$

Similarly, for a recently small shear deformation to obtain a linear viscoelastic response, $\Delta n(t) = 2n_{12}(t)\sin[\chi_n(t)]$, so that since in this case $\sin[2\chi_n(t)] \approx 1$, the preceding gives

$$\Delta n(t) = 2C\sigma(t) = 2C\int_0^t du\, G(t-u)\frac{\partial \gamma(u)}{\partial u} \tag{113}$$

for a strain-defined history. For stress relaxation following a small step-strain γ_o,

$$\Delta n(t) = 2C\gamma_o G(t) \tag{114}$$

For a slow shear flow at shear rate $\dot{\gamma}$, such that $\tau_c\dot{\gamma} << 1$,

$$\Delta n(t) = 2C\dot{\gamma}\int_0^t du\, G(u) \tag{115}$$

so that the steady-state flow birefringence Δn is given by

$$\Delta n = 2C\dot\gamma \int_0^\infty du\, G(u) = 2C\eta\dot\gamma = 2(C/J_s)\hat\gamma_R(\dot\gamma) \qquad (116)$$

as expected, with $\hat\gamma_R(\dot\gamma)$ the total strain recoil on cessation of flow.

An important use of strain-induced birefringence measurements is in the estimation of the first-normal stress difference $N_1(t)$ in a transient response in a strongly nonlinear response. Neither $N_1(t; \gamma_o)$ in relaxation following a step-strain γ_o nor $N_1(t; \dot\gamma)$ in shear deformation in nonlinear flows at a constant shear rate are trivial to measure mechanically. For example, although $N_1(t; \dot\gamma)$ may be determined from the force required to prevent separation of a cone and plate during a shear deformation, the slight movement unavoidable in the feedback mechanism to produce a measure of the required force may complicate the interpretation of the transient response.[128] The error should be less serious in a steady flow.

Although normal stresses are absent in shear deformation with the preceding model, as noted above, a first-normal stress N_1 does appear with use of the strain tensor $\mathbf{Q_o}$, with several predicted results given above. Assumption of a similar form may be adopted in the expressions given above introduces normal stresses in the refractive index tensor. For example during stress relaxation following a step strain γ_o,

$$\Delta n \sin[2\chi_n((t, \gamma_o))] = 2C\sigma(t; \gamma_o) = 2C\gamma_o G(t) \qquad (117a)$$

$$\Delta n \cos[2\chi_n((t, \gamma_o))] = CN_1(t; \gamma_o) = C\gamma_o^2 G(t) \qquad (117b)$$

$$\cot[2\chi_n((t, \gamma_o))] = N_1(t, \gamma_o)/2\sigma(t; \gamma_o) = \gamma_o/2 \qquad (117c)$$

for the 1,2-plane. Similarly, in the transient response for deformation at constant shear rate $\dot\gamma$,

$$\Delta n \sin[2\chi_n(t, \dot\gamma)] = 2C\sigma(t, \dot\gamma) = 2C\dot\gamma \int_0^t du\, G(u) \qquad (118a)$$

$$\Delta n \cos[2\chi_n(t, \dot\gamma)] = CN_1(t, \dot\gamma) = C\dot\gamma^2 \int_0^t du\, uG(u) \qquad (118b)$$

$$\cot[2\chi_n(t, \dot\gamma)] = N_1(t, \dot\gamma)/2\sigma(t; \dot\gamma) = \dot\gamma\int_0^t du\, uG(u)/2\int_0^t du\, G(u) \qquad (118c)$$

so that in steady-state flow at shear rate $\dot\gamma$ and shear stress $\sigma(\dot\gamma) = \dot\gamma\eta(\dot\gamma)$:

$$\Delta n \sin[2\chi_n(\dot\gamma)] = 2C\sigma(\dot\gamma) = 2(C/J_s)\hat\gamma_R(\dot\gamma) \quad (119a)$$

$$\Delta n \cos[2\chi_n(\dot\gamma)] = CN_1(\dot\gamma) = CS^{(1)}(\dot\gamma)2\sigma(\dot\gamma)^2 = 2(C/J_s)\hat\gamma_R(\dot\gamma)^2 \quad (119b)$$

$$\cot[2\chi_n(\dot\gamma)] = S^{(1)}(\dot\gamma)\sigma(\dot\gamma) = \hat\gamma_R(\dot\gamma) \quad (119c)$$

for the 1,2-plane, where in this regime, $S^{(1)}(\dot\gamma) = N_1(\dot\gamma)/2\sigma(\dot\gamma)^2 \approx J_s(\dot\gamma) \approx J_s$, and the $\hat\gamma_R(\dot\gamma)$ is the total recoverable strain following cessation of the slow steady shear flow is given by $\hat\gamma_R(\dot\gamma) \approx J_s\sigma(\dot\gamma)$. Based on the preceding, the birefringence in steady-state slow flow at shear rate $\dot\gamma$, for which $\sin[2\chi_n(\dot\gamma)] \approx 1$, is given by $\Delta n_{1,3}(\dot\gamma) = C(1 - \hat\psi)N_1(\dot\gamma) \approx 2(C/J_s)(1 - \hat\beta)(\tau_c\dot\gamma)^2$ for shear in the 1,3-flow plane, or $\cot[2\chi_n(\dot\gamma)] \approx \tau_c\dot\gamma = \gamma_R(\dot\gamma)$ in the 1,2-flow plane. These expressions, which appear to be in accord with experiment in this response range,[16; 27e; 119] make use of the relation $J_s = N_1/2\sigma^2$, which is obtained under rather general considerations for in a steady slow flow,[98] and further emphasizes the direct connection between the birefringence behavior and the total recoverable strain $\gamma_R(\dot\gamma)$.

Birefringence measurements are often of interest in steady-state flow for a nonlinear response for which the use of $\mathbf{Q_o}$ is inadequate. For example, the stress-optic relation given above has been invoked to estimate $N_1(\dot\gamma)$ in nonlinear steady-state shear flow ($\tau_c\dot\gamma > 1$), with apparent success.[16; 27; 109; 110] Following the examples given above, the use the strain tensor $\mathbf{Q}$ to encompass nonlinear behavior in the response to a step-strain γ_o in the 1,2-plane gives

$$\Delta n \sin[2\chi_n(t; \gamma_o)] = 2C\sigma(t; \gamma_o) = 2C\gamma_o F(\gamma_o)G(t) \quad (120a)$$

$$\Delta n \cos[2\chi_n(t; \gamma_o)] = CN_1(t; \gamma_o) = C\gamma_o^2 F(\gamma_o)G(t) \quad (120b)$$

$$\cot[2\chi_n(t; \gamma_o)] = N_1(t; \gamma_o)/2\sigma(t; \gamma_o) = \gamma_o/2 \quad (120c)$$

for the 1,2-plane, in accord with data on some polymeric fluids.[129; 130] Similarly, for a shear deformation in steady-state flow,

$$\Delta n \sin[2\chi_n(t; \dot\gamma)] = 2C\sigma(t; \dot\gamma) \quad (121a)$$

$$\Delta n \cos[2\chi_n(t; \dot\gamma)] = CN_1(t; \dot\gamma) \quad (121b)$$

$$\cot[2\chi_n(t; \dot\gamma)] = N_1(t; \dot\gamma)/2\sigma(t; \dot\gamma) = S^{(1)}(t; \dot\gamma)\sigma(t; \dot\gamma) \quad (121c)$$

for the 1,2-plane, with $\sigma(t; \dot\gamma)$ and $N_1(t; \dot\gamma)$ computed as discussed in the section on nonlinear viscoelasticity, $\chi_n(t; \dot\gamma) \le \pi/4$ decreases with increasing $\dot\gamma$, and $S^{(1)}(t; \dot\gamma) = N_1(t; \dot\gamma)/2[\sigma(t; \dot\gamma)]^2$. Similarly, $\Delta n_{1,3}(t; \dot\gamma) = C(1 - \hat\psi)N_1(t; \dot\gamma)$ in the 1,3-flow plane in this approximation if it is assumed that $\hat\psi$ is independent of t and $\dot\gamma$. At steady-state flow, these relations become

$$\Delta n \sin[2\chi_n(\dot\gamma)] = 2C\sigma(\dot\gamma) = 2(C/J_s)[J_s/J_s(\dot\gamma)]\hat\gamma_R(\dot\gamma) \quad (122a)$$

$$\Delta n \cos[2\chi_n(\dot\gamma)] = CN_1(\dot\gamma) = 2(C/J_s)[S^{(1)}(\dot\gamma)/J_s(\dot\gamma)][J_s/J_s(\dot\gamma)]\hat\gamma_R(\dot\gamma)^2 \quad (122b)$$

$$\cot[2\chi_n(\dot\gamma)] = S^{(1)}(\dot\gamma)\sigma(\dot\gamma) = [S^{(1)}(\dot\gamma)/J_s(\dot\gamma)]\hat\gamma_R(\dot\gamma) \quad (122c)$$

where $\sigma(\dot\gamma) = \dot\gamma\eta(\dot\gamma)$, $\hat\gamma_R(\dot\gamma) = J_s(\dot\gamma)\dot\gamma\eta(\dot\gamma)$ is the total recoverable strain following cessation of steady-state flow. Similarly, $\Delta n_{1,3}(\dot\gamma) = C(1 - \hat\psi)N_1(\dot\gamma)$ in the 1,3-flow plane if it is assumed that $\hat\psi$ is independent of $\dot\gamma$. The final forms emphasize the relation of the birefringence to the constrained recoil $\hat\gamma_R(\dot\gamma)$ on cessation of flow, and are analogous to the relations given above for an elastic solid (i.e., replace $\dot\gamma$ by γ, J_s by J_e and $S^{(1)}(\dot\gamma)/J_s(\dot\gamma)$ by m). As discussed in the previous section, $S^{(1)}(\dot\gamma)/J_S(\dot\gamma)$ depends on the distribution of components (e.g., the molecular weight distribution), where $S^{(1)}(\dot\gamma)/J_S(\dot\gamma) \le 1$, with the equality occurring for flows of monodisperse polymer with $\tau_c\dot\gamma < 1$. The analogy with the behavior for a linear elastic solid is strengthened by noting that $S^{(1)}(\dot\gamma)/J_s(\dot\gamma)$ tends toward 0.5 with increasing $\tau_c\dot\gamma$, similar to the value of m noted above for a linear elastic solid, as remarked above. Estimates of $N_1(t; \dot\gamma)$ made in this way appear to be similar to those obtained by direct mechanical measurements.[106; 107; 109; 110] This correspondence could reflect the marked weighting of the response toward the longer time response in $G_n(t)$, and may not provide definitive evidence for constant $G_n(t)/G(t)$ for all t. In part, the use of the stress-optic approximation here is motivated by statistical mechanical theories which suggest that Δn and ΔS depend on similar averages over chain conformations for flexible chain polymers,[16h; 22h; 27b; 120] but the similarity with the expression for an elastic solid given above is evident, and is not accidental since the theories in both cases are based on additivity of incremental stresses attributed to molecular deformations, similar to the treatment of a collection of macroscopic beads and dashpots.[22h]

Relations comparable to the preceding do not appear to be available for a stress-defined history. Moreover, there are few data to evaluate the nature of $J_n(t)$, a situation that may change with the availability of commercial rheo-optical instrumentation to permit the implementation of stress-

defined histories. The lack of experimental and theoretical attention may reflect both the lack of commercially available equipment to study the transient response with a stress-defined shear deformation and the perception that $J_n(t)$ is a constant, as required by the stress optic approximation with constant $G_n(t)/G(t)$, in which case birefringence measurements for a stress-defined history would be relatively uninteresting. However, as remarked in the preceding, the evidence that $G_n(t)/G(t)$ must be considered to be independent of t is not definitive. For example, $G_n(t)$ could relax more slowly than G(t) for large t, but still decay fast enough to give the response $G_n'(\omega) \propto \omega^2$ and $G_n''(\omega) \propto \omega$ reported experimentally for small ω.[100] In addition, as may be seen in the expression for $J_n(t)$, deviation of $G_n(t)/G(t)$ from a constant for small t will have an impact on $J_n(t)$ at large t. As mentioned above, birefringence measurements are sometimes made on amorphous materials near T_g, with the finding that a single constant C cannot be applied over the entire range of ω at a given T.[126; 127] This result is readily accommodated in terms of a distribution of retardation times to represent $\alpha(t)$, with the response corresponding to an Andrade creep region having a different value of C than that associated with the portion of the retardation times associated with the Rouse-like or entanglement responses.

Given the uncertain status of the stress-optic approximation, it is of interest to consider the consequences of a strain-optic approximation for use with stress-defined experiments. Since the birefringence is a constant in steady-state flow, it is apparent that $J_n(t)$ must not have the term proportional to t found in J(t), even if $J_n(t)$ is not a constant as required by the stress-optic approximation. Further, the preceding provides a clear relationship between the birefringence and the recoverable strain for an elastic solid under a small deformation and a fluid in a slow steady-state flow. For lack of a definitive treatment, it will be assumed that these features are preserved in a transient deformation, and that the birefringence at arbitrary time is related to the total constrained recoil that would be recovered if the stress were suddenly reduced to zero at that time; the calculation of this following an arbitrary stress history is discussed above in the section on creep and recovery in the section on linear viscoelastic phenomenology. Thus, for recently small deformations on an incompressible sample relaxed at the beginning of the deformation, such that the linear viscoelastic response functions may be used, it is presumed that $J_n(t) = (C/J_\infty)R(t)$, and that the deviatoric components of the refraction tensor are given by,

$$\{n_{ij}(t)\}_{\text{Deviatoric}} = (C/J_\infty)\int_0^t ds\, R(t-s)\left[\frac{\partial S_{ij}(s)}{\partial s} - \frac{1}{3}\delta_{ij}\frac{\partial S_{\alpha\alpha}(s)}{\partial s}\right] \qquad (123)$$

Consequently, for elongational or shear deformations, with total recoverable strains $\hat{\varepsilon}_R(t)$ and $\hat{\gamma}_R(t)$, respectively,

$$\Delta n(t) = (C/D_\infty)\hat{\varepsilon}_R(t) = (C/3D_\infty)\int_0^t du\, R(t-u)\frac{\partial \tau(u)}{\partial u} \tag{124a}$$

$$\Delta n(t) = 2(C/J_\infty)\hat{\gamma}_R(t) = 2(C/J_\infty)\int_0^t du\, R(t-u)\frac{\partial \sigma(u)}{\partial u} \tag{124b}$$

For example, for a step stress σ_o initiated at zero time, and terminated at time T_e on a linear viscoelastic fluid

$$\Delta n(t) = 2(C/J_s)\sigma_o\int_0^t du\, R(t-u)\,\delta(u-0) = 2(C/J_s)R(t)\sigma_o \tag{125}$$

At a time ϑ following the onset of constrained recoil after creep terminated at time $t = T_e$,

$$\Delta n(\vartheta) = 2(C/J_s)\{\hat{\gamma}_R(T_e) - \hat{\gamma}_R(\vartheta)\} \tag{126a}$$

$$= 2(C/J_s)\{R(\vartheta + T_e) - R(\vartheta)\}\sigma_o \tag{126b}$$

Strict application of the stress-optic approximation would make Δn independent of time by contrast with these expressions, but data to evaluate these alternatives do not seem to be available. In an alternative deformation history, the total recoverable strain $\hat{\gamma}_R(T_e, \gamma_o)$ that would be measured if the stress were dropped to zero at time T_e during stress relaxation of a fluid following a jump γ_o in the strain is given above by $\hat{\gamma}_R(T_e, \gamma_o) = \gamma_o[1 - \eta^{-1}\int_0^{T_e} ds\, G(s)]$. With this expression, $\Delta n(t) \approx 2(C/J_s)\hat{\gamma}_R(t,\gamma_o)$ is not equal to the relation $\Delta n(t) \approx 2CG(t)$ given above using the stress-optic approximation, unless G(t) is given by an exponential function, in which case R(t) is a constant, as would be consistent with the stress-optic approximation.

A few studies are available for a step stress τ_o initiated at zero time, and terminated at time T_e on a linear viscoelastic solid, for which $D(t) \approx R(t)/3$,

$$\Delta n(t) = (C/D_e)\tau_o D(t) \qquad 0 < t < T_e \qquad (127a)$$

$$\Delta n(\vartheta) = (C/D_e)\tau_o [D(\vartheta + T_e) - D(\vartheta)] \qquad t \geq T_e \qquad (127b)$$

where $\vartheta = t - T_e$. Thus, if T_e is large enough that D(t) approaches its equilibrium value D_e during creep, then $\Delta n(\vartheta)/C\tau_o = D_e - D(\vartheta)$ during recovery ($t \geq T_e$). A recent study on a loosely crosslinked rubber may illustrate the delicacy of birefringence measurements.[131] Whereas the data on the strain in creep and recovery appear qualitatively normal, the birefringence was observed to be positive in creep, and negative in recovery. The numerous dangling chains (chains attached only once to the network) may provide an explanation for this unexpected behavior if these chains relaxed during creep, and were subsequently oriented orthogonal to the stretch direction during the relatively large initial recovery, so that Δn was subsequently negative during recovery for $t > T_e$. This would provide an example of the failure of the initial assumption concerning the origin of the birefringence introduced above.

Application of this approximation to a steady oscillatory with a small amplitude stress-defined deformation would give a result with $J_n'(\omega) = (C/J_s)J'(\omega)$ and $J_n''(\omega) = (C/J_s)[J''(\omega) - (1/\omega\eta)]$, reflecting the absence of a term involving η in the form assumed for $J_n(t)$. Experimental assessment of this feature does not appear to be available; most (all?) of the available data on fluids in an oscillatory deformation use a strain-defined history. Since $J_n^*(\omega) = G_n^*(\omega)J^*(\omega)$ according to the relations given above,[99; 132] it follows that

$$J_n'(\omega) = G_n'(\omega)J'(\omega) + G_n''(\omega)J''(\omega) \qquad (128a)$$

$$J_n''(\omega) = G_n'(\omega)J''(\omega) - G_n''(\omega)J'(\omega) \qquad (128b)$$

Consequently, the reported responses $G_n'(\omega) \propto \omega^2$ and $G_n''(\omega) \propto \omega$ for small ω give $J_n'(\omega) \propto$ constant and $J_n''(\omega) \propto \omega$ for small ω, consistent with the result obtained with the $J_n(t)$ postulated above for a viscoelastic fluid. However, inspection shows that if $G_n'(\omega)/G'(\omega) = G_n''(\omega)/G''(\omega) = C$, for small ω, then $J_n''(\omega)$ is zero and $J_n'(\omega)$ is a constant in that same limit, so that the birefringence is predicted to be exactly in phase with the oscillating stress. These extremes should be relatively easy to assess.

Application to nonlinear deformations is less readily evaluated. Steady-state shear flow reached by a stress or strain defined histories must be equivalent. As seen in the preceding, in such a case

$\cot[2\chi_n(\dot\gamma)] = [S^{(1)}(\dot\gamma)/J_s(\dot\gamma)]\hat\gamma_R(\dot\gamma)$, with $S^{(1)}(\dot\gamma)/J_s(\dot\gamma) \approx 1$ if the flow deformation may be characterized by use of $\mathbf{Q_o}$. The function $\cot[2\chi_n(t; \sigma_o)]$ in linear or nonlinear creep under a step-stress σ_o must approach this behavior in steady-state flow. Thus, using the constrained recoil $\hat\gamma_R(t; \sigma_o)$ on removal of the stress at time t, one might expect that

$$\cot[2\chi_n(t; \sigma_o)] \quad = \quad \Phi(t; \sigma_o)\hat\gamma_R(t; \sigma_o) \tag{129}$$

where $\eta(t; \dot\gamma) = \sigma(t; \dot\gamma)/\dot\gamma$, $R(t; \sigma_o) = \hat\gamma_R(t; \sigma_o)/\sigma_o$, and $\Phi(t; \sigma_o) = S^{(1)}(t; \sigma_o)/R(t; \sigma_o)$. Presumably, $\Phi(t; \sigma_o)$ will vary from about unity for small t, since then the strain must be recently small, to its limiting value of about 0.5 in steady-state nonlinear flow. In principle, $\Phi(t; \sigma_o)$ could be estimated by an interative calculation involving the relations given in the section on nonlinear rheological behavior, as has been done for $J_s(\dot\gamma)$.[43]

In summary, it appears that the stress-optic approximation, embodied in the expression $G_n(t)/G(t) \approx C$ for all t, may sometimes be used for strain-defined deformations to estimate the first-normal stress and the shear stress in a shear deformation, and the tensile stress in an elongational deformation, although it is clear that the approximation is not always valid, especially for deformation involving the short-time features of the response, e.g., the transition from the Andrade creep to the Rouse-like response in the retardation spectrum. The experimental situation is not clear for stress-defined deformations, with strict compliance with the relation $G_n(t)/G(t) \approx C$ requiring that $J_n(t)$ be independent of time. An alternative approximation may be to put $J_n(t)/R(t) \approx C/J_\infty$ in a strain-optic approximation, with neither the stress-optic or strain-optic relations expected to be exact.

9. Linear and nonlinear viscoelastic behavior of colloidal dispersions.

The viscoelastic behavior of colloidal dispersions is an enormous topic, the subject of numerous reviews and monographs,[54; 70; 133] and one that can only receive incomplete discussion here. The interactions among colloidally dispersed particles can involve diverse phenomena, including dispersion forces, electrostatic interactions, interactions with dissolved polymeric components, interactions mediated by adsorbed surfactants, etc.[54b,c,d; 70] In many, perhaps most, cases there is a tendency for cluster formation among the colloidal particles, leading to complex behavior, including yield phenomena in which the material may be considered to be a solid provided the strain is small, but will flow if the strain is increased beyond some value γ°, similar to the behavior discussed above for certain polymeric systems.

The simplest behavior, that of dilute dispersion of spheres interacting only through a hard-core potential, was discussed above in terms of a virial expansion for the viscosity, rewritten here in a form to emphasize the dependence on the volume fraction φ of spheres:

$$\eta = \eta_{LOC}^{(c)}\{1 + (5/2)\varphi + k'(5/2)^2\varphi^2 + \ldots\} \quad (130)$$

where $(5/2)\varphi = [\eta]c$, and it is usually assumed that $\eta_{LOC}^{(c)} \approx \eta_{solv}$.[15a; 54a; 70] As noted above, $k' \approx 1.0$ for this model, and as usual, the virial expansion is inadequate with increasing concentration. A number of expressions have been developed to approximate η as φ is increased toward the maximum value φ_{max} possible with hard-core spheres. Several general approximate forms designed to approximate the behavior exactly for dilute suspensions, and approximate the rapid increase in η as φ approaches φ_{max},[15c; 54e; 70; 133] The simple expressions

$$\eta \approx \eta_{LOC}^{(c)}\{1 - \varphi/n_1\}^{-5n_1/2} \quad (131)$$

$$\eta \approx \eta_{LOC}^{(c)}\{1 - (5/2)\varphi[1 - \varphi/n_2]^{-5n_2k'/2}\} \quad (132)$$

are designed to force agreement with the virial expansion at least to order φ and φ^2, respectively, where n_1 and n_2 are a constant and again, it is usual to assume that $\eta_{LOC}^{(c)} \approx \eta_{solv}$. The second expression will be recognized to involve a variation of the relation $[\eta]^{(c)} \approx [\eta]\{1 + [\eta]c\}^{k'}$ introduced above in the discussion of the viscosity of dilute solutions of polymers. An application of the first expression puts $n_1 = \varphi_{max}$;[70; 133] the value of $n_1 = 5/8$ would be required to give $k' \approx 1.0$, which is close to the estimate $\varphi \approx 0.64$ for spontaneous ordering of the spheres in this model.[134] It is noteworthy that η does not depend on the sphere radius R in these expressions, but only on the volume fraction of spheres.

Certain theoretical treatments may be put in the form

$$\eta = \eta_{LOC}^{(c)}\{1 + (5/2)\varphi + k'[\psi_1(\varphi) + \psi_2(\varphi)](5/2)^2\varphi^2\} \quad (133)$$

where it is assumed that $\eta_{LOC}^{(c)} \approx \eta_{solv}$. The functions $\psi_1(\varphi)$ and $\psi_2(\varphi)$, reflecting hydrodynamic and thermodynamic effects, respectively, depend on the form of the particle interaction potential; $\psi_1(0) + \psi_2(0) = 1$, and both $\psi_1(\varphi)$ and $\psi_2(\varphi)$ increase with increasing φ.[54f; 70; 134-139] Experimental

data for η from slow steady flow and $\eta = \eta'(0)$ from small strain amplitude dynamic measurements for dispersions of spheres over a range of R from different investigators in Figure 19 for systems artfully designed to behave as hard spheres demonstrate the dependence of η on φ.[135; 137; 140] The solid curve is calculated with the semi-empirical expressions $\psi_1(\varphi) \approx (4/5)(1 - \varphi/\varphi_{max})$ and $\psi_2(\varphi) \approx (1/5)(1 - \varphi/\varphi_{max})^2$, based on more complex theoretical expressions.[134; 136; 138; 139; 141; 142] The semi-empirical expression provides a reasonable representation is given over the entire range of φ by the empirical relations, as would the second of the empirical relation above with $n_2 = 0.605$. The situation is more complex with nonspherical particles, with the possibility of producing ordered phases with plate or rod shaped particles, even with the simple hard-core interaction.[143] In any case, η will involve a measure of the particle shape, such as the L/d ratio for a rod, or the ratio of the principal axes for spheroids of revolution.[68]

Linear viscoelastic behavior has been predicted and observed for dispersions of rigid spheres.[54f; 134-139; 142] Experimental data on dispersions designed exhibit the behavior of hard spheres are shown in Figure 20;[137] similar data are available over a range of particle size in reference [137] as well as from other investigators.[135; 144] The data for several temperatures have been superposed, assuming that $b(T, T_{REF}) = 1$. The data on $\eta'(\omega)$ exhibit a limiting value $\eta'(0)$ for small ω, as expected, but also show a plateau $\eta'(\omega_L)$ for a regime at an intermediate range of $\omega \approx \omega_L$, before decreasing to zero with increasing ω, beyond the range of ω usually accessible. Since only the frequency range $\omega \leq \omega_L$ is of usual interest, the models lump the effects at high ω (say, $\omega > 1/\tau_1$) into an additive term $(G_o - G_1)\delta(t)$ to G(t), as discussed in the first section, so that $\eta'(\omega_L) \approx (G_o - G_1)\tau_1$. Since J'($\omega$) would tend to a constant for small ω, but would decrease with increasing ω for larger ω, reflecting the term $(G_o - G_1)\delta(t)/\tau_1$ in G(t), it is convenient to remove the latter by use of $G''_{EFF}(\omega) = \omega[\eta'(\omega) - \eta'(\omega_L)]$ instead of G"(ω) to compute a $J'_{EFF}(\omega)$ from the reported moduli to suppress the response for $\omega > \omega_L$. The data in Figure 20 show that $J'_{EFF}(\omega)$ decreases with increasing ω, to reach a plateau $J'_{EFF}(\omega_L) \approx 1/G'(\omega_L) \approx 1/G_1$ for ω in the regime for which $\eta'(\omega) \approx \eta'(\omega_L)$. The theoretical expression given above for η is taken to estimate $\eta'(0) = \eta$, and it is assumed that $\eta'(\omega_L)$ is given by the theoretical relation for η, with $\psi_2(\varphi) = 0$, reflecting the suppression of thermodynamic interactions at high ω; comparison with experimental data in Figure 19 shows this to be reasonably accurate. For most models, $J'_{EFF}(\omega_L) \approx 1/G'(\omega_L) \approx 1/G_1$ is expected to vary markedly with φ, with $G_1R^3/kT\varphi^2 \approx \psi_0(\varphi)$ for spheres of radius R. The expression $\psi_0(\varphi) \approx 0.78(\eta'(\omega_L)/\eta_{solv})g(2, \varphi)$ given by an approximate model[138] is in reasonable accord with numerical results from a more rigorous treatment, where $g(2, \varphi)$ is the value of the radial distribution

$g(r/R, \varphi)$ at the contact condition $r/R = 2$; $g(2, \varphi) = (1 - \varphi/2)^2/(1 - \varphi)^3$ for $\varphi < 0.5$ and $g(2, \varphi) = (6/5)(1 - \varphi/\varphi_{max})$ for $\varphi \geq 0.5$.[136-138] These expressions are compared with experimental data on dispersions of spherical particles in Figure 19,[137] revealing reasonable agreement with the theoretical model. Theoretical models predict a region of the response which would have $J'_{EFF}(\omega) \propto \omega^{-1/2}$;[136; 138] as shown in Figure 20, experimental data are consistent with this, even though the agreement is not definitive.

The nonlinear steady-state viscosity of dispersions of spherical particles is frequently characterized by a plateau $\eta_{plateau}(\dot{\gamma})$ over a range of shear rate with $\dot{\gamma} \approx \omega_L$.[54e; 70; 133] It has been suggested that $\eta_{plateau}(\dot{\gamma}) \approx \eta'(\omega_L)$, reflecting suppression of the same contributions to $\eta(\dot{\gamma})$ that are lost in $\eta'(\omega)$ for $\omega \approx \omega_L$.[54f; 134]. Comparison of $\eta(\dot{\gamma}) \approx \eta'(\omega = \dot{\gamma})$ shows that the approximation is qualitatively useful, but not fully accurate.[144] The behavior is similar to the Cox-Merz approximation $\eta(\dot{\gamma}) \approx \eta'(\omega = \dot{\gamma})$ discussed above, but the paucity of relaxation times may play a role in rendering the approximation less accurate than sometimes found with polymers, which display a relative an abundance of relaxation times.

The effect of more specific or long-range interparticle interactions can substantially modify the behavior described above. For example, charged spheres dispersed in a solvent with a very low ionic strength may form an ordered phase, with the spheres tending to lie on a lattice through the effects of electrostatic repulsions among the spheres, forming a viscoelastic solid with an equilibrium modulus if the deformation is small and the sphere concentration is large enough.[54g] Alternatively, with a lower concentration of spheres, the spheres may phase separate into clusters of ordered arrays, in equilibrium with essentially pure solvent.[145-147] Similar clusters may be formed by the addition of a polymeric solute that does not adsorb on the particles, with the particle flocculation stabilized by the loss of entropy associated with a polymer chain inserted between two closely spaced spheres.[54g; 148] In either case, the clusters may be disrupted by an imposed strain, often leading to a behavior in which $\eta(\dot{\gamma})$ appears to be nearly proportional to $\dot{\gamma}^{-1}$, so that the stress $\dot{\gamma}\,\eta(\dot{\gamma})$ is essentially constant in flow.[54g] For example, studies on a dispersion of polystyrene beads in a polystyrene solution ($w = 0.15$ for the polymer, with 170 nm beads at weight fractions w_B of 0.05, 0.10, 0.15 and 0.20 dispersed in polystyrene solutions in either tritoylphospate, TCP, or 1,2-di(2-ethyl hexyl)pthtalate, DOP, a Flory theta solvent at 22°C) revealed interconnected strings of close packed beads coexisting with regions essentially free of beads,[148] similar to structures reported for charged beads in a low ionic strength solvent.[146] The filled polymer solution exhibited a weak yield stress determined as the maximum stress permitting fully recoverable strain

in creep, with the yield stress in good accord with that expected from the osmotic pressure of the polymer solution.[148] Data on the steady-state viscosity and the recoverable compliance following steady flow are shown in Figure 21 for the filled polymeric system. The data reveal a plateau viscosity η_P with $\eta(\dot\gamma)$ essentially independent of $\dot\gamma$ at intermediate $\dot\gamma$, and a limiting value J_s of $J(\dot\gamma)$ at low $\dot\gamma$. Except for the increase of $\eta(\dot\gamma)$ with decreasing $\dot\gamma$ at low $\dot\gamma$, with $\partial\ln(\eta(\dot\gamma)/\partial\ln\dot\gamma < -1$, the behavior is similar to that observed with polymers and their solutions, with remarkable reduction over a range of bead concentration and solution temperature in two solvents. The data on $\eta(\dot\gamma)$ at low $\dot\gamma$ for the dispersion with $w_B = 0.05$ exhibiting largest deviation. The data on η_P are seen to exceed η for the bead-free polymer solution by about the amount expected for dispersed beads, but the data on the recoverable compliance show a much enhanced J_s, attributed to the elasticity from distortion of the strings of close packed beads in steady-flow. These rheological features will have a substantial impact on the processing characteristics of such filled suspensions.

As indicated above, the subject of this section is very broad, and many additional examples could be discussed, including electrostatic interactions among particles and dissolved polymer, the effects with polymer adsorbed on a particle, interactions of polymeric solute with micelle structures, the effects of non spherical shapes of the dispersed particles, and more. Some of these are elaborated in reference [70].

10. References

1 Society of Rheology Website, http://www.umecheme.maine.edu/sor/default.htm., 1999.

2 Staverman, A. J.; Schwarzl, F. "Linear deformation behavior of high polymers" In *Die Physik der Hochpolymeren*; H. A. Stuart, ed.; Vol. IV; Springer-Verlag; Berlin, 1956; Chapt. 1.

3 Treloar, L. R. G. *The Physics of Rubber Elasticity*; 2rd ed.; Oxford University Press; London, 1958, (a) 156, (b) 64, (c) 177.

4 Coleman, B. D., Markovitz, H., and Noll, W. *Viscometric Flows of Non-Newtonian Fluids*; Springer-Verlag; New York, 1966, (a) 34, (b) 55, (c) 54, (d) 46.

5 McCrum, N. G.; Read, B. E.; Williams, G. *Anelastic and Dielectric Effects in Polymeric Solids*; Wiley; New York, 1967.

6 Aklonis, J. J.; MacKnight, W. J.; Shen, M. C. *Introduction to Polymer Viscoelasticity*; Wiley-Interscience; New York, 1972.

7 Bartenev, G. M.; Zelenev, Y. V., eds. *Relaxation Phenomena in Polymers*; John Wiley & Sons (Halsted Press); New York, 1974.

8 Walters, K. *Rheometry*; John Wiley & Sons; New York, 1975, (a) 44, (b) 48, (c) 52, (d) 93, (e) 102, (f) 100.

9 Markovitz, H. "Rheology" In *Physics Vade Mecum*; H. L. Anderson, ed.; Am. Inst. Phys.; New York, 1981; p. 274-86.

10 Plazek, D. J. "Viscoelastic and steady-state rheological response" In *Methods of Experimental Physics*; R. A. Fava, ed.; Vol. 16C; Academic Press; New York, 1980; Chapt. 11.

11 Ferry, J. D. *Viscoelastic Properties of Polymers*; 3rd ed.; John Wiley & Sons Inc.; New York, 1980, (a) 37, (b) 40, (c) 48, (d) 96, (e) 132, (f) 154, (g) 603, (h) 168, (i) 1, (j) 177, (k) 224, (m) 17, (n) 3, (p) 5, (q) 68, (r) 33, (s) 103, (t) 70, (u) 69, (v) 60, (w) 83, (x) 63, (y) 91, (z) 287, (a') 227, (b') 266, (c') 366, (d') 229, (e') 232, (f') 390, (g') 388, (h') 411, (i') 545.

12 Bailey, R. T.; North, A. M.; Pethrick, R. A. *Molecular Motion in High Polymers* The International Series of Monographs on Chemistry, J. E. Baldwin, *et al.*, eds.; Clarendon Press; Oxford, 1981.

13 Christensen, R. M. *Theory of Viscoelasticity*; 2nd. ed.; Academic; New York, 1982, (a) 353, (b) 1, (c) 5, (d) 7.

14 Dealy, J. M. *Rheometers for Molten Plastics*; Van Nostrand Reinhold Co.; New York, 1982, (a) 1, (b) 116, (c) 126, (d) 148, (e) 75, (f) 61.

15 Bohdanecký, M.; Kovář, J. *Viscosity of Polymer Solutions* Polymer Science Library, A. D. Jenkins, ed.; Vol. 2; Elsevier Scientific Publ. Co.; Amsterdam, 1982, (a) 167, (b) 175, (c) 177.

16 Janeschitz-Kriegl, H. *Polymer Melt Rheology and Flow Birefringence*; Springer-Verlag; Berlin ; New York, 1983, (a) 455, (b) 4, (c) 467, (d) 464, (e) 355, (f) 60, (g) 177, (h) 217.

17 Doi, M.; Edwards, S. F. *The Theory of Polymer Dynamics*; Clarendon Press; Oxford, UK, 1986, (a) 222, (b) 366, (c) 218, (d) 91, (e) 226, (f) 281, (g) 255, (h) 121, (i) 166.
18 Berry, G. C.; Plazek, D. J. "Rheology of polymeric fluids" In *Glass: Science and Technology*; D. R. Uhlmann; N. J. Kreidl, ed.; Vol. 3; Academic Press; New York, 1986; 319-62.
19 Bird, R. B.; Armstrong, R. C.; Hassager, O. *Dynamics of Polymeric Liquids. Vol. 1. Fluid Mechanics*; 2nd ed.; John Wiley & Sons, Inc.; New York, 1987, (a) 158, (b) 269, (c) 290.
20 Bird, R. B.; Curtiss, C. C.; Armstrong, R. C.; Hassager, O. *Dynamics of Polymeric Liquids. Vol. 2. Kinetic Theory*; 2nd ed.; John Wiley & Sons, Inc.; New York, 1987.
21 Collyer, A. A.; Clegg, D. W., eds. *Rheological Measurement*; Elsevier Science Co.; New York, 1988.
22 Larson, R. G. *Constitutive Equations for Polymer Melts and Solutions*; Butterworths; Boston, 1988, (a) 49, (b) 93, (c) 318, (d) 118, (e) 120, (f) 233, (g)120, (h) 95.
23 Tschoegl, N. W. *The Phenomenological Theory of Linear Viscoelastic Behavior*; Springer-Verlag; Berlin, 1989, (a) 513, (b) 551, (c) 69, (d) 47, (e) 560, (f) 21, (g) 508, (h) 55, (i) 413, (j) 401, (k) 406, (m) 157, (n) 409, (p) 157, (q) 425.
24 White, J. L. *Principles of Polymer Engineering Rheology*; John Wiley & Sons, Inc.; New York, 1990, (a) 83, (b) 163, (c) 174.
25 Matsuoka, S. *Relaxation Phenomena in Polymers*; Hanser; Munich, 1992.
26 Yanovsky, Y. G. *Polymer Rheology: Theory and Practice*; Chapman & Hall; New York, 1993, (a) 200, (b) 235.
27 Fuller, G. G. *Optical Rheometry of Complex Fluids* Topics in Chemical Engineering, K. E. Gubbins, ed.; Oxford University Press; New York, Oxford, 1995, (a) 117, (b) 109, (c) 149, (d) 167, (e) 193.
28 Coleman, B. D.; Noll, W. "Foundations of linear viscoelasticity" *Rev. Modern Phys.* **1961**, *33*, 239-49.
29 Petrie, C. J. S. *Elongational Flows: Aspects of the Behaviour of Model Elasticoviscous Fluids*; Pitman; London ; San Francisco, 1979.
30 Meissner, J.; Hostettler, J. "A new elongational rheometer for polymer melts and other highly viscoelastic liquids" *Rheol. Acta* **1994**, *33*, 1-21.
31 Macosko, C.; Starita, J. M. "New rheometer is put to the test" *SPE-J.* **1971**, *27 (11)*, 38-42.
32 Plazek, D. J. "Magnetic bearing torsional creep apparatus" *J. Polym. Sci. A-2* **1968**, *6*, 621.
33 Berry, G. C.; Birnboim, M. H.; Park, J. O.; Meitz, D. W.; Plazek, D. J. "A rotational rheometer for rheological rtudies with prescribed strain or stress history" *J. Polym. Sci.: Part B: Polym. Phys.* **1989**, *27*, 273.
34 Rabinowitsch, B. "Über die Viskosität und Elastizität von Solen" *Z. Phys. Chem., Abt. A* **1929**, *145*, 1-26.

35 Barr, G. *A Monograph of Viscometry*; Oxford University Press (Authorized facsimile by University Microfilms, Ann Arbor, MI, 1967); London, 1931.
36 Carslaw, H. S.; Jaeger, J. C. *Operational Methods in Applied Mathematics*; Dover Publications, Inc.; New York, 1948.
37 Shermergor, T. D. "Description of relaxation phenomena in structurally nonhomogeneous polymers by correlation functions" In *Relaxation Phenomena in Polymers*; G. M. Bartenev; Yu. V. Zelenev, eds.; John Wiley & Sons (Halsted Press); New York, 1974.
38 Berry, G. C. "Rheological and rheo-optical studies on nematic solutions of a rodlike polymer: Bingham Award Lecture" *J. Rheology* **1991**, *35*, 943.
39 Meissner, J. "Experimental problems and recent results in polymer melt rheometry" *J. Macromol. Chem., Macromol. Symp.* **1992**, *56*, 25-42.
40 Ostrowsky, N.; Sornette, D.; Parker, R.; Pike, E. R. "Exponential sampling method for light scattering polydispersity analysis" *Opt. Acta* **1981**, *28*, 1059-70.
41 Baumgaertel, M.; Winter, H. H. "Determination of discrete relaxation and retardation time spectra from dynamic mechanical data" *Rheol. Acta* **1989**, *28*, 511-19.
42 Sips, R. "General theory of deformation of viscoelastic substances" *J. Polym. Sci.* **1951**, *7*, 191-205.
43 Nakamura, K.; Wong, C. P.; Berry, G. C. "Strain criterion in nonlinear creep and recovery in concentrated polymer solutions" *J. Polym. Sci.: Polym. Phys. Ed.* **1984**, *22*, 1119-48.
44 Berry, G. C.; Plazek, D. J. "On the use of stretched-exponential functions for both linear viscoelastic creep and stress relaxation" *Rheol. Acta* **1997**, *36*, 320-9.
45 Riande, E.; Markovitz, H. "Approximate relations among compliance functions of linear viscoelasticity for amorphous polymers" *J. Polym. Sci.: Polm. Phys. Ed.* **1975**, *13*, 947-51.
46 Plazek, D. J.; Raghupathi, N.; Orbon, S. J. "Determination of dynamic storage and loss compliances from creep data" *J. Rheol.* **1979**, *23*, 477-88.
47 Markovitz, H. "The reduction principle in linear viscoelasticity" *J. Phys. Chem* **1965**, *69*, 671.
48 Markovitz, H. "Superposition in rheology" *J. Polym. Sci.: Symp.* **1975**, *50*, 431-56.
49 Berry, G. C.; "The viscosity of polymers and their concentrated solutions" *Adv. in Polym. Sci.* **1968**, *5*, 261-357.
50 Berry, G. C. "Crossover behavior in the viscosity of semiflexible polymers: Intermolecular interactions as a function of concentration and molecular weight" *J. Rheol.* **1996**, *40*, 1129-54.
51 Boyer, R. F. "The relation of transition temperatures to chemical structure in high polymers" *Rubber Rev.* **1963**, *36*, 1303-421.
52 Berry, G. C. "Thermodynamic and conformational studies of polystyrene. II. Intrinsic viscosity studies on dilute solutions of linear polystyrenes" *J. Chem. Phys.* **1967**, *46*, 1338.

53 Berry, G. C. "Molecular weight distribution" In *Encyclopedia of Materials Science and Engineering*; M. B. Bever, ed.; Pergamon Press; Oxford, 1986; 3759.
54 Russel, W. B.; Saville, D. A.; Schowalter., W. R. *Colloidal Dispersions*; Cambridge University Press; Cambridge, 1989, (a) 498, (b) 88, (c) 129, (d) 162, (e) 466, (f) 469, (g) 474.
55 Berry, G. C. "Remarks on a relation among the intrinsic viscosity, the radius of gyration, and the translational friction coefficient" *Journal of Polymer Science, Part B: Polymer Physics* **1988**, *26*, 1137-42.
56 Yamakawa, H. *Modern Theory of Polymer Solutions*; Harper and Row; New York, 1971, (a) 266, (b) 314.
57 Flory, P. J.; "Molecular configuration and thermodynamic properties from intrinsic viscosities" *J. Polym. Sci.* **1950**, *5*, 745-7.
58 Casassa, E. F.; Berry, G. C. "Reflections and comments on "Molecular configuration and thermodynamic properties from intrinsic viscosities" by Paul J. Flory and Thomas G Fox" *J. Polym. Sci., Pt. B: Polym. Phys.* **1996**, *34*, 203-6.
59 Casassa, E. F.; Berry, G. C. "Polymer solutions" In *Comprehensive Polymer Science*; G. Allen, ed.; Vol. 2; Pergamon Press; New York, 1988; Chapt. 3.
60 Brandrup, J.; Immergut, E. H., eds. *Polymer Handbook*; 3rd ed.; Wiley; New York, 1989.
61 Casassa, E. F.; Berry, G. C. "Angular distribution of intensity of Rayleigh scattering from comblike branched molecules" *J. Polym. Sci.: Part A-2* **1966**, *4*, 881.
62 Lodge, T. P. "Solvent dynamics, local friction, and the viscoelastic properties of polymer solutions" *J. Phys. Chem.* **1993**, *97*, 1480-7.
63 Harrison, G.; Lamb, J.; Matheson, A. J. "The viscoelastic properties of dilute solutions of polystyrene in toluene" *J. Phys. Chem.* **1966**, *68*, 1072-8.
64 Osaki, K. "Viscoelastic properties of dilute polymer solutions" *Adv. Polym. Sci.* **1973**, *12*, 1-64.
65 Birnboim, M. H. "The viscoelastic properties of low molecular weight polystyrene solutions in high frequency regime: Polymer-solvent interaction" *Proc. IUPAC Macro 82* **1982**, *July 12-16*, 872.
66 Schrag, J. L., *et al.* "Local modification of solvent dynamics by polymeric solutes" *J. Non-Cryst. Solids* **1991**, *131*, 537-43.
67 Yoshizaki, T.; Takaeda, Y.; Yamakawa, H. "On the correlation between the negative intrinsic viscosity and the rotatory relaxation time of solvent molecules in dilute polymer solutions" *Macromolecules* **1993**, *26*, 6891-6.
68 Yamakawa, H. "Concentration dependence of polymer chain configurations in solution" *J. Chem. Phys.* **1961**, *34*, 1360-72.

69 Batchelor, G. K. "The effect of Brownian motion on the bulk stress in a suspension of spherical particles" *J. Fluid Mech.* **1977**, *83*, 97-117.
70 Pal, R. "Rheology of emulsions containing polymeric liquids" In *Encyclopedia of Emulsion Technology*; Paul Becher, ed.; Vol. 4; Marcel Dekker, Inc.; New York, 1996; 93-263.
71 Park, J. O.; Berry, G. C. "Moderately concentrated solutions of polystyrene. 3. Viscoelastic measurements at the Flory Theta temperature" *Macromolecules* **1989**, *22*, 3022-9.
72 de Gennes, P.-G. *Scaling Concepts in Polymer Physics*; Cornell University Press; Ithaca, NY, 1979.
73 Narayanaswamy, O. S. "Annealing of glass" In *Glass: Science and Technology*; D. R. Uhlmann; N. J. Kreidl, ed.; Vol. 3; Academic Press; New York, 1986; 275-318.
74 Plazek, D. J.; Berry, G. C. "Physical aging of polymer glasses" In *Glass: Science and Technology*; D. R. Uhlmann; N. J. Kreidl, ed.; Vol. 3; Academic Press; New York, 1986; 363-99.
75 Graessley, W. W. "The entanglement concept in polymer rheology" *Adv. Polym. Sci.* **1974**, *16*, 1-179.
76 Berry, G. C.; Nakayasu, H.; "Viscosity of poly(vinyl acetate) and its concentrated solutions" *Journal of Polymer Science, Polymer Physics Edition* **1979**, *17*, 1825-44.
77 da Andrade, E. N. *Viscosity and Plasticity*; Chemical Publishing Co.; New York, 1951.
78 Berry, G. C. "The stress-strain behavior of materials exhibiting Andrade creep" *Polym Eng Sci* **1976**, *16*, 777-81.
79 Orbon, S. J.; Plazek, D. J. "The recoverable compliance of a series of bimodal molecular weight blends of polystyrene" *J. Polym. Sci.: Polym. Phys. Ed.* **1979**, *17*, 1871.
80 Berry, G. C. "Terminal retardation times and weights for the Rouse model for a crosslinked network" *J. Polym. Sci.: Part B: Polym. Phys.* **1987**, *25*, 2203-5.
81 Masuda, T.; Takahashi, M.; Onogi, S. "Steady-state compliance of polymer blends" *Appl. Polym. Symp.* **1973**, *20*, 49-60.
82 Kurata, M. "Effect of molecular weight distribution on viscoelastic properties of polymers. 2. Terminal relaxation time and steady-state compliance" *Macromolecules* **1984**, *17*, 895-8.
83 Fujita, H.; Einaga, Y. "Self diffusion and viscoelasticity in entangled systems. II. Steady-state viscosity and compliance of binary blends" *Polymer J.* **1985**, *17*, 1189-95.
84 Montfort, J. P.; Marin, G.; Monge, P. "Molecular weight distribution dependence of the viscoelastic properties of linear polymers: The coupling of reptation and tube-renewal effects" *Macromolecules* **1986**, *19*, 1979-88.
85 des Cloizeaux, J. "Relaxation of entangled polymeric melts" *Macromolecules* **1990**, *23*, 3992-4006.

86 Tsenoglou, C. "Molecular weight polydispersity effects on the viscoelasticity of entangled linear polymers" *Macromoleucules* **1991**, *24*, 1762-7.
87 Berry, G. C. "Rheological properties of blends of rodlike chains with flexible or semiflexible chains" *Trends in Polymer Science* **1993**, *1*, 309.
88 Berry, G. C. "Rheology of blends of liquid crystalline and flexible chain polymers" *Trends Poly. Sci.* **1996**, *4*, 289-92.
89 Plazek, D. J.; Chay, I. C. "The evolution of the viscoelastic retardation spectrum during the development of an epoxy resin network" *J. Polym. Sci.: Part B: Polym. Phys.* **1991**, *29*, 17-29.
90 Winter, H. H.; Mours, M. "Rheology of polymers near liquid-solid transitions" *Adv. Polym. Sci.* **1997**, *134*, 167-234.
91 Plazek, D. J. "Oh, thermorheological simplicity, wherefore art thou?" *J. Rheol.* **1996**, *40*, 987-1014.
92 Plazek, D. J.; Chelko, A. J., Jr. "Temperature dependence of the steady state recoverable compliance of amorphous polymers" *Polymer* **1977**, *18*, 15-8.
93 Inoue, T.; Mizukami, Y.; Okamoto, H.; Matsui, H.; Watanabe, H.; Kanaya, T.; Osaki, K. "Dynamic birefringence of vinyl polymers" *Macromolecules* **1996**, *29*, 6240-5.
94 Struik, L. C. E. *Physical Aging in Amorphous Polymers and Other Materials*; Elsevier; Amsterdam, 1978.
95 Bero, C. A.; Plazek, D. J. "Volume-dependent rate processes in an epoxy resin" *J. Polym. Sci.: Part B: Polym. Phys.* **1991**, *29*, 39-47.
96 Lodge, A. S.; Meissner, J. "On the use of instantaneous strains, superposed on shear and elongational flows of polymeric liquids to test the Gaussian network hypothesis and to estimate the segment concentration and its variation during flow" *Rheol. Acta* **1971**, *11*, 351-2.
97 Coleman, B. D.; Markovitz, H. "Asymptotic relations between shear stresses and normal stresses in general incompressible fluids" *J. Polym. Sci.: Polym. Phys. Ed.* **1974**, *12*, 2195-207.
98 Coleman, B. D.; Markovitz, H. "Normal stress effects in second-order fluids" *J. Appl. Phys.* **1964**, *35*, 1-9.
99 Coleman, B. D.; Dill, E. H.; Toupin, R. A. "A phenomenological theory of streaming birefringence" *Arch. Rational Mech. Anal.* **1970**, *39*, 358-99.
100 Kannan, R. M.; Kornfield, J. A. "The third-normal stress difference in entangled melts: Quantitative stress-optical measurements in oscillatory shear" *Rheol. Acta* **1992**, *31*, 535-44.
101 Bernstein, B.; Kearsley, E. A.; Zapas, L. J. "A study of stress relaxation with finite strain" *Trans. Soc. Rheol.* **1963**, *7*, 391-410.
102 Wagner, M. H.; Laun, H. M. "Nonlinear shear creep and constrained recovery of a LDPE melt" *Rheol. Acta* **1978**, *17*, 138-48.

103 Wagner, M. H.; Stephenson, S. E. "The irreversibility assumption of network disentanglement in flowing polymer melts and its effects on elastic recoil predictions" *J. Rheol.* **1979**, *23*, 489-504.

104 Graessley, W. W.; Park, W. S.; Crawley, R. L. "Experimental tests of constitutive relations for polymers undergoing uniaxial shear flows" *Rheol. Acta* **1977**, *16*, 291-301.

105 Cox, W. P.; Merz, B. H. "Correlation of dynamic and steady flow viscosities" *J. Polym. Sci.* **1958**, *28*, 619-22.

106 Osaki, K.; Bessho, N.; Kojimoto, T.; Kurata, M. "Flow birefringence of polymer solutions in time-dependence field" *J. Rheol.* **1979**, *23*, 457-75.

107 Takahashi, M.; Masuda, T.; Bessho, N.; Osaki, K. "Stress measurements at the start of shear flow: Comparison of data from a modified Weissenberg Rheogoniometer and from flow birefringence" *J. Rheol.* **1980**, *24*, 516-20.

108 Menezes, E. V.; Graessley, W. W. "Nonlinear rheological behavior of polymer systems for several shear-flow histories" *J. Polym. Sci., Polym. Phys. Ed.* **1982**, *20*, 1817-33.

109 Pearson, D. S.; Kiss, A. D.; Fetters, L. J.; Doi, M. "Flow-induced birefringence of concentrated polyisoprene solutions" *J. Rheol.* **1989**, *33*, 517-35.

110 Rochefort, W. E.; Heffner, G. W.; Pearson, D. S.; Miller, R. D.; Cotts, P. M. "Rheological and rheooptical studies of poly(alkylsilanes)" *Macromolecules* **1991**, *24*, 4861-4.

111 Wong, C. P.; Berry, G. C. "Rheological studies on concentrated solutions of heterocyclic polymers" *Polymer* **1979**, *20*, 229-40.

112 Casson, N. "A flow equation for pigment-oil suspensions of the printing ink type" In *Rheology of Disperse Systems*; C. C. Mill, ed.; Pergamon Press; London, 1959; 84-104.

113 Markovitz, H. "Relative rates of creep and relaxation in shear, elongation and isotropic compression" *J. Polym. Sci.: Polym. Phys. Ed.* **1973**, *11*, 1769-77.

114 Kovacs, A. J.; Aklonis, J. J.; Hutchinson, J. M.; Ramos, A. R. "Isobaric volume and enthalpy recovery of glasses. II. A transparent multiparameter theory" *J. Polym. Sci.: Polym. Phys. Ed.* **1979**, *17*, 1097-162.

115 Philippoff, W. "Flow birefringence and stress" *J. Appl. Phys.* **1956**, *27*, 984-9.

116 Philippoff "Elastic stresses and birefringence in flow" *Trans. Soc. Rheol.* **1961**, *5*, 163-91.

117 Janeschitz-Kriegl, H. "Flow birefringence of elastico-viscous polymer systems" *Adv. Polym. Sci.* **1969**, *6*, 170-318.

118 Coleman, B. D.; Dill, E. H. "Photoviscoelasticity: Theory and practice" In *The photoelastic effect and its applications*; J. Kestens, ed.; Springer-Verlag; Berlin, New York, 1975; 455-505.

119 Wales, J. L. S. *The Application of Flow Birefringence to Rheological Studies of Polymer Melts.*; Delft University Press; Delft, 1976.

120 Riande, E.; Saiz, E. *Dipole Moments and Birefringence of Polymers*; Prentice Hall; Englewood Cliffs, N.J., 1992.
121 Read, B. E. "Viscoelastic behavior of amorphous polymers in the glass-rubber transition region: Birefringence studies" *Polym. Eng. Sci.* **1983**, *23*, 835-43.
122 Kornfield, J. A.; Fuller, G. G.; Pearson, D. S. "Third normal stress difference and component relaxation spectra for bidisperse melts under oscillatory shear" *Macromolecules* **1991**, *24*, 5429-41.
123 Takahashi, T. "Measurement of first and second normal stress difference of a polystyrene solution using a simultaneous mechanical and optical measurement technique" In *Fluid Measurement and Instrumentation: 1995*; G. L. Morrison, *et al.*, eds.; Vol. FWD-Vol. 211; Am. Soc. Mech. Eng.; New York, 1995; 31-4.
124 Olson, D. I.; Brown, E. F.; Burghardt, W. R. "Second normal stress difference relaxation in a linear polymer melt following step-strain" *J. Polym. Sci. Part B: Polym. Phys.* **1998**, *36*, 2671-5.
125 Coleman, B. D.; Dill, E. H. "Theory of induced birefringence in materials with memory" *J. Mech. Phys. Solids* **1971**, *19*, 215-43.
126 Osaki, K.; Okamoto, H.; Inoue, T.; Hwang, E.-J. "Molecular interpretation of dynamic birefringence and viscoelasticity of amorphous polymers" *Macromolecules* **1995**, *28*, 3625-30.
127 Mott, P. H.; Roland, C. M. "Birefringence of polymers in the softening zone" *Macromolecules* **1998**, *31*, 7095-8.
128 Lodge, A. S. "Stress relaxation after a sudden shear strain" *Rheol. Acta* **1975**, *14*, 664-5.
129 Osaki, K.; Bessho, N.; Kojimoto, T.; Kurata, M. "Flow birefringence of polymer solutions in time-dependent field. Relation between normal and shear stresses on application of step-shear strain" *J. Rheol.* **1979**, *23*, 617-24.
130 Osaki, K.; Kimura, S.; Kurata, M. "Relaxation of shear and normal stresses in step-shear deformation of a polystyrene solution. Comparison with the predictions of the Doi-Edwards theory" *J. Polym. Sci.: Polym. Phys. Ed.* **1981**, *19*, 517-27.
131 Mott, P. H.; Roland, C. M. "Birefringence of rubber during creep and recovery" *Macromolecules* **1996**, *29*, 8492-6.
132 Osaki, K.; Inoue, T. "Some phenomenological relations for strain-induced birefringence of amorphous polymers" *Nihon Reoroji Gakkaishi* **1991**, *19*, 130-2 (In English).
133 Krieger, I. M. "Rheology of monodisperse latices" *Adv. Colloid Interface Sci.* **1972**, *3*, 111-36.
134 Russel, W. B.; Gast, A. P. "Nonequilibrium statistical mechanics of concentrated colloidal dispersions: Hard spheres in weak flows" *J. Chem. Phys.* **1986**, *84*, 1815-26.
135 van der Werff, J. C.; de Kruif, C. G.; Blom, C.; Mellema, J. "Linear viscoelastic behavior of dense hard-sphere dispersions" *Phys. Rev. A* **1989**, *39*, 795-807.

136 Brady, J. F. "The rheological behavior of concentrated colloidal dispersions" *J. Chem. Phys.* **1993**, *99*, 567-81.
137 Shikata, T.; Pearson, D. S. "Viscoelastic behavior of concentrated spherical suspensions" *J. Rheol.* **1994**, *38*, 601-16.
138 Lionberger, R. A.; Russel, W. B. "High frequency modulus of hard sphere colloids" *J. Rheol.* **1994**, *38*, 1885-908.
139 Lionberger, R. A.; Russel, W. B. "Effectiveness of nonequilibrium closures for the many body forces in concentrated colloidal dispersions" *J. Chem. Phys.* **1997**, *106*, 402-16.
140 Chong, J. S.; Christiansen, E. B.; Baer, A. D. "Rheology of concentrated suspensions" *J. Appl. Polym. Sci.* **1971**, *15*, 2007-21.
141 Beenakker, C. W. J. "The effective viscosity of a concentrated suspension of spheres (And its relation to diffusion)" *Physica A* **1984**, *128A*, 48-81.
142 Beenakker, C. W. J.; Mazur, P. "Diffusion of spheres in a concentrated suspension. II" *Physica A* **1984**, *126A*, 349-70.
143 de Gennes, P. G.; Prost, J. *The Physics of Liquid Crystals*; Oxford U. P.; New York, 1993.
144 Mellema, J.; de Kurif, C. G.; Blom, C.; Vrij, A. "Hard sphere colloidal dispersions: Mechanical relaxation pertaining to thermodynamic forces" *Rheol. Acta* **1987**, *26*, 40-4.
145 Arora, A. K.; Tata, B. V. R., eds. *Ordering and Phase Transitions in Charged Colloids*; VCH Publisher; New York, 1996.
146 Yoshida, J.; Yamanaka, J.; Koka, T.; Ise, N.; Hashimoto, T. "Novel crystallization process in dilute ionic colloids" *Langmuir* **1998**, *14*, 569-74.
147 Weiss, J. A.; Larsen, A. E.; Grier, D. G. "Interactions, dynamics, and elasticity in charge-stabilized colloidal crystals" *J. Chem. Phys.* **1998**, *109*, 8659-66.
148 Meitz, D. W.; Yen, L.; Berry, G. C.; Markovitz, H. "Rheological studies of dispersions of spherical particles in a polymer solution" *J. Rheology* **1988**, *32*, 309-51.

Table 1 Linear Viscoelastic Functions

Shear Compliance	***J(t)***
Shear Modulus	***G(t)***
Bulk Compliance	***B(t)***
Bulk Modulus	***K(t)***
Tensile Compliance	$D(t) = J(t)/3 + B(t)/9$
Tensile Modulus[a]	$1/\hat{E}(s) = 1/3\hat{G}(s) + 1/9\hat{K}(s)$

a. The superscript "^" denotes a Laplace transform.

Table 2 Functions and Parameters Used

Function/Parameter	Symbol	Units
Time	t	T
Frequency	ω	T^{-1}
Strain Component	ε_{ij}	---
Elongational strain	ε	---
Shear strain	γ	---
Rate of shear	$\dot{\gamma}$, $\dot{\varepsilon}$	T^{-1}
Stress Component	S_{ij}	$ML^{-1}T^{-2}$
Shear stress	σ	$ML^{-1}T^{-2}$
Modulus	G, K, E	$ML^{-1}T^{-2}$
Compliance	J, B, D	$M^{-1}LT^{2}$
Viscosity	η	$ML^{-1}T^{-1}$

Table 3 Relations Among Elastic Constants

	K, G	**E, G**	**K, E**	**K, ν**	**E, ν**	**G, ν**
K	K	$\frac{EG}{3[3G - E]}$	K	K	$\frac{E}{3[1 - 2\nu]}$	$\frac{2G[1 + \nu]}{3[1 - 2\nu]}$
E	$\frac{9KG}{3K + G}$	E	E	$3K(1 - 2\nu)$	E	$2G(1 + \nu)$
G	G	G	$\frac{3KE}{9K - E}$	$\frac{3K[1 - 2\nu]}{2[1 + \nu]}$	$\frac{E}{2[1 + \nu]}$	G
ν	$\frac{3K - 2G}{6K + 2G}$	$\frac{E}{2G} - 1$	$\frac{3K - E}{6K}$	ν	ν	ν

$J = 1/G$, $B = 1/K$, $D = 1/E$

Table 4: Geometric Factors in Rheometry

Geometry	Measured		Calculated[a]	
Translational geometries				
Parallel Plate	Force:	$\mathfrak{F}$	Stress:	$\sigma = \mathfrak{F}/wb$
width,w; breadth b; separation h	Displacement:	D	Strain:	$\gamma = D/h$
Concentric Cylinders	Force:	$\mathfrak{F}$	Stress:	$\sigma = \mathfrak{F}/2\pi Rh$
inner radius R; gap Δ; height h	Displacement:	D	Strain:	$\gamma = D/R\ln(1 + \Delta/R)$
Rotational geometries				
Parallel Plate	Torque:	$\mathfrak{M}$	Stress:	$\sigma = (2r/R)\mathfrak{M}/\pi R^3$
outer radius R; separation h	Rotation:	Ω	Strain:	$\gamma(r) = (r/h)\,\Omega$
Cone & Plate	Torque:	$\mathfrak{M}$	Stress:	$\sigma = (3/2)\mathfrak{M}/\pi R^3$
outer radius R; cone angle $\pi - \alpha$	Rotation:	Ω	Strain:	$\gamma = (1/\alpha)\,\Omega$
Concentric Cylinders	Torque:	$\mathfrak{M}$	Stress:	$\sigma = (R/2h)\mathfrak{M}/\pi R^3$
inner radius R; gap Δ; height h	Rotation:	Ω	Strain:	$\gamma(r) = (R/\Delta R)\,\Omega f(R,r)$
				$f(R,r) = (R/r)^2 \frac{1 + \Delta/R}{1 + \Delta/2R}$

a σ and γ are the shear stress and strain, respecgively

Table 5: Time-Temperature Superposition Approximation

Temperature Dependent Parameters

Fluid:	**Solid:**
$\eta'(0) = \eta$	$\eta'(0) = \text{cst.}$
$J_\infty = J_s$	$J_\infty = J_e = 1/G_e$
$\tau_c = \eta'(0)J_\infty = \eta J_s$	$\tau_c = \eta'(0)J_\infty = \eta'(0)J_s$

Functions approximately independent of Temperature

Compliances:	**Moduli:**	
$J(t/\tau_c)/J_\infty$	$J_\infty G(t/\tau_c)$	
$J'(\omega\tau_c)/J_\infty$	$J_\infty G'(\omega\tau_c)$	$\eta'(\omega\tau_c)/\eta'(0)$
$J''(\omega\tau_c)/J_\infty$	$J_\infty G''(\omega\tau_c)$	$\eta''(\omega\tau_c)/\eta'(0)$

Relative "Shift Factors" at temperature T_{REF}

$$b_T = b(T,T_{REF}) = J_\infty(T)/J_\infty(T_{REF})$$
$$h_T = h(T,T_{REF}) = \eta(T)/\eta(T_{REF})$$
$$a_T = a(T,T_{REF}) = \tau_c(T)/\tau_c(T_{REF}) = h_T\, b_T$$

Use of relative shift factors to produce a "Master Curve"

Compliances:	**Moduli:**
$J(t/a_T;T)/b_T \approx J(t;T_{REF})$	$b_T G(t/a_T;T) \approx G(t;T_{REF})$
$J'(\omega a_T;T)/b_T \approx J'(\omega;T_{REF})$	$b_T G'(\omega a_T;T) \approx G'(\omega;T_{REF})$
$J''(\omega a_T;T)/b_T \approx J''(\omega;T_{REF})$	$b_T G''(\omega a_T;T) \approx G''(\omega;T_{REF})$
	$\eta'(\omega a_T;T)/h_T \approx \eta'(\omega;T_{REF})$
	$\eta''(\omega a_T;T)/h_T \approx \eta''(\omega;T_{REF})$

Figure Caption

1. Schematic diagram of some of the principal components of a rheometer under the control of a computer and the output signals.

2. Schematic drawing of a device for elongational (tensile) creep and recovery on a strip or fiber. The table at the bottom gives the input/output for the instrument.

3. Schematic drawing of a device for a torsional shear rheometer with a controlled torque input. The table at the bottom gives the input/output for the instrument.

4. Schematic drawing of a device for a torsional shear rheometer with a controlled deformation input. The table at the bottom gives the input/output for the instrument.

5. Schematic drawings of several fixtures used with torsional shear rheometers.

6. Schematic drawings of idealized rheological experiments:
   Upper: The shear stress $\sigma(t)$ resulting from successive jumps in the strain $\gamma(t)$;
   Lower: The shear strain $\gamma(t)$ resulting from successive jumps in the stress $\sigma(t)$

7. Schematic drawings for four viscoelastic experiments discussed in the text.

8. Schematic drawing to illustrate the application of time-temperature superposition for data on the shear creep compliance (assuming that $b_T = 1$ for simplicity). The shifts of the data at each temperature to the reference plot at temperature $T_{REF} = T_5$ are shown by the dashed lines. The indicated experimental range is given as a guideline of actual practice, but could be extended to shorter or longer times on occasion. After an example in reference [18].

9. Illustrative example of isochronal data (for a fixed frequency) corresponding to isothermal data (reduced to the glass transition temperature) for a linear viscoelastic solid. The isochronal data were computed from the isothermal data by the use of the "universal" expression for the temperature dependence of the viscosity discussed in the text; with $b_T = 1$ for simplicity. The vertical dashed lines mark positions of frequency and temperature common to the two representations.

10. Schematic drawing of the viscosity (lower) and the concentration dependent excluded volume factor (upper) vs R_G/Λ based on a relations discussed in the text to illustrate regimes over which various approximations apply; $\Lambda = (M/N_A c)^{1/3}$ equal to the mean separation of molecular centers. From reference [50].

11. Bilogarithmic plot of the viscosity versus $X = \tilde{X}/\pi N_A m_a/M_L$ for various polymers (with m_a/M_L essentially a constant for the examples shown). The variation of $\eta^{(c)}_{LOC}$ with M_n owing to effects on T_g is included in the "constant", which also includes a term to provide vertical separation of the data. From reference [49].

12. Bilogarithmic plot of the viscosity versus φM_w for fractions of poly(vinyl acetate) and its concentrated solutions. Each data set is for the fixed volume fraction φ indicated. The dashed lines indicate the curve that would be obtained if data would be plotted after reduction for the change in T_g with molecular weight and φ. The downward displacement of the data sets for $\varphi < 1$ reflects the suppression of $\eta^{(c)}_{LOC}$ as T_g decreases with decreasing T. The filled points are for data under Flory theta conditions. After an example in reference [76].

13. Schematic drawings to illustrate various linear viscoelastic functions for an oligomer with a low M (top), a polymer with M less than that for entanglement effects (middle), and a polymer with M large enough to exhibit entanglement effects (bottom).

14. Examples of creep compliances and shear moduli for a high molecular weight polymer; the data exhibit entanglement effects for large t (or small frequency). After an example in reference [9].

15. Schematic drawings to illustrate various the linear recoverable compliance and the associated retardation spectrum for several cases.
    Upper: The recoverable compliance and the associated retardation spectra for a polymers with narrow and broad molecular weight distributions, and with M large enough to exhibit entanglement effects.
    Lower: The effect of random crosslinking on the retardation spectrum for a polymer initially with a narrow molecular weight distribution, and with M large enough to exhibit entanglement effects.

16. Bilogarithmic plots of the several reduce functions for a high molecular weight polyethylene with a broad molecular weight distribution: the viscosity $\eta(\dot\gamma)/\eta(0)$, the total recoverable compliance $J_s(\dot\gamma)/J_s$ and the first-normal stress difference $S^{(1)}(\dot\gamma)J_s$ as functions of $\tau_c\dot\gamma = J_s\eta(0)\dot\gamma$. The curves are calculated as described in the text. After an example in reference [43] based on data in reference [102] .

17. Bilogarithmic plots of the several reduce functions for a high molecular weight polysytrene with a narrow molecular weight distribution: the viscosity $\eta(\dot\gamma)/\eta(0)$, the dynamic viscosity $\eta'(\omega)/\eta(0)$, the total recoverable compliance $J_s(\dot\gamma)/J_s$, the dynamic storage compliance $J'(\omega)/J_s$, and the first-normal stress difference $S^{(1)}(\dot\gamma)J_s$ as functions of $\tau_c\dot\gamma = J_s\eta(0)\dot\gamma$. After an example in reference [104].

18. An example of the elongational creep and recovery compliances for a material exhibiting a yield strain behavior. The unfilled and filled symbols in (b) show the strain versus $\vartheta^{1/3}$ and the recoverable strain versus the function $(\vartheta + T_e)^{1/3} - \vartheta^{1/3}$ computed for a linear viscoelastic response; the data exhibit quasi-linear response in recovery following creep beyond the yield strain. After an example in reference [111].

19. Semilogarithmic plots the relative viscosity $\eta_{rel} = \eta/\eta_{solv}$ and a reduced modulus $(G_1)_{red}$ versus volume fraction for hard spheres over a range of sphere radius R; $(G_1)_{red} = G_1R^3/kT$, with $G_1 \approx G'(\omega_L)$ in a certain range of frequency for which $G'(\omega_L)$ is about constant, see the text. The data for η_{rel} are from references [135; 137; 140] for unfilled circles, filled circles and squares, respectively; the data from reference [140] represent data from several sources. The data for $(G_1)_{red}$ are from reference [137], for spheres with R/μm equal to 0.060 (pip down), 0.125 (no pip) and 0.225 (pip up). The curves in the lower figure labeled "U", and "L" correspond to the formulae discussed in the text for $\eta'(0)$ and $\eta'(\omega_L)$, respectively, and the curved labeled "D" corresponds to the dilute solution virial series truncated at the term in φ^2, with k' = 1.0. The curve in the upper figure is calculated as described in the text.

20. Data on the dynamic viscosity $\eta'(\omega)$ and an effective storage creep compliance $J'_{EFF}(\omega)$ versus reduced frequency ωa_T for hard spheres (R = 0.060 μm, φ = 0.37) over a range of temperatures as indicated. The dashed line has slope – 1/3, as expected in some treatments discussed in the text. From data given in reference [137].

21. Bilogarithmic plots of the reduce functions for a solution of a high molecular weight polysytrene with a narrow molecular weight distribution filled with crosslinked polystyrene spheres: the viscosity $\eta(\dot\gamma)/\eta_P$ and the total recoverable compliance $J_s(\dot\gamma)/J_s$ as functions of $\tau_c\dot\gamma = J_s\eta_P\dot\gamma$, where η_P is the value of $\eta(\dot\gamma)$ over an intermediate range of $\dot\gamma$ for which $\eta(\dot\gamma)$ is essentially a constant. The weight fraction w_B of beads covers the range shown in the insets; the data for $\eta(\dot\gamma)/\eta_P$ tending to lie below the bulk of the data are for $w_B = 0.05$. One of the two solvents used corresponded Flory theta conditions for polystyrene at the experimental temperature. After an example in reference [148].

1 Website, S. o. R.; in *http://www.umecheme.maine.edu/sor/default.htm*. 1999,.

2 Staverman, A. J.; Schwarzl, F. "Linear deformation behavior of high polymers" In *Die Physik der Hochpolymeren*; H. A. Stuart, ed.; Vol. IV; Springer-Verlag; Berlin, 1956; Chapt. 1.

3 Treloar, L. R. G. *The Physics of Rubber Elasticity*; 2rd ed.; Oxford University Press; London, 1958, (a) 156, (b) 64, (c) 177.

4 Coleman, B. D., Markovitz, H., and Noll, W. *Viscometric Flows of Non-Newtonian Fluids*; Springer-Verlag; New York, 1966, (a) 34, (b) 55, (c) 54, (d) 46.

5 McCrum, N. G.; Read, B. E.; Williams, G. *Anelastic and Dielectric Effects in Polymeric Solids*; Wiley; New York, 1967.

6 Aklonis, J. J.; MacKnight, W. J.; Shen, M. C. *Introduction to Polymer Viscoelasticity*; Wiley-Interscience; New York, 1972.

7 Bartenev, G. M.; Zelenev, Y. V., eds. *Relaxation Phenomena in Polymers*; John Wiley & Sons (Halsted Press); New York, 1974.

8 Walters, K. *Rheometry*; John Wiley & Sons; New York, 1975, (a) 44, (b) 48, (c) 52, (d) 93, (e) 102, (f) 100.

9 Markovitz, H. "Rheology" In *Physics Vade Mecum*; H. L. Anderson, ed.; Am. Inst. Phys.; New York, 1981; p. 274-86.

10 Plazek, D. J. "Viscoelastic and steady-state rheological response" In *Methods of Experimental Physics*; R. A. Fava, ed.; Vol. 16C; Academic Press; New York, 1980; Chapt. 11.

11 Ferry, J. D. *Viscoelastic Properties of Polymers*; 3rd ed.; John Wiley & Sons Inc.; New York, 1980, (a) 37, (b) 40, (c) 48, (d) 96, (e) 132, (f) 154, (g) 603, (h) 168, (i) 1, (j) 177, (k) 224, (m) 17, (n) 3, (p) 5, (q) 68, (r) 33, (s) 103, (t) 70, (u) 69, (v) 60, (w) 83, (x) 63, (y) 91, (z) 287, (a') 227, (b') 266, (c') 366, (d') 229, (e') 232, (f') 390, (g') 388, (h') 411, (i') 545.

12 Bailey, R. T.; North, A. M.; Pethrick, R. A. *Molecular Motion in High Polymers* The International Series of Monographs on Chemistry, J. E. Baldwin, *et al.*, eds.; Clarendon Press; Oxford, 1981.

13 Christensen, R. M. *Theory of Viscoelasticity*; 2nd. ed.; Academic; New York, 1982, (a) 353, (b) 1, (c) 5, (d) 7.
14 Dealy, J. M. *Rheometers for Molten Plastics*; Van Nostrand Reinhold Co.; New York, 1982, (a) 1, (b) 116, (c) 126, (d) 148, (e) 75, (f) 61.
15 BohdaneckO(´y), M.; KováO(˘r), J. *Viscosity of Polymer Solutions* Polymer Science Library, A. D. Jenkins, ed.; Vol. 2; Elsevier Scientific Publ. Co.; Amsterdam, 1982, (a) 167, (b) 175, (c) 177.
16 Janeschitz-Kriegl, H. *Polymer Melt Rheology and Flow Birefringence*; Springer-Verlag; Berlin ; New York, 1983, (a) 455, (b) 4, (c) 467, (d) 464, (e) 355, (f) 60, (g) 177, (h) 217.
17 Doi, M.; Edwards, S. F. *The Theory of Polymer Dynamics*; Clarendon Press; Oxford, UK, 1986, (a) 222, (b) 366, (c) 218, (d) 91, (e) 226, (f) 281, (g) 255, (h) 121, (i) 166.
18 Berry, G. C.; Plazek, D. J. "Rheology of polymeric fluids" In *Glass: Science and Technology*; D. R. Uhlmann; N. J. Kreidl, ed.; Vol. 3; Academic Press; New York, 1986; 319-62.
19 Bird, R. B.; Armstrong, R. C.; Hassager, O. *Dynamics of Polymeric Liquids. Vol. 1. Fluid Mechanics*; 2nd ed.; John Wiley & Sons, Inc.; New York, 1987, (a) 158, (b) 269, (c) 290.
20 Bird, R. B.; Curtiss, C. C.; Armstrong, R. C.; Hassager, O. *Dynamics of Polymeric Liquids. Vol. 2. Kinetic Theory*; 2nd ed.; John Wiley & Sons, Inc.; New York, 1987.
21 Collyer, A. A.; Clegg, D. W., eds. *Rheological Measurement*; Elsevier Science Co.; New York, 1988.
22 Larson, R. G. *Constitutive Equations for Polymer Melts and Solutions*; Butterworths; Boston, 1988, (a) 49, (b) 93, (c) 318, (d) 118, (e) 120, (f) 233, (g)120, (h) 95.
23 Tschoegl, N. W. *The Phenomenological Theory of Linear Viscoelastic Behavior*; Springer-Verlag; Berlin, 1989, (a) 513, (b) 551, (c) 69, (d) 47, (e) 560, (f) 21, (g) 508, (h) 55, (i) 413, (j) 401, (k) 406, (m) 157, (n) 409, (p) 157, (q) 425.
24 White, J. L. *Principles of Polymer Engineering Rheology*; John Wiley & Sons, Inc.; New York, 1990, (a) 83, (b) 163, (c) 174.
25 Matsuoka, S. *Relaxation Phenomena in Polymers*; Hanser; Munich, 1992.
26 Yanovsky, Y. G. *Polymer Rheology: Theory and Practice*; Chapman & Hall; New York, 1993, (a) 200, (b) 235.
27 Fuller, G. G. *Optical Rheometry of Complex Fluids* Topics in Chemical Engineering, K. E. Gubbins, ed.; Oxford University Press; New York, Oxford, 1995, (a) 117, (b) 109, (c) 149, (d) 167, (e) 193.
28 Coleman, B. D.; Noll, W. "Foundations of linear viscoelasticity" *Rev. Modern Phys.* **1961**, *33*, 239-49.
29 Petrie, C. J. S. *Elongational Flows: Aspects of the Behaviour of Model Elasticoviscous Fluids*; Pitman; London ; San Francisco, 1979.

30 Meissner, J.; Hostettler, J. "A new elongational rheometer for polymer melts and other highly viscoelastic liquids" *Rheol. Acta* **1994**, *33*, 1-21.
31 Macosko, C.; Starita, J. M. "New rheometer is put to the test" *SPE-J.* **1971**, *27 (11)*, 38-42.
32 Plazek, D. J. "Magnetic bearing torsional creep apparatus" *J. Polym. Sci. A-2* **1968**, *6*, 621.
33 Berry, G. C.; Birnboim, M. H.; Park, J. O.; Meitz, D. W.; Plazek, D. J. "A rotational rheometer for rheological rtudies with prescribed strain or stress history" *J. Polym. Sci.: Part B: Polym. Phys.* **1989**, *27*, 273.
34 Rabinowitsch, B. "Über die Viskosität und Elastizität von Solen" *Z. Phys. Chem., Abt. A* **1929**, *145*, 1-26.
35 Barr, G. *A Monograph of Viscometry*; Oxford University Press (Authorized facsimile by University Microfilms, Ann Arbor, MI, 1967); London, 1931.
36 Carslaw, H. S.; Jaeger, J. C. *Operational Methods in Applied Mathematics*; Dover Publications, Inc.; New York, 1948.
37 Shermergor, T. D. "Description of relaxation phenomena in structurally nonhomogeneous polymers by correlation functions" In *Relaxation Phenomena in Polymers*; G. M. Bartenev; Yu. V. Zelenev, eds.; John Wiley & Sons (Halsted Press); New York, 1974.
38 Berry, G. C. "Rheological and rheo-optical studies on nematic solutions of a rodlike polymer: Bingham Award Lecture" *J. Rheology* **1991**, *35*, 943.
39 Meissner, J. "Experimental problems and recent results in polymer melt rheometry" *J. Macromol. Chem., Macromol. Symp.* **1992**, *56*, 25-42.
40 Ostrowsky, N.; Sornette, D.; Parker, R.; Pike, E. R. "Exponential sampling method for light scattering polydispersity analysis" *Opt. Acta* **1981**, *28*, 1059-70.
41 Baumgaertel, M.; Winter, H. H. "Determination of discrete relaxation and retardation time spectra from dynamic mechanical data" *Rheol. Acta* **1989**, *28*, 511-19.
42 Sips, R. "General theory of deformation of viscoelastic substances" *J. Polym. Sci.* **1951**, *7*, 191-205.
43 Nakamura, K.; Wong, C. P.; Berry, G. C. "Strain criterion in nonlinear creep and recovery in concentrated polymer solutions" *J. Polym. Sci.: Polym. Phys. Ed.* **1984**, *22*, 1119-48.
44 Berry, G. C.; Plazek, D. J. "On the use of stretched-exponential functions for both linear viscoelastic creep and stress relaxation" *Rheol. Acta* **1997**, *36*, 320-9.
45 Riande, E.; Markovitz, H. "Approximate relations among compliance functions of linear viscoelasticity for amorphous polymers" *J. Polym. Sci.: Polm. Phys. Ed.* **1975**, *13*, 947-51.
46 Plazek, D. J.; Raghupathi, N.; Orbon, S. J. "Determination of dynamic storage and loss compliances from creep data" *J. Rheol.* **1979**, *23*, 477-88.
47 Markovitz, H. "The reduction principle in linear viscoelasticity" *J. Phys. Chem* **1965**, *69*, 671.
48 Markovitz, H. "Superposition in rheology" *J. Polym. Sci.: Symp.* **1975**, *50*, 431-56.

49 Berry, G. C.; "The viscosity of polymers and their concentrated solutions" *Adv. in Polym. Sci.* **1968**, *5*, 261-357.
50 Berry, G. C. "Crossover behavior in the viscosity of semiflexible polymers: Intermolecular interactions as a function of concentration and molecular weight" *J. Rheol.* **1996**, *40*, 1129-54.
51 Boyer, R. F. "The relation of transition temperatures to chemical structure in high polymers" *Rubber Rev.* **1963**, *36*, 1303-421.
52 Berry, G. C. "Thermodynamic and conformational studies of polystyrene. II. Intrinsic viscosity studies on dilute solutions of linear polystyrenes" *J. Chem. Phys.* **1967**, *46*, 1338.
53 Berry, G. C. "Molecular weight distribution" In *Encyclopedia of Materials Science and Engineering*; M. B. Bever, ed.; Pergamon Press; Oxford, 1986; 3759.
54 Russel, W. B.; Saville, D. A.; Schowalter., W. R. *Colloidal Dispersions*; Cambridge University Press; Cambridge, 1989, (a) 498, (b) 88, (c) 129, (d) 162, (e) 466, (f) 469, (g) 474.
55 Berry, G. C. "Remarks on a relation among the intrinsic viscosity, the radius of gyration, and the translational friction coefficient" *Journal of Polymer Science, Part B: Polymer Physics* **1988**, *26*, 1137-42.
56 Yamakawa, H. *Modern Theory of Polymer Solutions*; Harper and Row; New York, 1971, (a) 266, (b) 314.
57 Flory, P. J.; "Molecular configuration and thermodynamic properties from intrinsic viscosities" *J. Polym. Sci.* **1950**, *5*, 745-7.
58 Casassa, E. F.; Berry, G. C. "Reflections and comments on "Molecular configuration and thermodynamic properties from intrinsic viscosities" by Paul J. Flory and Thomas G Fox" *J. Polym. Sci., Pt. B: Polym. Phys.* **1996**, *34*, 203-6.
59 Casassa, E. F.; Berry, G. C. "Polymer solutions" In *Comprehensive Polymer Science*; G. Allen, ed.; Vol. 2; Pergamon Press; New York, 1988; Chapt. 3.
60 Brandrup, J.; Immergut, E. H., eds. *Polymer Handbook*; 3rd ed.; Wiley; New York, 1989.
61 Casassa, E. F.; Berry, G. C. "Angular distribution of intensity of Rayleigh scattering from comblike branched molecules" *J. Polym. Sci.: Part A-2* **1966**, *4*, 881.
62 Lodge, T. P. "Solvent dynamics, local friction, and the viscoelastic properties of polymer solutions" *J. Phys. Chem.* **1993**, *97*, 1480-7.
63 Harrison, G.; Lamb, J.; Matheson, A. J. "The viscoelastic properties of dilute solutions of polystyrene in toluene" *J. Phys. Chem.* **1966**, *68*, 1072-8.
64 Osaki, K. "Viscoelastic properties of dilute polymer solutions" *Adv. Polym. Sci.* **1973**, *12*, 1-64.
65 Birnboim, M. H. "The viscoelastic properties of low molecular weight polystyrene solutions in high frequency regime: Polymer-solvent interaction" *Proc. IUPAC Macro 82* **1982**, *July 12-16*, 872.

66 Schrag, J. L., *et al.* "Local modification of solvent dynamics by polymeric solutes" *J. Non-Cryst. Solids* **1991**, *131*, 537-43.
67 Yoshizaki, T.; Takaeda, Y.; Yamakawa, H. "On the correlation between the negative intrinsic viscosity and the rotatory relaxation time of solvent molecules in dilute polymer solutions" *Macromolecules* **1993**, *26*, 6891-6.
68 Yamakawa, H. "Concentration dependence of polymer chain configurations in solution" *J. Chem. Phys.* **1961**, *34*, 1360-72.
69 Batchelor, G. K. "The effect of Brownian motion on the bulk stress in a suspension of spherical particles" *J. Fluid Mech.* **1977**, *83*, 97-117.
70 Pal, R. "Rheology of emulsions containing polymeric liquids" In *Encyclopedia of Emulsion Technology*; Paul Becher, ed.; Vol. 4; Marcel Dekker, Inc.; New York, 1996; 93-263.
71 Park, J. O.; Berry, G. C. "Moderately concentrated solutions of polystyrene. 3. Viscoelastic measurements at the Flory Theta temperature" *Macromolecules* **1989**, *22*, 3022-9.
72 de Gennes, P.-G. *Scaling Concepts in Polymer Physics*; Cornell University Press; Ithaca, NY, 1979.
73 Narayanaswamy, O. S. "Annealing of glass" In *Glass: Science and Technology*; D. R. Uhlmann; N. J. Kreidl, ed.; Vol. 3; Academic Press; New York, 1986; 275-318.
74 Plazek, D. J.; Berry, G. C. "Physical aging of polymer glasses" In *Glass: Science and Technology*; D. R. Uhlmann; N. J. Kreidl, ed.; Vol. 3; Academic Press; New York, 1986; 363-99.
75 Graessley, W. W. "The entanglement concept in polymer rheology" *Adv. Polym. Sci.* **1974**, *16*, 1-179.
76 Berry, G. C.; Nakayasu, H.; "Viscosity of poly(vinyl acetate) and its concentrated solutions" *Journal of Polymer Science, Polymer Physics Edition* **1979**, *17*, 1825-44.
77 da Andrade, E. N. *Viscosity and Plasticity*; Chemical Publishing Co.; New York, 1951.
78 Berry, G. C. "The stress-strain behavior of materials exhibiting Andrade creep" *Polym Eng Sci* **1976**, *16*, 777-81.
79 Orbon, S. J.; Plazek, D. J. "The recoverable compliance of a series of bimodal molecular weight blends of polystyrene" *J. Polym. Sci.: Polym. Phys. Ed.* **1979**, *17*, 1871.
80 Berry, G. C. "Terminal retardation times and weights for the Rouse model for a crosslinked network" *J. Polym. Sci.: Part B: Polym. Phys.* **1987**, *25*, 2203-5.
81 Masuda, T.; Takahashi, M.; Onogi, S. "Steady-state compliance of polymer blends" *Appl. Polym. Symp.* **1973**, *20*, 49-60.
82 Kurata, M. "Effect of molecular weight distribution on viscoelastic properties of polymers. 2. Terminal relaxation time and steady-state compliance" *Macromolecules* **1984**, *17*, 895-8.

83 Fujita, H.; Einaga, Y. "Self diffusion and viscoelasticity in entangled systems. II. Steady-state viscosity and compliance of binary blends" *Polymer J.* **1985**, *17*, 1189-95.
84 Montfort, J. P.; Marin, G.; Monge, P. "Molecular weight distribution dependence of the viscoelastic properties of linear polymers: The coupling of reptation and tube-renewal effects" *Macromolecules* **1986**, *19*, 1979-88.
85 des Cloizeaux, J. "Relaxation of entangled polymeric melts" *Macromolecules* **1990**, *23*, 3992-4006.
86 Tsenoglou, C. "Molecular weight polydispersity effects on the viscoelasticity of entangled linear polymers" *Macromoleucules* **1991**, *24*, 1762-7.
87 Berry, G. C. "Rheological properties of blends of rodlike chains with flexible or semiflexible chains" *Trends in Polymer Science* **1993**, *1*, 309.
88 Berry, G. C. "Rheology of blends of liquid crystalline and flexible chain polymers" *Trends Poly. Sci.* **1996**, *4*, 289-92.
89 Plazek, D. J.; Chay, I. C. "The evolution of the viscoelastic retardation spectrum during the development of an epoxy resin network" *J. Polym. Sci.: Part B: Polym. Phys.* **1991**, *29*, 17-29.
90 Winter, H. H.; Mours, M. "Rheology of polymers near liquid-solid transitions" *Adv. Polym. Sci.* **1997**, *134*, 167-234.
91 Plazek, D. J. "Oh, thermorheological simplicity, wherefore art thou?" *J. Rheol.* **1996**, *40*, 987-1014.
92 Plazek, D. J.; Chelko, A. J., Jr. "Temperature dependence of the steady state recoverable compliance of amorphous polymers" *Polymer* **1977**, *18*, 15-8.
93 Inoue, T.; Mizukami, Y.; Okamoto, H.; Matsui, H.; Watanabe, H.; Kanaya, T.; Osaki, K. "Dynamic birefringence of vinyl polymers" *Macromolecules* **1996**, *29*, 6240-5.
94 Struik, L. C. E. *Physical Aging in Amorphous Polymers and Other Materials*; Elsevier; Amsterdam, 1978.
95 Bero, C. A.; Plazek, D. J. "Volume-dependent rate processes in an epoxy resin" *J. Polym. Sci.: Part B: Polym. Phys.* **1991**, *29*, 39-47.
96 Lodge, A. S.; Meissner, J. "On the use of instantaneous strains, superposed on shear and elongational flows of polymeric liquids to test the Gaussian network hypothesis and to estimate the segment concentration and its variation during flow" *Rheol. Acta* **1971**, *11*, 351-2.
97 Coleman, B. D.; Markovitz, H. "Asymptotic relations between shear stresses and normal stresses in general incompressible fluids" *J. Polym. Sci.: Polym. Phys. Ed.* **1974**, *12*, 2195-207.
98 Coleman, B. D.; Markovitz, H. "Normal stress effects in second-order fluids" *J. Appl. Phys.* **1964**, *35*, 1-9.
99 Coleman, B. D.; Dill, E. H.; Toupin, R. A. "A phenomenological theory of streaming birefringence" *Arch. Rational Mech. Anal.* **1970**, *39*, 358-99.

100 Kannan, R. M.; Kornfield, J. A. "The third-normal stress difference in entangled melts: Quantitative stress-optical measurements in oscillatory shear" *Rheol. Acta* **1992**, *31*, 535-44.
101 Bernstein, B.; Kearsley, E. A.; Zapas, L. J. "A study of stress relaxation with finite strain" *Trans. Soc. Rheol.* **1963**, *7*, 391-410.
102 Wagner, M. H.; Laun, H. M. "Nonlinear shear creep and constrained recovery of a LDPE melt" *Rheol. Acta* **1978**, *17*, 138-48.
103 Wagner, M. H.; Stephenson, S. E. "The irreversibility assumption of network disentanglement in flowing polymer melts and its effects on elastic recoil predictions" *J. Rheol.* **1979**, *23*, 489-504.
104 Graessley, W. W.; Park, W. S.; Crawley, R. L. "Experimental tests of constitutive relations for polymers undergoing uniaxial shear flows" *Rheol. Acta* **1977**, *16*, 291-301.
105 Cox, W. P.; Merz, B. H. "Correlation of dynamic and steady flow viscosities" *J. Polym. Sci.* **1958**, *28*, 619-22.
106 Osaki, K.; Bessho, N.; Kojimoto, T.; Kurata, M. "Flow birefringence of polymer solutions in time-dependence field" *J. Rheol.* **1979**, *23*, 457-75.
107 Takahashi, M.; Masuda, T.; Bessho, N.; Osaki, K. "Stress measurements at the start of shear flow: Comparison of data from a modified Weissenberg Rheogoniometer and from flow birefringence" *J. Rheol.* **1980**, *24*, 516-20.
108 Menezes, E. V.; Graessley, W. W. "Nonlinear rheological behavior of polymer systems for several shear-flow histories" *J. Polym. Sci., Polym. Phys. Ed.* **1982**, *20*, 1817-33.
109 Pearson, D. S.; Kiss, A. D.; Fetters, L. J.; Doi, M. "Flow-induced birefringence of concentrated polyisoprene solutions" *J. Rheol.* **1989**, *33*, 517-35.
110 Rochefort, W. E.; Heffner, G. W.; Pearson, D. S.; Miller, R. D.; Cotts, P. M. "Rheological and rheooptical studies of poly(alkylsilanes)" *Macromolecules* **1991**, *24*, 4861-4.
111 Wong, C. P.; Berry, G. C. "Rheological studies on concentrated solutions of heterocyclic polymers" *Polymer* **1979**, *20*, 229-40.
112 Casson, N. "A flow equation for pigment-oil suspensions of the printing ink type" In *Rheology of Disperse Systems*; C. C. Mill, ed.; Pergamon Press; London, 1959; 84-104.
113 Markovitz, H. "Relative rates of creep and relaxation in shear, elongation and isotropic compression" *J. Polym. Sci.: Polym. Phys. Ed.* **1973**, *11*, 1769-77.
114 Kovacs, A. J.; Aklonis, J. J.; Hutchinson, J. M.; Ramos, A. R. "Isobaric volume and enthalpy recovery of glasses. II. A transparent multiparameter theory" *J. Polym. Sci.: Polym. Phys. Ed.* **1979**, *17*, 1097-162.
115 Philippoff, W. "Flow birefringence and stress" *J. Appl. Phys.* **1956**, *27*, 984-9.
116 Philippoff "Elastic stresses and birefringence in flow" *Trans. Soc. Rheol.* **1961**, *5*, 163-91.

117 Janeschitz-Kriegl, H. "Flow birefringence of elastico-viscous polymer systems" *Adv. Polym. Sci.* **1969**, *6*, 170-318.

118 Coleman, B. D.; Dill, E. H. "Photoviscoelasticity: Theory and practice" In *The photoelastic effect and its applications*; J. Kestens, ed.; Springer-Verlag; Berlin, New York, 1975; 455-505.

119 Wales, J. L. S. *The Application of Flow Birefringence to Rheological Studies of Polymer Melts.*; Delft University Press; Delft, 1976.

120 Riande, E.; Saiz, E. *Dipole Moments and Birefringence of Polymers*; Prentice Hall; Englewood Cliffs, N.J., 1992.

121 Read, B. E. "Viscoelastic behavior of amorphous polymers in the glass-rubber transition region: Birefringence studies" *Polym. Eng. Sci.* **1983**, *23*, 835-43.

122 Kornfield, J. A.; Fuller, G. G.; Pearson, D. S. "Third normal stress difference and component relaxation spectra for bidisperse melts under oscillatory shear" *Macromolecules* **1991**, *24*, 5429-41.

123 Takahashi, T. "Measurement of first and second normal stress difference of a polystyrene solution using a simultaneous mechanical and optical measurement technique" In *Fluid Measurement and Instrumentation: 1995*; G. L. Morrison, *et al.*, eds.; Vol. FWD-Vol. 211; Am. Soc. Mech. Eng.; New York, 1995; 31-4.

124 Olson, D. I.; Brown, E. F.; Burghardt, W. R. "Second normal stress difference relaxation in a linear polymer melt following step-strain" *J. Polym. Sci. Part B: Polym. Phys.* **1998**, *36*, 2671-5.

125 Coleman, B. D.; Dill, E. H. "Theory of induced birefringence in materials with memory" *J. Mech. Phys. Solids* **1971**, *19*, 215-43.

126 Osaki, K.; Okamoto, H.; Inoue, T.; Hwang, E.-J. "Molecular interpretation of dynamic birefringence and viscoelasticity of amorphous polymers" *Macromolecules* **1995**, *28*, 3625-30.

127 Mott, P. H.; Roland, C. M. "Birefringence of polymers in the softening zone" *Macromolecules* **1998**, *31*, 7095-8.

128 Lodge, A. S. "Stress relaxation after a sudden shear strain" *Rheol. Acta* **1975**, *14*, 664-5.

129 Osaki, K.; Bessho, N.; Kojimoto, T.; Kurata, M. "Flow birefringence of polymer solutions in time-dependent field. Relation between normal and shear stresses on application of step-shear strain" *J. Rheol.* **1979**, *23*, 617-24.

130 Osaki, K.; Kimura, S.; Kurata, M. "Relaxation of shear and normal stresses in step-shear deformation of a polystyrene solution. Comparison with the predictions of the Doi-Edwards theory" *J. Polym. Sci.: Polym. Phys. Ed.* **1981**, *19*, 517-27.

131 Mott, P. H.; Roland, C. M. "Birefringence of rubber during creep and recovery" *Macromolecules* **1996**, *29*, 8492-6.

132 Osaki, K.; Inoue, T. "Some phenomenological relations for strain-induced birefringence of amorphous polymers" *Nihon Reoroji Gakkaishi* **1991**, *19*, 130-2 (In English).
133 Krieger, I. M. "Rheology of monodisperse latices" *Adv. Colloid Interface Sci.* **1972**, *3*, 111-36.
134 Russel, W. B.; Gast, A. P. "Nonequilibrium statistical mechanics of concentrated colloidal dispersions: Hard spheres in weak flows" *J. Chem. Phys.* **1986**, *84*, 1815-26.
135 van der Werff, J. C.; de Kruif, C. G.; Blom, C.; Mellema, J. "Linear viscoelastic behavior of dense hard-sphere dispersions" *Phys. Rev. A* **1989**, *39*, 795-807.
136 Brady, J. F. "The rheological behavior of concentrated colloidal dispersions" *J. Chem. Phys.* **1993**, *99*, 567-81.
137 Shikata, T.; Pearson, D. S. "Viscoelastic behavior of concentrated spherical suspensions" *J. Rheol.* **1994**, *38*, 601-16.
138 Lionberger, R. A.; Russel, W. B. "High frequency modulus of hard sphere colloids" *J. Rheol.* **1994**, *38*, 1885-908.
139 Lionberger, R. A.; Russel, W. B. "Effectiveness of nonequilibrium closures for the many body forces in concentrated colloidal dispersions" *J. Chem. Phys.* **1997**, *106*, 402-16.
140 Chong, J. S.; Christiansen, E. B.; Baer, A. D. "Rheology of concentrated suspensions" *J. Appl. Polym. Sci.* **1971**, *15*, 2007-21.
141 Beenakker, C. W. J. "The effective viscosity of a concentrated suspension of spheres (And its relation to diffusion)" *Physica A* **1984**, *128A*, 48-81.
142 Beenakker, C. W. J.; Mazur, P. "Diffusion of spheres in a concentrated suspension. II" *Physica A* **1984**, *126A*, 349-70.
143 de Gennes, P. G.; Prost, J. *The Physics of Liquid Crystals*; Oxford U. P.; New York, 1993.
144 Mellema, J.; de Kurif, C. G.; Blom, C.; Vrij, A. "Hard sphere colloidal dispersions: Mechanical relaxation pertaining to thermodynamic forces" *Rheol. Acta* **1987**, *26*, 40-4.
145 Arora, A. K.; Tata, B. V. R., eds. *Ordering and Phase Transitions in Charged Colloids*; VCH Publisher; New York, 1996.
146 Yoshida, J.; Yamanaka, J.; Koka, T.; Ise, N.; Hashimoto, T. "Novel crystallization process in dilute ionic colloids" *Langmuir* **1998**, *14*, 569-74.
147 Weiss, J. A.; Larsen, A. E.; Grier, D. G. "Interactions, dynamics, and elasticity in charge-stabilized colloidal crystals" *J. Chem. Phys.* **1998**, *109*, 8659-66.
148 Meitz, D. W.; Yen, L.; Berry, G. C.; Markovitz, H. "Rheological studies of dispersions of spherical particles in a polymer solution" *J. Rheology* **1988**, *32*, 309-51.

Table 1 Linear Viscoelastic Functions

Shear Compliance	***J(t)***
Shear Modulus	***G(t)***
Bulk Compliance	***B(t)***
Bulk Modulus	***K(t)***
Tensile Compliance	***D(t) = J(t)/3 + B(t)/9***
Tensile Modulus[a]	$1/\hat{E}(s) = 1/3\hat{G}(s) + 1/9\hat{K}(s)$

a. The superscript "^" denotes a Laplace transform.

Table 2 Functions and Parameters Used

Function/Parameter	Symbol	Units
Time	t	T
Frequency	ω	T^{-1}
Strain Component	ε_{ij}	---
Elongational strain	ε	---
Shear strain	γ	---
Rate of shear	$\dot{\gamma}$, $\dot{\varepsilon}$	T^{-1}
Stress Component	S_{ij}	$ML^{-1}T^{-2}$
Shear stress	σ	$ML^{-1}T^{-2}$
Modulus	G, K, E	$ML^{-1}T^{-2}$
Compliance	J, B, D	$M^{-1}LT^{2}$
Viscosity	η	$ML^{-1}T^{-1}$

Table 3 Relations Among Elastic Constants

	K, G	**E, G**	**K, E**	**K, ν**	**E, ν**	**G, ν**
K	K	$\frac{EG}{3[3G - E]}$	K	K	$\frac{E}{3[1 - 2\nu]}$	$\frac{2G[1 + \nu]}{3[1 - 2\nu]}$
E	$\frac{9KG}{3K + G}$	E	E	$3K(1 - 2\nu)$	E	$2G(1 + \nu)$
G	G	G	$\frac{3KE}{9K - E}$	$\frac{3K[1 - 2\nu]}{2[1 + \nu]}$	$\frac{E}{2[1 + \nu]}$	G
ν	$\frac{3K - 2G}{6K + 2G}$	$\frac{E}{2G} - 1$	$\frac{3K - E}{6K}$	ν	ν	ν

$J = 1/G$, $B = 1/K$, $D = 1/E$

Table 4: Geometric Factors in Rheometry

Geometry	Measured		Calculated[a]	
Translational geometries				
Parallel Plate	Force:	$\mathcal{F}$	Stress:	$\sigma = \mathcal{F}/wb$
width,w; breadth b; separation h	Displacement:	D	Strain:	$\gamma = D/h$
Concentric Cylinders	Force:	$\mathcal{F}$	Stress:	$\sigma = \mathcal{F}/2\pi Rh$
inner radius R; gap Δ; height h	Displacement:	D	Strain:	$\gamma = D/R\ln(1 + \Delta/R)$
Rotational geometries				
Parallel Plate	Torque:	$\mathcal{M}$	Stress:	$\sigma = (2r/R)\mathcal{M}/\pi R^3$
outer radius R; separation h	Rotation:	Ω	Strain:	$\gamma(r) = (r/h)\,\Omega$
Cone & Plate	Torque:	$\mathcal{M}$	Stress:	$\sigma = (3/2)\mathcal{M}/\pi R^3$
outer radius R; cone angle $\pi - \alpha$	Rotation:	Ω	Strain:	$\gamma = (1/\alpha)\,\Omega$
Concentric Cylinders	Torque:	$\mathcal{M}$	Stress:	$\sigma = (R/2h)\mathcal{M}/\pi R^3$
inner radius R; gap Δ; height h	Rotation:	Ω	Strain:	$\gamma(r) = (R/\Delta R)\,\Omega f(R,r)$
				$f(R,r) = (R/r)^2 \frac{1 + \Delta/R}{1 + \Delta/2R}$

a σ and γ are the shear stress and strain, respecgively

Table 5: Time-Temperature Superposition Approximation

Temperature Dependent Parameters

Fluid:	**Solid:**
$\eta'(0) = \eta$	$\eta'(0) = \text{cst.}$
$J_\infty = J_s$	$J_\infty = J_e = 1/G_e$
$\tau_c = \eta'(0)J_\infty = \eta J_s$	$\tau_c = \eta'(0)J_\infty = \eta'(0)J_s$

Functions approximately independent of Temperature

Compliances:	**Moduli:**	
$J(t/\tau_c)/J_\infty$	$J_\infty G(t/\tau_c)$	
$J'(\omega\tau_c)/J_\infty$	$J_\infty G'(\omega\tau_c)$	$\eta'(\omega\tau_c)/\eta'(0)$
$J''(\omega\tau_c)/J_\infty$	$J_\infty G''(\omega\tau_c)$	$\eta''(\omega\tau_c)/\eta'(0)$

Relative "Shift Factors" at temperature T_{REF}

$$b_T = b(T,T_{REF}) = J_\infty(T)/J_\infty(T_{REF})$$
$$h_T = h(T,T_{REF}) = \eta(T)/\eta(T_{REF})$$
$$a_T = a(T,T_{REF}) = \tau_c(T)/\tau_c(T_{REF}) = h_T\, b_T$$

Use of relative shift factors to produce a "Master Curve"

Compliances:	**Moduli:**
$J(t/a_T;T)/b_T \approx J(t;T_{REF})$	$b_T G(t/a_T;T) \approx G(t;T_{REF})$
$J'(\omega a_T;T)/b_T \approx J'(\omega;T_{REF})$	$b_T G'(\omega a_T;T) \approx G'(\omega;T_{REF})$
$J''(\omega a_T;T)/b_T \approx J''(\omega;T_{REF})$	$b_T G''(\omega a_T;T) \approx G''(\omega;T_{REF})$
	$\eta'(\omega a_T;T)/h_T \approx \eta'(\omega;T_{REF})$
	$\eta''(\omega a_T;T)/h_T \approx \eta''(\omega;T_{REF})$

Figure Caption

1. Schematic diagram of some of the principal components of a rheometer under the control of a computer and the output signals.

2. Schematic drawing of a device for elongational (tensile) creep and recovery on a strip or fiber. The table at the bottom gives the input/output for the instrument.

3. Schematic drawing of a device for a torsional shear rheometer with a controlled torque input. The table at the bottom gives the input/output for the instrument.

4. Schematic drawing of a device for a torsional shear rheometer with a controlled deformation input. The table at the bottom gives the input/output for the instrument.

5. Schematic drawings of several fixtures used with torsional shear rheometers.

6. Schematic drawings of idealized rheological experiments:
   Upper: The shear stress $\sigma(t)$ resulting from successive jumps in the strain $\gamma(t)$;
   Lower: The shear strain $\gamma(t)$ resulting from successive jumps in the stress $\sigma(t)$

7. Schematic drawings for four viscoelastic experiments discussed in the text.

8. Schematic drawing to illustrate the application of time-temperature superposition for data on the shear creep compliance (assuming that $b_T = 1$ for simplicity). The shifts of the data at each temperature to the reference plot at temperature $T_{REF} = T_5$ are shown by the dashed lines. The indicated experimental range is given as a guideline of actual practice, but could be extended to shorter or longer times on occasion. After an example in reference [18].

9. Illustrative example of isochronal data (for a fixed frequency) corresponding to isothermal data (reduced to the glass transition temperature) for a linear viscoelastic solid. The isochronal data were computed from the isothermal data by the use of the "universal" expression for the temperature dependence of the viscosity discussed in the text; with $b_T = 1$ for simplicity. The vertical dashed lines mark positions of frequency and temperature common to the two representations.

10. Schematic drawing of the viscosity (lower) and the concentration dependent excluded volume factor (upper) vs R_G/Λ based on a relations discussed in the text to illustrate regimes over which various approximations apply; $\Lambda = (M/N_A c)^{1/3}$ equal to the mean separation of molecular centers. From reference [50].

11. Bilogarithmic plot of the viscosity versus $X = \tilde{X}/\pi N_A m_a/M_L$ for various polymers (with m_a/M_L essentially a constant for the examples shown). The variation of $\eta^{(c)}_{LOC}$ with M_n owing to effects on T_g is included in the "constant", which also includes a term to provide vertical separation of the data. From reference [49].

12. Bilogarithmic plot of the viscosity versus φM_w for fractions of poly(vinyl acetate) and its concentrated solutions. Each data set is for the fixed volume fraction φ indicated. The dashed lines indicate the curve that would be obtained if data would be plotted after reduction for the change in T_g with molecular weight and φ. The downward displacement of the data sets for $\varphi < 1$ reflects the suppression of $\eta^{(c)}_{LOC}$ as T_g decreases with decreasing T. The filled points are for data under Flory theta conditions. After an example in reference [76].

13. Schematic drawings to illustrate various linear viscoelastic functions for an oligomer with a low M (top), a polymer with M less than that for entanglement effects (middle), and a polymer with M large enough to exhibit entanglement effects (bottom).

14. Examples of creep compliances and shear moduli for a high molecular weight polymer; the data exhibit entanglement effects for large t (or small frequency). After an example in reference [9].

15. Schematic drawings to illustrate various the linear recoverable compliance and the associated retardation spectrum for several cases.
    Upper: The recoverable compliance and the associated retardation spectra for a polymers with narrow and broad molecular weight distributions, and with M large enough to exhibit entanglement effects.
    Lower: The effect of random crosslinking on the retardation spectrum for a polymer initially with a narrow molecular weight distribution, and with M large enough to exhibit entanglement effects.

16. Bilogarithmic plots of the several reduce functions for a high molecular weight polyethylene with a broad molecular weight distribution: the viscosity $\eta(\dot{\gamma})/\eta(0)$, the total recoverable

compliance $J_s(\dot\gamma)/J_s$ and the first-normal stress difference $S^{(1)}(\dot\gamma)J_s$ as functions of $\tau_c\dot\gamma = J_s\eta(0)\dot\gamma$. The curves are calculated as described in the text. After an example in reference [43] based on data in reference [102] .

17. Bilogarithmic plots of the several reduce functions for a high molecular weight polysytrene with a narrow molecular weight distribution: the viscosity $\eta(\dot\gamma)/\eta(0)$, the dynamic viscosity $\eta'(\omega)/\eta(0)$, the total recoverable compliance $J_s(\dot\gamma)/J_s$, the dynamic storage compliance $J'(\omega)/J_s$, and the first-normal stress difference $S^{(1)}(\dot\gamma)J_s$ as functions of $\tau_c\dot\gamma = J_s\eta(0)\dot\gamma$. After an example in reference [104].

18. An example of the elongational creep and recovery compliances for a material exhibiting a yield strain behavior. The unfilled and filled symbols in (b) show the strain versus $\vartheta^{1/3}$ and the recoverable strain versus the function $(\vartheta + T_e)^{1/3} - \vartheta^{1/3}$ computed for a linear viscoelastic response; the data exhibit quasi-linear response in recovery following creep beyond the yield strain. After an example in reference [111].

19. Semilogarithmic plots the relative viscosity $\eta_{rel} = \eta/\eta_{solv}$ and a reduced modulus $(G_1)_{red}$ versus volume fraction for hard spheres over a range of sphere radius R; $(G_1)_{red} = G_1R^3/kT$, with $G_1 \approx G'(\omega_L)$ in a certain range of frequency for which $G'(\omega_L)$ is about constant, see the text. The data for η_{rel} are from references [135; 137; 140] for unfilled circles, filled circles and squares, respectively; the data from reference [140] represent data from several sources. The data for $(G_1)_{red}$ are from reference [137], for spheres with R/μm equal to 0.060 (pip down), 0.125 (no pip) and 0.225 (pip up). The curves in the lower figure labeled "U", and "L" correspond to the formulae discussed in the text for $\eta'(0)$ and $\eta'(\omega_L)$, respectively, and the curved labeled "D" corresponds to the dilute solution virial series truncated at the term in φ^2, with k' = 1.0. The curve in the upper figure is calculated as described in the text.

20. Data on the dynamic viscosity $\eta'(\omega)$ and an effective storage creep compliance $J'_{EFF}(\omega)$ versus reduced frequency ωa_T for hard spheres (R = 0.060 μm, φ = 0.37) over a range of temperatures as indicated. The dashed line has slope – 1/3, as expected in some treatments discussed in the text. From data given in reference [137].

21. Bilogarithmic plots of the reduce functions for a solution of a high molecular weight polysytrene with a narrow molecular weight distribution filled with crosslinked polystyrene spheres: the viscosity $\eta(\dot\gamma)/\eta_P$ and the total recoverable compliance $J_s(\dot\gamma)/J_s$ as functions of $\tau_c\dot\gamma$

= $J_s\eta_P\dot{\gamma}$, where η_P is the value of $\eta(\dot{\gamma})$ over an intermediate range of $\dot{\gamma}$ for which $\eta(\dot{\gamma})$ is essentially a constant. The weight fraction w_B of beads covers the range shown in the insets; the data for $\eta(\dot{\gamma})/\eta_P$ tending to lie below the bulk of the data are for $w_B = 0.05$. One of the two solvents used corresponded Flory theta conditions for polystyrene at the experimental temperature. After an example in reference [148].

1 Website, S. o. R.; in *http://www.umecheme.maine.edu/sor/default.htm*. 1999,.

2 Staverman, A. J.; Schwarzl, F. "Linear deformation behavior of high polymers" In *Die Physik der Hochpolymeren*; H. A. Stuart, ed.; Vol. IV; Springer-Verlag; Berlin, 1956; Chapt. 1.

3 Treloar, L. R. G. *The Physics of Rubber Elasticity*; 2rd ed.; Oxford University Press; London, 1958, (a) 156, (b) 64, (c) 177.

4 Coleman, B. D., Markovitz, H., and Noll, W. *Viscometric Flows of Non-Newtonian Fluids*; Springer-Verlag; New York, 1966, (a) 34, (b) 55, (c) 54, (d) 46.

5 McCrum, N. G.; Read, B. E.; Williams, G. *Anelastic and Dielectric Effects in Polymeric Solids*; Wiley; New York, 1967.

6 Aklonis, J. J.; MacKnight, W. J.; Shen, M. C. *Introduction to Polymer Viscoelasticity*; Wiley-Interscience; New York, 1972.

7 Bartenev, G. M.; Zelenev, Y. V., eds. *Relaxation Phenomena in Polymers*; John Wiley & Sons (Halsted Press); New York, 1974.

8 Walters, K. *Rheometry*; John Wiley & Sons; New York, 1975, (a) 44, (b) 48, (c) 52, (d) 93, (e) 102, (f) 100.

9 Markovitz, H. "Rheology" In *Physics Vade Mecum*; H. L. Anderson, ed.; Am. Inst. Phys.; New York, 1981; p. 274-86.

10 Plazek, D. J. "Viscoelastic and steady-state rheological response" In *Methods of Experimental Physics*; R. A. Fava, ed.; Vol. 16C; Academic Press; New York, 1980; Chapt. 11.

11 Ferry, J. D. *Viscoelastic Properties of Polymers*; 3rd ed.; John Wiley & Sons Inc.; New York, 1980, (a) 37, (b) 40, (c) 48, (d) 96, (e) 132, (f) 154, (g) 603, (h) 168, (i) 1, (j) 177, (k) 224, (m) 17, (n) 3, (p) 5, (q) 68, (r) 33, (s) 103, (t) 70, (u) 69, (v) 60, (w) 83, (x) 63, (y) 91, (z) 287, (a') 227, (b') 266, (c') 366, (d') 229, (e') 232, (f') 390, (g') 388, (h') 411, (i') 545.

12 Bailey, R. T.; North, A. M.; Pethrick, R. A. *Molecular Motion in High Polymers* The International Series of Monographs on Chemistry, J. E. Baldwin, *et al.*, eds.; Clarendon Press; Oxford, 1981.

13 Christensen, R. M. *Theory of Viscoelasticity*; 2nd. ed.; Academic; New York, 1982, (a) 353, (b) 1, (c) 5, (d) 7.

14 Dealy, J. M. *Rheometers for Molten Plastics*; Van Nostrand Reinhold Co.; New York, 1982, (a) 1, (b) 116, (c) 126, (d) 148, (e) 75, (f) 61.

15 BohdaneckO(´y), M.; KováO(˘r), J. *Viscosity of Polymer Solutions* Polymer Science Library, A. D. Jenkins, ed.; Vol. 2; Elsevier Scientific Publ. Co.; Amsterdam, 1982, (a) 167, (b) 175, (c) 177.

16 Janeschitz-Kriegl, H. *Polymer Melt Rheology and Flow Birefringence*; Springer-Verlag; Berlin ; New York, 1983, (a) 455, (b) 4, (c) 467, (d) 464, (e) 355, (f) 60, (g) 177, (h) 217.

17 Doi, M.; Edwards, S. F. *The Theory of Polymer Dynamics*; Clarendon Press; Oxford, UK, 1986, (a) 222, (b) 366, (c) 218, (d) 91, (e) 226, (f) 281, (g) 255, (h) 121, (i) 166.

18 Berry, G. C.; Plazek, D. J. "Rheology of polymeric fluids" In *Glass: Science and Technology*; D. R. Uhlmann; N. J. Kreidl, ed.; Vol. 3; Academic Press; New York, 1986; 319-62.

19 Bird, R. B.; Armstrong, R. C.; Hassager, O. *Dynamics of Polymeric Liquids. Vol. 1. Fluid Mechanics*; 2nd ed.; John Wiley & Sons, Inc.; New York, 1987, (a) 158, (b) 269, (c) 290.

20 Bird, R. B.; Curtiss, C. C.; Armstrong, R. C.; Hassager, O. *Dynamics of Polymeric Liquids. Vol. 2. Kinetic Theory*; 2nd ed.; John Wiley & Sons, Inc.; New York, 1987.

21 Collyer, A. A.; Clegg, D. W., eds. *Rheological Measurement*; Elsevier Science Co.; New York, 1988.

22 Larson, R. G. *Constitutive Equations for Polymer Melts and Solutions*; Butterworths; Boston, 1988, (a) 49, (b) 93, (c) 318, (d) 118, (e) 120, (f) 233, (g)120, (h) 95.

23 Tschoegl, N. W. *The Phenomenological Theory of Linear Viscoelastic Behavior*; Springer-Verlag; Berlin, 1989, (a) 513, (b) 551, (c) 69, (d) 47, (e) 560, (f) 21, (g) 508, (h) 55, (i) 413, (j) 401, (k) 406, (m) 157, (n) 409, (p) 157, (q) 425.

24 White, J. L. *Principles of Polymer Engineering Rheology*; John Wiley & Sons, Inc.; New York, 1990, (a) 83, (b) 163, (c) 174.

25 Matsuoka, S. *Relaxation Phenomena in Polymers*; Hanser; Munich, 1992.

26 Yanovsky, Y. G. *Polymer Rheology: Theory and Practice*; Chapman & Hall; New York, 1993, (a) 200, (b) 235.

27 Fuller, G. G. *Optical Rheometry of Complex Fluids* Topics in Chemical Engineering, K. E. Gubbins, ed.; Oxford University Press; New York, Oxford, 1995, (a) 117, (b) 109, (c) 149, (d) 167, (e) 193.

28 Coleman, B. D.; Noll, W. "Foundations of linear viscoelasticity" *Rev. Modern Phys.* **1961**, *33*, 239-49.

29 Petrie, C. J. S. *Elongational Flows: Aspects of the Behaviour of Model Elasticoviscous Fluids*; Pitman; London ; San Francisco, 1979.

30 Meissner, J.; Hostettler, J. "A new elongational rheometer for polymer melts and other highly viscoelastic liquids" *Rheol. Acta* **1994**, *33*, 1-21.

31 Macosko, C.; Starita, J. M. "New rheometer is put to the test" *SPE-J.* **1971**, *27 (11)*, 38-42.

32 Plazek, D. J. "Magnetic bearing torsional creep apparatus" *J. Polym. Sci. A-2* **1968**, *6*, 621.

33 Berry, G. C.; Birnboim, M. H.; Park, J. O.; Meitz, D. W.; Plazek, D. J. "A rotational rheometer for rheological rtudies with prescribed strain or stress history" *J. Polym. Sci.: Part B: Polym. Phys.* **1989**, *27*, 273.

34 Rabinowitsch, B. "Über die Viskosität und Elastizität von Solen" *Z. Phys. Chem., Abt. A* **1929**, *145*, 1-26.

35 Barr, G. *A Monograph of Viscometry*; Oxford University Press (Authorized facsimile by University Microfilms, Ann Arbor, MI, 1967); London, 1931.

36 Carslaw, H. S.; Jaeger, J. C. *Operational Methods in Applied Mathematics*; Dover Publications, Inc.; New York, 1948.

37 Shermergor, T. D. "Description of relaxation phenomena in structurally nonhomogeneous polymers by correlation functions" In *Relaxation Phenomena in Polymers*; G. M. Bartenev; Yu. V. Zelenev, eds.; John Wiley & Sons (Halsted Press); New York, 1974.

38 Berry, G. C. "Rheological and rheo-optical studies on nematic solutions of a rodlike polymer: Bingham Award Lecture" *J. Rheology* **1991**, *35*, 943.

39 Meissner, J. "Experimental problems and recent results in polymer melt rheometry" *J. Macromol. Chem., Macromol. Symp.* **1992**, *56*, 25-42.

40 Ostrowsky, N.; Sornette, D.; Parker, R.; Pike, E. R. "Exponential sampling method for light scattering polydispersity analysis" *Opt. Acta* **1981**, *28*, 1059-70.

41 Baumgaertel, M.; Winter, H. H. "Determination of discrete relaxation and retardation time spectra from dynamic mechanical data" *Rheol. Acta* **1989**, *28*, 511-19.

42 Sips, R. "General theory of deformation of viscoelastic substances" *J. Polym. Sci.* **1951**, *7*, 191-205.

43 Nakamura, K.; Wong, C. P.; Berry, G. C. "Strain criterion in nonlinear creep and recovery in concentrated polymer solutions" *J. Polym. Sci.: Polym. Phys. Ed.* **1984**, *22*, 1119-48.

44 Berry, G. C.; Plazek, D. J. "On the use of stretched-exponential functions for both linear viscoelastic creep and stress relaxation" *Rheol. Acta* **1997**, *36*, 320-9.

45 Riande, E.; Markovitz, H. "Approximate relations among compliance functions of linear viscoelasticity for amorphous polymers" *J. Polym. Sci.: Polm. Phys. Ed.* **1975**, *13*, 947-51.

46 Plazek, D. J.; Raghupathi, N.; Orbon, S. J. "Determination of dynamic storage and loss compliances from creep data" *J. Rheol.* **1979**, *23*, 477-88.

47 Markovitz, H. "The reduction principle in linear viscoelasticity" *J. Phys. Chem* **1965**, *69*, 671.

48 Markovitz, H. "Superposition in rheology" *J. Polym. Sci.: Symp.* **1975**, *50*, 431-56.

49 Berry, G. C.; "The viscosity of polymers and their concentrated solutions" *Adv. in Polym. Sci.* **1968**, *5*, 261-357.

50 Berry, G. C. "Crossover behavior in the viscosity of semiflexible polymers: Intermolecular interactions as a function of concentration and molecular weight" *J. Rheol.* **1996**, *40*, 1129-54.

51 Boyer, R. F. "The relation of transition temperatures to chemical structure in high polymers" *Rubber Rev.* **1963**, *36*, 1303-421.
52 Berry, G. C. "Thermodynamic and conformational studies of polystyrene. II. Intrinsic viscosity studies on dilute solutions of linear polystyrenes" *J. Chem. Phys.* **1967**, *46*, 1338.
53 Berry, G. C. "Molecular weight distribution" In *Encyclopedia of Materials Science and Engineering*; M. B. Bever, ed.; Pergamon Press; Oxford, 1986; 3759.
54 Russel, W. B.; Saville, D. A.; Schowalter., W. R. *Colloidal Dispersions*; Cambridge University Press; Cambridge, 1989, (a) 498, (b) 88, (c) 129, (d) 162, (e) 466, (f) 469, (g) 474.
55 Berry, G. C. "Remarks on a relation among the intrinsic viscosity, the radius of gyration, and the translational friction coefficient" *Journal of Polymer Science, Part B: Polymer Physics* **1988**, *26*, 1137-42.
56 Yamakawa, H. *Modern Theory of Polymer Solutions*; Harper and Row; New York, 1971, (a) 266, (b) 314.
57 Flory, P. J.; "Molecular configuration and thermodynamic properties from intrinsic viscosities" *J. Polym. Sci.* **1950**, *5*, 745-7.
58 Casassa, E. F.; Berry, G. C. "Reflections and comments on "Molecular configuration and thermodynamic properties from intrinsic viscosities" by Paul J. Flory and Thomas G Fox" *J. Polym. Sci., Pt. B: Polym. Phys.* **1996**, *34*, 203-6.
59 Casassa, E. F.; Berry, G. C. "Polymer solutions" In *Comprehensive Polymer Science*; G. Allen, ed.; Vol. 2; Pergamon Press; New York, 1988; Chapt. 3.
60 Brandrup, J.; Immergut, E. H., eds. *Polymer Handbook*; 3rd ed.; Wiley; New York, 1989.
61 Casassa, E. F.; Berry, G. C. "Angular distribution of intensity of Rayleigh scattering from comblike branched molecules" *J. Polym. Sci.: Part A-2* **1966**, *4*, 881.
62 Lodge, T. P. "Solvent dynamics, local friction, and the viscoelastic properties of polymer solutions" *J. Phys. Chem.* **1993**, *97*, 1480-7.
63 Harrison, G.; Lamb, J.; Matheson, A. J. "The viscoelastic properties of dilute solutions of polystyrene in toluene" *J. Phys. Chem.* **1966**, *68*, 1072-8.
64 Osaki, K. "Viscoelastic properties of dilute polymer solutions" *Adv. Polym. Sci.* **1973**, *12*, 1-64.
65 Birnboim, M. H. "The viscoelastic properties of low molecular weight polystyrene solutions in high frequency regime: Polymer-solvent interaction" *Proc. IUPAC Macro 82* **1982**, *July 12-16*, 872.
66 Schrag, J. L., *et al.* "Local modification of solvent dynamics by polymeric solutes" *J. Non-Cryst. Solids* **1991**, *131*, 537-43.

67 Yoshizaki, T.; Takaeda, Y.; Yamakawa, H. "On the correlation between the negative intrinsic viscosity and the rotatory relaxation time of solvent molecules in dilute polymer solutions" *Macromolecules* **1993**, *26*, 6891-6.
68 Yamakawa, H. "Concentration dependence of polymer chain configurations in solution" *J. Chem. Phys.* **1961**, *34*, 1360-72.
69 Batchelor, G. K. "The effect of Brownian motion on the bulk stress in a suspension of spherical particles" *J. Fluid Mech.* **1977**, *83*, 97-117.
70 Pal, R. "Rheology of emulsions containing polymeric liquids" In *Encyclopedia of Emulsion Technology*; Paul Becher, ed.; Vol. 4; Marcel Dekker, Inc.; New York, 1996; 93-263.
71 Park, J. O.; Berry, G. C. "Moderately concentrated solutions of polystyrene. 3. Viscoelastic measurements at the Flory Theta temperature" *Macromolecules* **1989**, *22*, 3022-9.
72 de Gennes, P.-G. *Scaling Concepts in Polymer Physics*; Cornell University Press; Ithaca, NY, 1979.
73 Narayanaswamy, O. S. "Annealing of glass" In *Glass: Science and Technology*; D. R. Uhlmann; N. J. Kreidl, ed.; Vol. 3; Academic Press; New York, 1986; 275-318.
74 Plazek, D. J.; Berry, G. C. "Physical aging of polymer glasses" In *Glass: Science and Technology*; D. R. Uhlmann; N. J. Kreidl, ed.; Vol. 3; Academic Press; New York, 1986; 363-99.
75 Graessley, W. W. "The entanglement concept in polymer rheology" *Adv. Polym. Sci.* **1974**, *16*, 1-179.
76 Berry, G. C.; Nakayasu, H.; "Viscosity of poly(vinyl acetate) and its concentrated solutions" *Journal of Polymer Science, Polymer Physics Edition* **1979**, *17*, 1825-44.
77 da Andrade, E. N. *Viscosity and Plasticity*; Chemical Publishing Co.; New York, 1951.
78 Berry, G. C. "The stress-strain behavior of materials exhibiting Andrade creep" *Polym Eng Sci* **1976**, *16*, 777-81.
79 Orbon, S. J.; Plazek, D. J. "The recoverable compliance of a series of bimodal molecular weight blends of polystyrene" *J. Polym. Sci.: Polym. Phys. Ed.* **1979**, *17*, 1871.
80 Berry, G. C. "Terminal retardation times and weights for the Rouse model for a crosslinked network" *J. Polym. Sci.: Part B: Polym. Phys.* **1987**, *25*, 2203-5.
81 Masuda, T.; Takahashi, M.; Onogi, S. "Steady-state compliance of polymer blends" *Appl. Polym. Symp.* **1973**, *20*, 49-60.
82 Kurata, M. "Effect of molecular weight distribution on viscoelastic properties of polymers. 2. Terminal relaxation time and steady-state compliance" *Macromolecules* **1984**, *17*, 895-8.
83 Fujita, H.; Einaga, Y. "Self diffusion and viscoelasticity in entangled systems. II. Steady-state viscosity and compliance of binary blends" *Polymer J.* **1985**, *17*, 1189-95.

84 Montfort, J. P.; Marin, G.; Monge, P. "Molecular weight distribution dependence of the viscoelastic properties of linear polymers: The coupling of reptation and tube-renewal effects" *Macromolecules* **1986**, *19*, 1979-88.
85 des Cloizeaux, J. "Relaxation of entangled polymeric melts" *Macromolecules* **1990**, *23*, 3992-4006.
86 Tsenoglou, C. "Molecular weight polydispersity effects on the viscoelasticity of entangled linear polymers" *Macromoleucules* **1991**, *24*, 1762-7.
87 Berry, G. C. "Rheological properties of blends of rodlike chains with flexible or semiflexible chains" *Trends in Polymer Science* **1993**, *1*, 309.
88 Berry, G. C. "Rheology of blends of liquid crystalline and flexible chain polymers" *Trends Poly. Sci.* **1996**, *4*, 289-92.
89 Plazek, D. J.; Chay, I. C. "The evolution of the viscoelastic retardation spectrum during the development of an epoxy resin network" *J. Polym. Sci.: Part B: Polym. Phys.* **1991**, *29*, 17-29.
90 Winter, H. H.; Mours, M. "Rheology of polymers near liquid-solid transitions" *Adv. Polym. Sci.* **1997**, *134*, 167-234.
91 Plazek, D. J. "Oh, thermorheological simplicity, wherefore art thou?" *J. Rheol.* **1996**, *40*, 987-1014.
92 Plazek, D. J.; Chelko, A. J., Jr. "Temperature dependence of the steady state recoverable compliance of amorphous polymers" *Polymer* **1977**, *18*, 15-8.
93 Inoue, T.; Mizukami, Y.; Okamoto, H.; Matsui, H.; Watanabe, H.; Kanaya, T.; Osaki, K. "Dynamic birefringence of vinyl polymers" *Macromolecules* **1996**, *29*, 6240-5.
94 Struik, L. C. E. *Physical Aging in Amorphous Polymers and Other Materials*; Elsevier; Amsterdam, 1978.
95 Bero, C. A.; Plazek, D. J. "Volume-dependent rate processes in an epoxy resin" *J. Polym. Sci.: Part B: Polym. Phys.* **1991**, *29*, 39-47.
96 Lodge, A. S.; Meissner, J. "On the use of instantaneous strains, superposed on shear and elongational flows of polymeric liquids to test the Gaussian network hypothesis and to estimate the segment concentration and its variation during flow" *Rheol. Acta* **1971**, *11*, 351-2.
97 Coleman, B. D.; Markovitz, H. "Asymptotic relations between shear stresses and normal stresses in general incompressible fluids" *J. Polym. Sci.: Polym. Phys. Ed.* **1974**, *12*, 2195-207.
98 Coleman, B. D.; Markovitz, H. "Normal stress effects in second-order fluids" *J. Appl. Phys.* **1964**, *35*, 1-9.
99 Coleman, B. D.; Dill, E. H.; Toupin, R. A. "A phenomenological theory of streaming birefringence" *Arch. Rational Mech. Anal.* **1970**, *39*, 358-99.
100 Kannan, R. M.; Kornfield, J. A. "The third-normal stress difference in entangled melts: Quantitative stress-optical measurements in oscillatory shear" *Rheol. Acta* **1992**, *31*, 535-44.

101 Bernstein, B.; Kearsley, E. A.; Zapas, L. J. "A study of stress relaxation with finite strain" *Trans. Soc. Rheol.* **1963**, *7*, 391-410.

102 Wagner, M. H.; Laun, H. M. "Nonlinear shear creep and constrained recovery of a LDPE melt" *Rheol. Acta* **1978**, *17*, 138-48.

103 Wagner, M. H.; Stephenson, S. E. "The irreversibility assumption of network disentanglement in flowing polymer melts and its effects on elastic recoil predictions" *J. Rheol.* **1979**, *23*, 489-504.

104 Graessley, W. W.; Park, W. S.; Crawley, R. L. "Experimental tests of constitutive relations for polymers undergoing uniaxial shear flows" *Rheol. Acta* **1977**, *16*, 291-301.

105 Cox, W. P.; Merz, B. H. "Correlation of dynamic and steady flow viscosities" *J. Polym. Sci.* **1958**, *28*, 619-22.

106 Osaki, K.; Bessho, N.; Kojimoto, T.; Kurata, M. "Flow birefringence of polymer solutions in time-dependence field" *J. Rheol.* **1979**, *23*, 457-75.

107 Takahashi, M.; Masuda, T.; Bessho, N.; Osaki, K. "Stress measurements at the start of shear flow: Comparison of data from a modified Weissenberg Rheogoniometer and from flow birefringence" *J. Rheol.* **1980**, *24*, 516-20.

108 Menezes, E. V.; Graessley, W. W. "Nonlinear rheological behavior of polymer systems for several shear-flow histories" *J. Polym. Sci., Polym. Phys. Ed.* **1982**, *20*, 1817-33.

109 Pearson, D. S.; Kiss, A. D.; Fetters, L. J.; Doi, M. "Flow-induced birefringence of concentrated polyisoprene solutions" *J. Rheol.* **1989**, *33*, 517-35.

110 Rochefort, W. E.; Heffner, G. W.; Pearson, D. S.; Miller, R. D.; Cotts, P. M. "Rheological and rheooptical studies of poly(alkylsilanes)" *Macromolecules* **1991**, *24*, 4861-4.

111 Wong, C. P.; Berry, G. C. "Rheological studies on concentrated solutions of heterocyclic polymers" *Polymer* **1979**, *20*, 229-40.

112 Casson, N. "A flow equation for pigment-oil suspensions of the printing ink type" In *Rheology of Disperse Systems*; C. C. Mill, ed.; Pergamon Press; London, 1959; 84-104.

113 Markovitz, H. "Relative rates of creep and relaxation in shear, elongation and isotropic compression" *J. Polym. Sci.: Polym. Phys. Ed.* **1973**, *11*, 1769-77.

114 Kovacs, A. J.; Aklonis, J. J.; Hutchinson, J. M.; Ramos, A. R. "Isobaric volume and enthalpy recovery of glasses. II. A transparent multiparameter theory" *J. Polym. Sci.: Polym. Phys. Ed.* **1979**, *17*, 1097-162.

115 Philippoff, W. "Flow birefringence and stress" *J. Appl. Phys.* **1956**, *27*, 984-9.

116 Philippoff "Elastic stresses and birefringence in flow" *Trans. Soc. Rheol.* **1961**, *5*, 163-91.

117 Janeschitz-Kriegl, H. "Flow birefringence of elastico-viscous polymer systems" *Adv. Polym. Sci.* **1969**, *6*, 170-318.

118 Coleman, B. D.; Dill, E. H. "Photoviscoelasticity: Theory and practice" In *The photoelastic effect and its applications*; J. Kestens, ed.; Springer-Verlag; Berlin, New York, 1975; 455-505.
119 Wales, J. L. S. *The Application of Flow Birefringence to Rheological Studies of Polymer Melts.*; Delft University Press; Delft, 1976.
120 Riande, E.; Saiz, E. *Dipole Moments and Birefringence of Polymers*; Prentice Hall; Englewood Cliffs, N.J., 1992.
121 Read, B. E. "Viscoelastic behavior of amorphous polymers in the glass-rubber transition region: Birefringence studies" *Polym. Eng. Sci.* **1983**, *23*, 835-43.
122 Kornfield, J. A.; Fuller, G. G.; Pearson, D. S. "Third normal stress difference and component relaxation spectra for bidisperse melts under oscillatory shear" *Macromolecules* **1991**, *24*, 5429-41.
123 Takahashi, T. "Measurement of first and second normal stress difference of a polystyrene solution using a simultaneous mechanical and optical measurement technique" In *Fluid Measurement and Instrumentation: 1995*; G. L. Morrison, *et al.*, eds.; Vol. FWD-Vol. 211; Am. Soc. Mech. Eng.; New York, 1995; 31-4.
124 Olson, D. I.; Brown, E. F.; Burghardt, W. R. "Second normal stress difference relaxation in a linear polymer melt following step-strain" *J. Polym. Sci. Part B: Polym. Phys.* **1998**, *36*, 2671-5.
125 Coleman, B. D.; Dill, E. H. "Theory of induced birefringence in materials with memory" *J. Mech. Phys. Solids* **1971**, *19*, 215-43.
126 Osaki, K.; Okamoto, H.; Inoue, T.; Hwang, E.-J. "Molecular interpretation of dynamic birefringence and viscoelasticity of amorphous polymers" *Macromolecules* **1995**, *28*, 3625-30.
127 Mott, P. H.; Roland, C. M. "Birefringence of polymers in the softening zone" *Macromolecules* **1998**, *31*, 7095-8.
128 Lodge, A. S. "Stress relaxation after a sudden shear strain" *Rheol. Acta* **1975**, *14*, 664-5.
129 Osaki, K.; Bessho, N.; Kojimoto, T.; Kurata, M. "Flow birefringence of polymer solutions in time-dependent field. Relation between normal and shear stresses on application of step-shear strain" *J. Rheol.* **1979**, *23*, 617-24.
130 Osaki, K.; Kimura, S.; Kurata, M. "Relaxation of shear and normal stresses in step-shear deformation of a polystyrene solution. Comparison with the predictions of the Doi-Edwards theory" *J. Polym. Sci.: Polym. Phys. Ed.* **1981**, *19*, 517-27.
131 Mott, P. H.; Roland, C. M. "Birefringence of rubber during creep and recovery" *Macromolecules* **1996**, *29*, 8492-6.
132 Osaki, K.; Inoue, T. "Some phenomenological relations for strain-induced birefringence of amorphous polymers" *Nihon Reoroji Gakkaishi* **1991**, *19*, 130-2 (In English).
133 Krieger, I. M. "Rheology of monodisperse latices" *Adv. Colloid Interface Sci.* **1972**, *3*, 111-36.

134 Russel, W. B.; Gast, A. P. "Nonequilibrium statistical mechanics of concentrated colloidal dispersions: Hard spheres in weak flows" *J. Chem. Phys.* **1986**, *84*, 1815-26.
135 van der Werff, J. C.; de Kruif, C. G.; Blom, C.; Mellema, J. "Linear viscoelastic behavior of dense hard-sphere dispersions" *Phys. Rev. A* **1989**, *39*, 795-807.
136 Brady, J. F. "The rheological behavior of concentrated colloidal dispersions" *J. Chem. Phys.* **1993**, *99*, 567-81.
137 Shikata, T.; Pearson, D. S. "Viscoelastic behavior of concentrated spherical suspensions" *J. Rheol.* **1994**, *38*, 601-16.
138 Lionberger, R. A.; Russel, W. B. "High frequency modulus of hard sphere colloids" *J. Rheol.* **1994**, *38*, 1885-908.
139 Lionberger, R. A.; Russel, W. B. "Effectiveness of nonequilibrium closures for the many body forces in concentrated colloidal dispersions" *J. Chem. Phys.* **1997**, *106*, 402-16.
140 Chong, J. S.; Christiansen, E. B.; Baer, A. D. "Rheology of concentrated suspensions" *J. Appl. Polym. Sci.* **1971**, *15*, 2007-21.
141 Beenakker, C. W. J. "The effective viscosity of a concentrated suspension of spheres (And its relation to diffusion)" *Physica A* **1984**, *128A*, 48-81.
142 Beenakker, C. W. J.; Mazur, P. "Diffusion of spheres in a concentrated suspension. II" *Physica A* **1984**, *126A*, 349-70.
143 de Gennes, P. G.; Prost, J. *The Physics of Liquid Crystals*; Oxford U. P.; New York, 1993.
144 Mellema, J.; de Kurif, C. G.; Blom, C.; Vrij, A. "Hard sphere colloidal dispersions: Mechanical relaxation pertaining to thermodynamic forces" *Rheol. Acta* **1987**, *26*, 40-4.
145 Arora, A. K.; Tata, B. V. R., eds. *Ordering and Phase Transitions in Charged Colloids*; VCH Publisher; New York, 1996.
146 Yoshida, J.; Yamanaka, J.; Koka, T.; Ise, N.; Hashimoto, T. "Novel crystallization process in dilute ionic colloids" *Langmuir* **1998**, *14*, 569-74.
147 Weiss, J. A.; Larsen, A. E.; Grier, D. G. "Interactions, dynamics, and elasticity in charge-stabilized colloidal crystals" *J. Chem. Phys.* **1998**, *109*, 8659-66.
148 Meitz, D. W.; Yen, L.; Berry, G. C.; Markovitz, H. "Rheological studies of dispersions of spherical particles in a polymer solution" *J. Rheology* **1988**, *32*, 309-51.

Schematic of Rheometer System

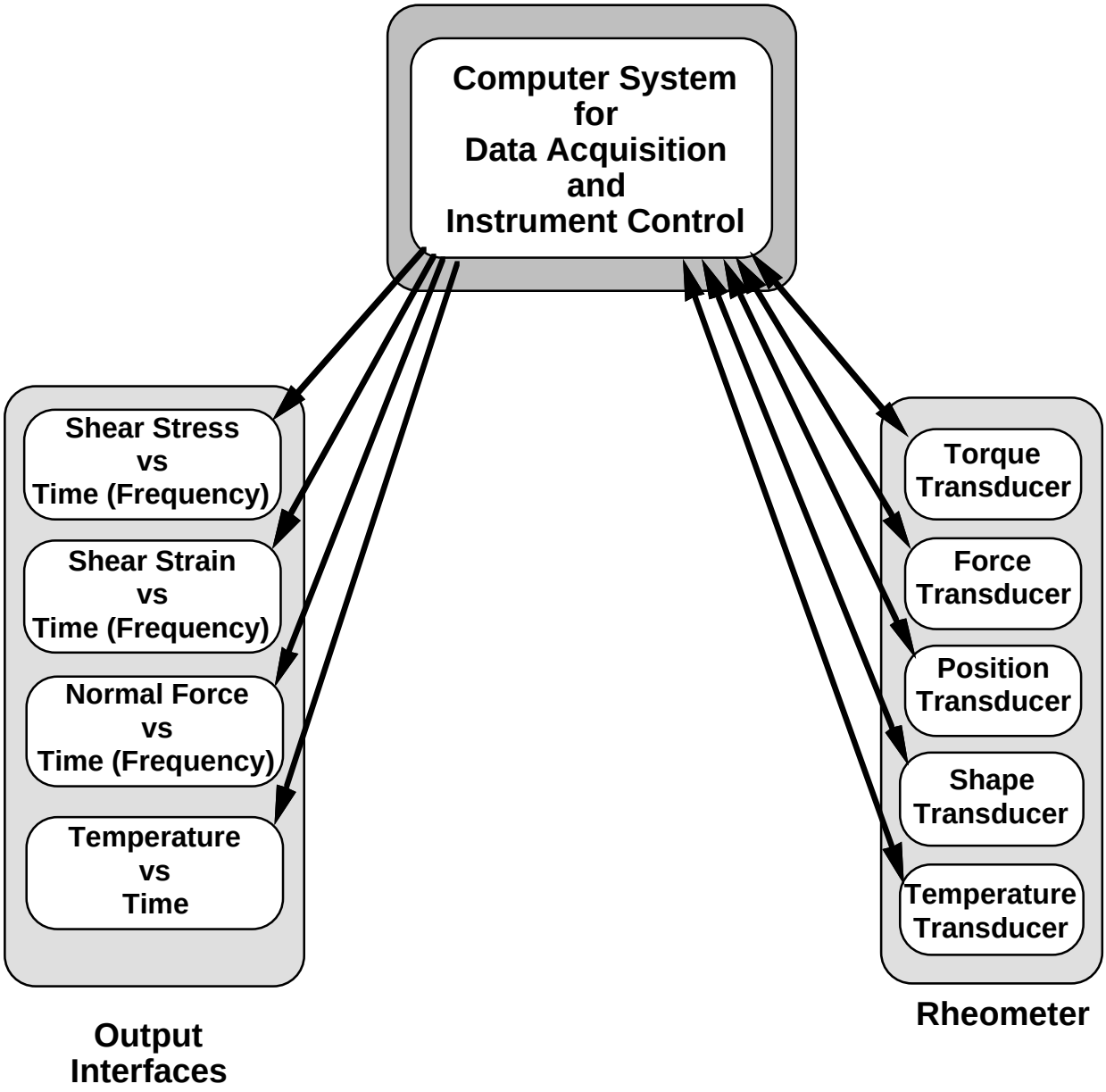

Figure 1

TENSILE CREEP AND RECOVERY

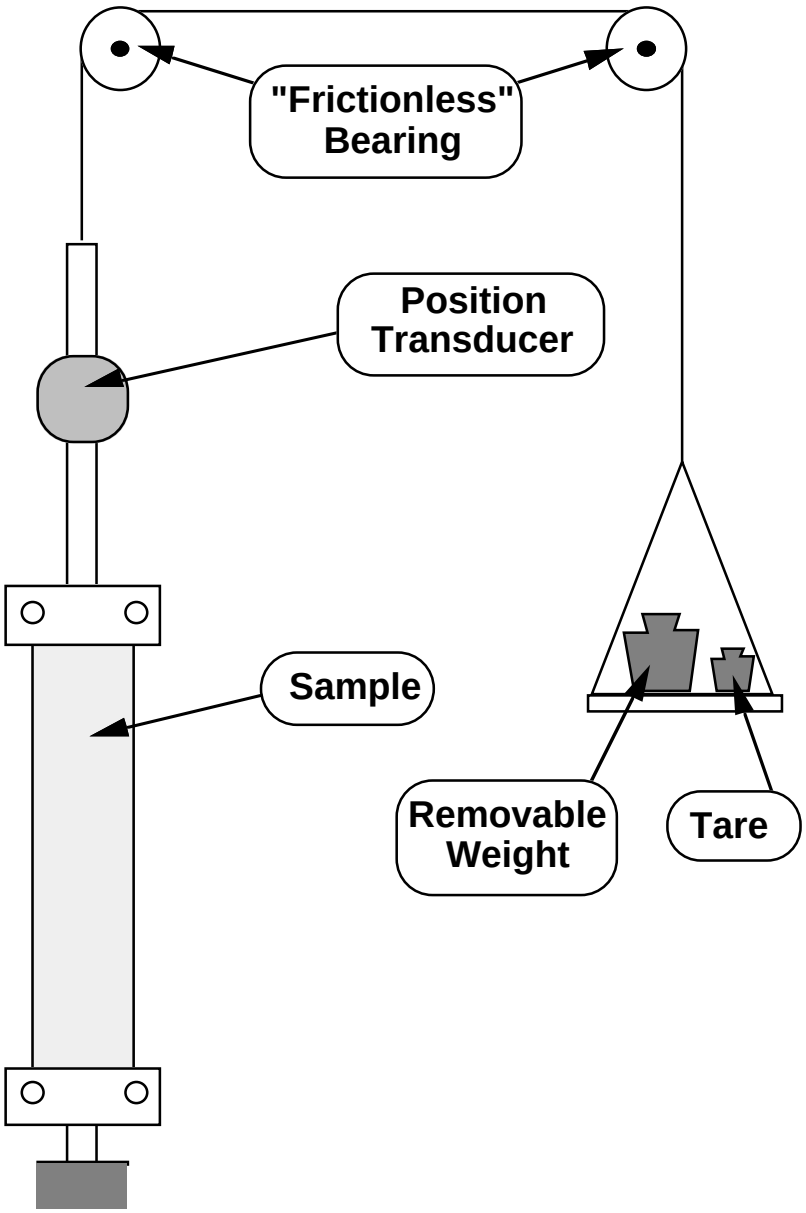

Device	Input	Output
Removable Weight	Controlled weight	Controlled force
Position Transducer	Measure of shaft position	Voltage (current)

Figure 2

CONTROLLED STRESS RHEOMETER

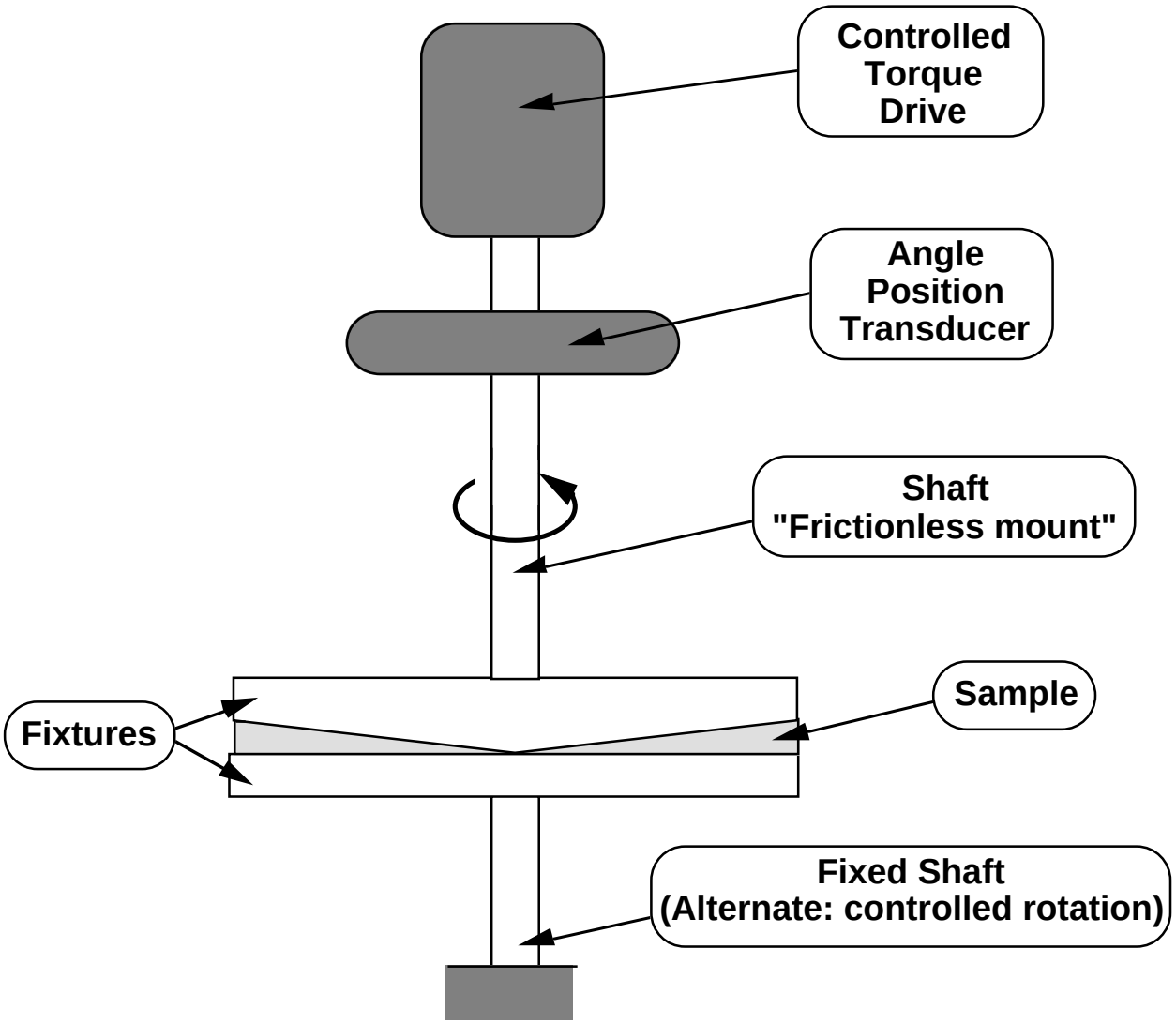

Device	Input	Output
Controlled Torque Drive	Controlled voltage	Controlled torque
Angle Position Transducer	Measure of shaft angle	Voltage (current)

Figure 3

CONTROLLED DEFORMATION RHEOMETER

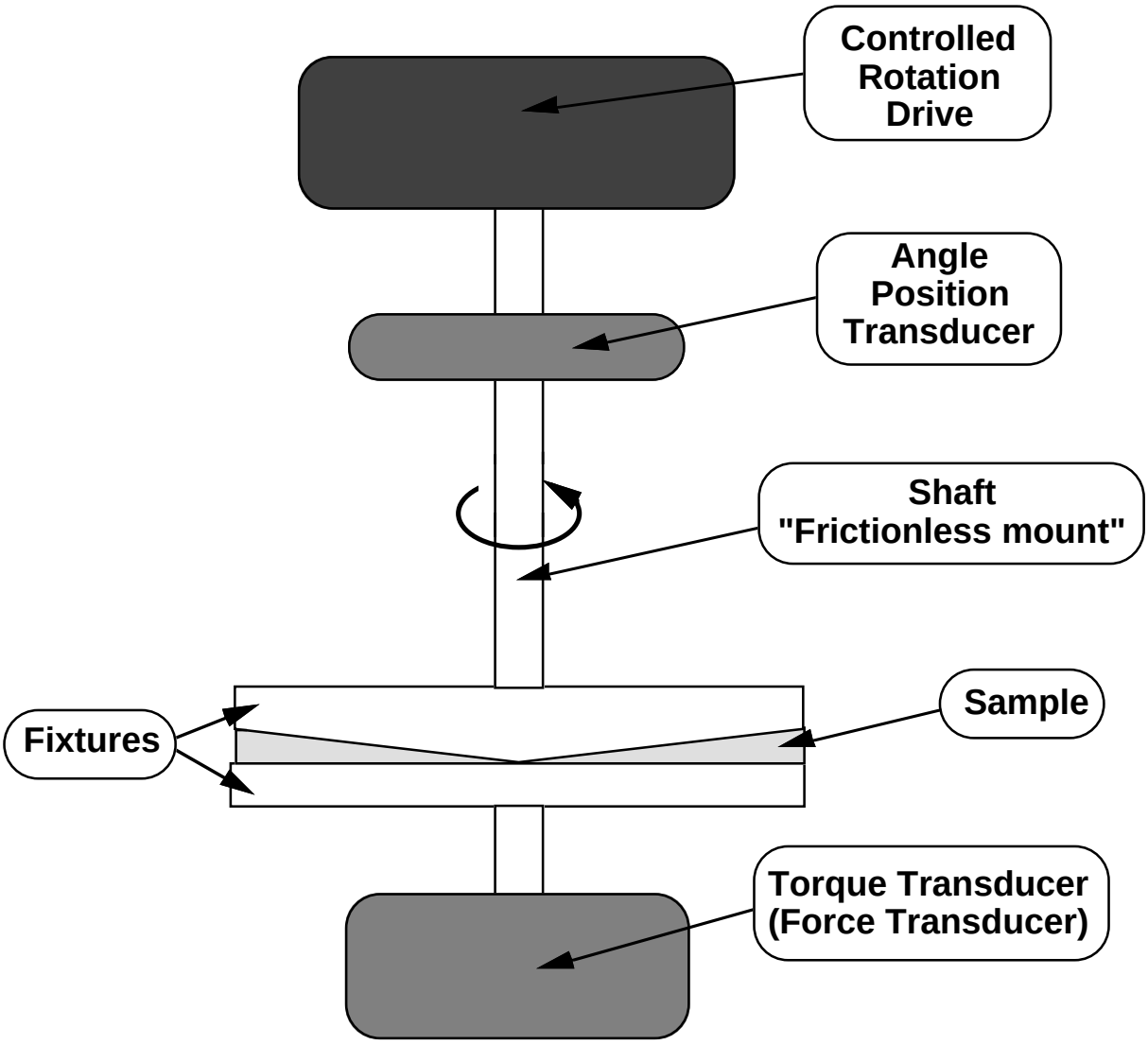

Device	Input	Output
Controlled Deformation Drive	Controlled voltage	Controlled shaft rotation

Figure 4

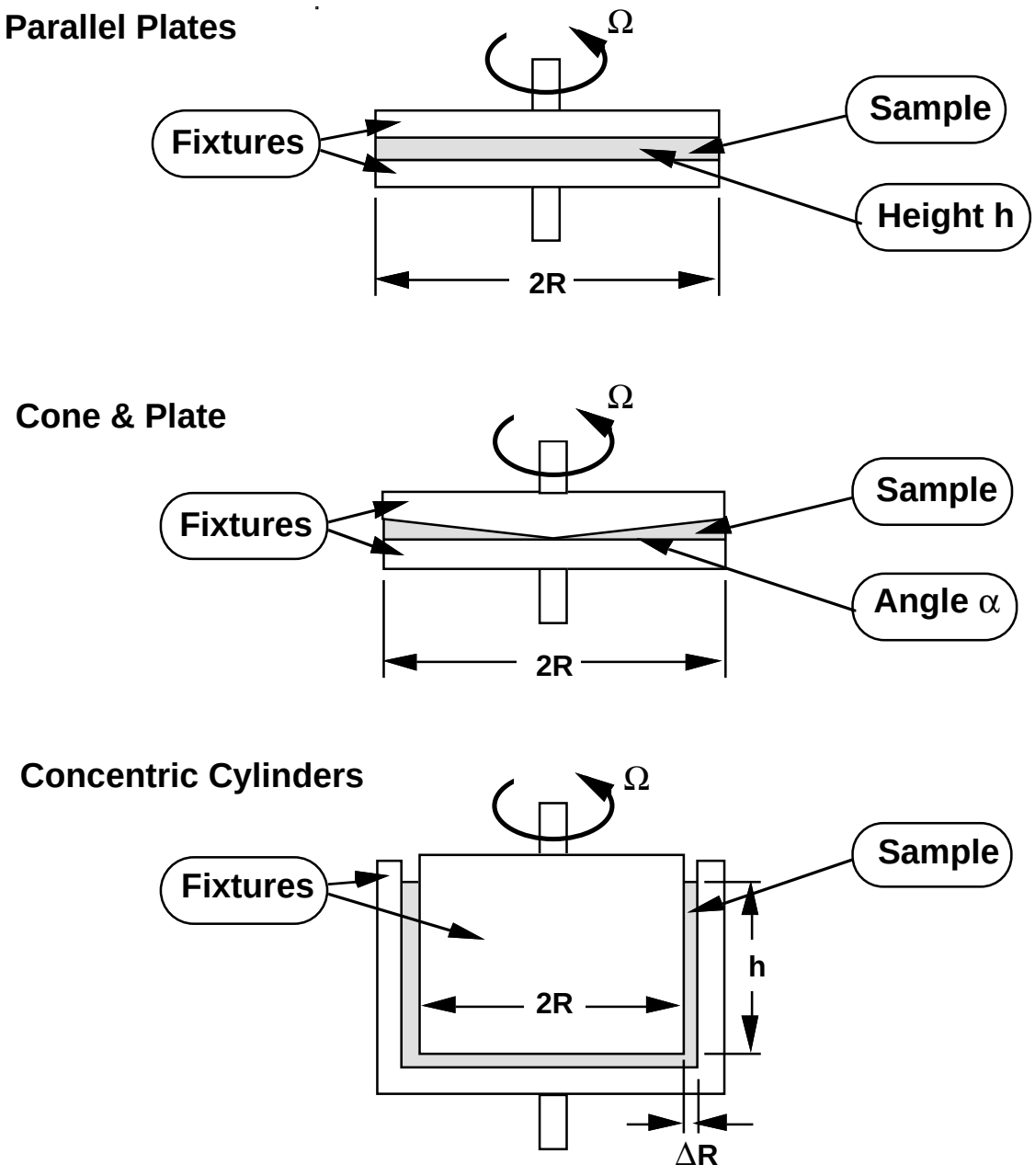
Parallel Plates
Ω
Fixtures
Sample
Height h
2R
Cone & Plate
Ω
Fixtures
Sample
Angle α
2R
Concentric Cylinders
Ω
Fixtures
Sample
h
2R
ΔR

Figure 5

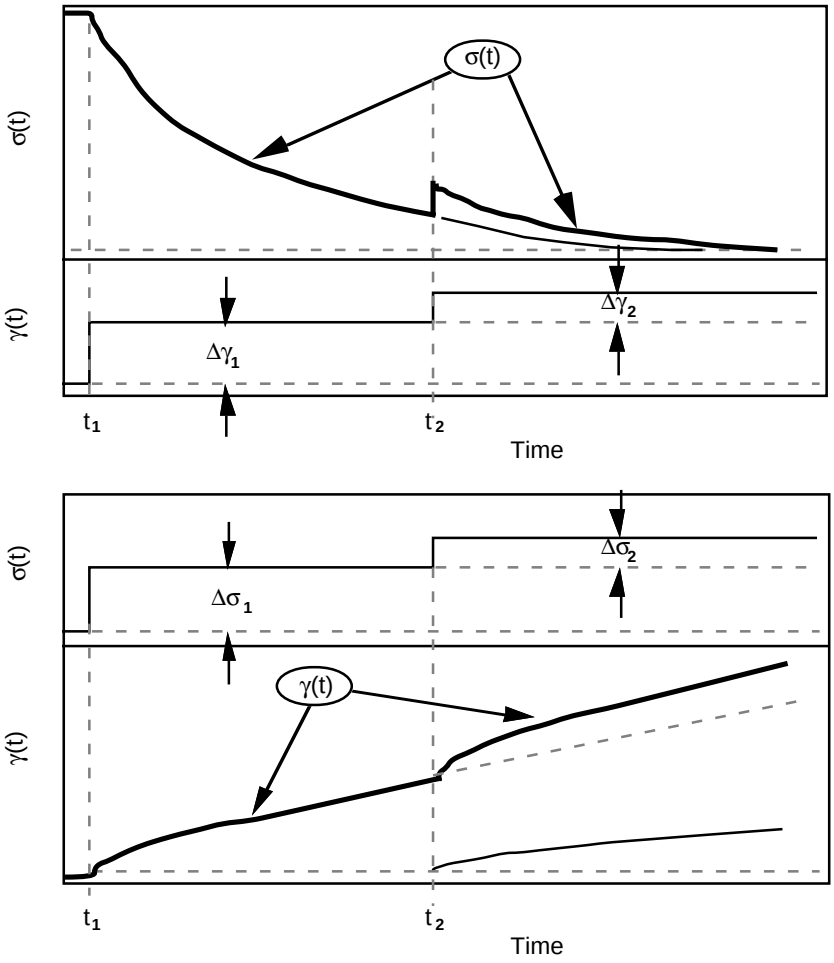

Figure 6

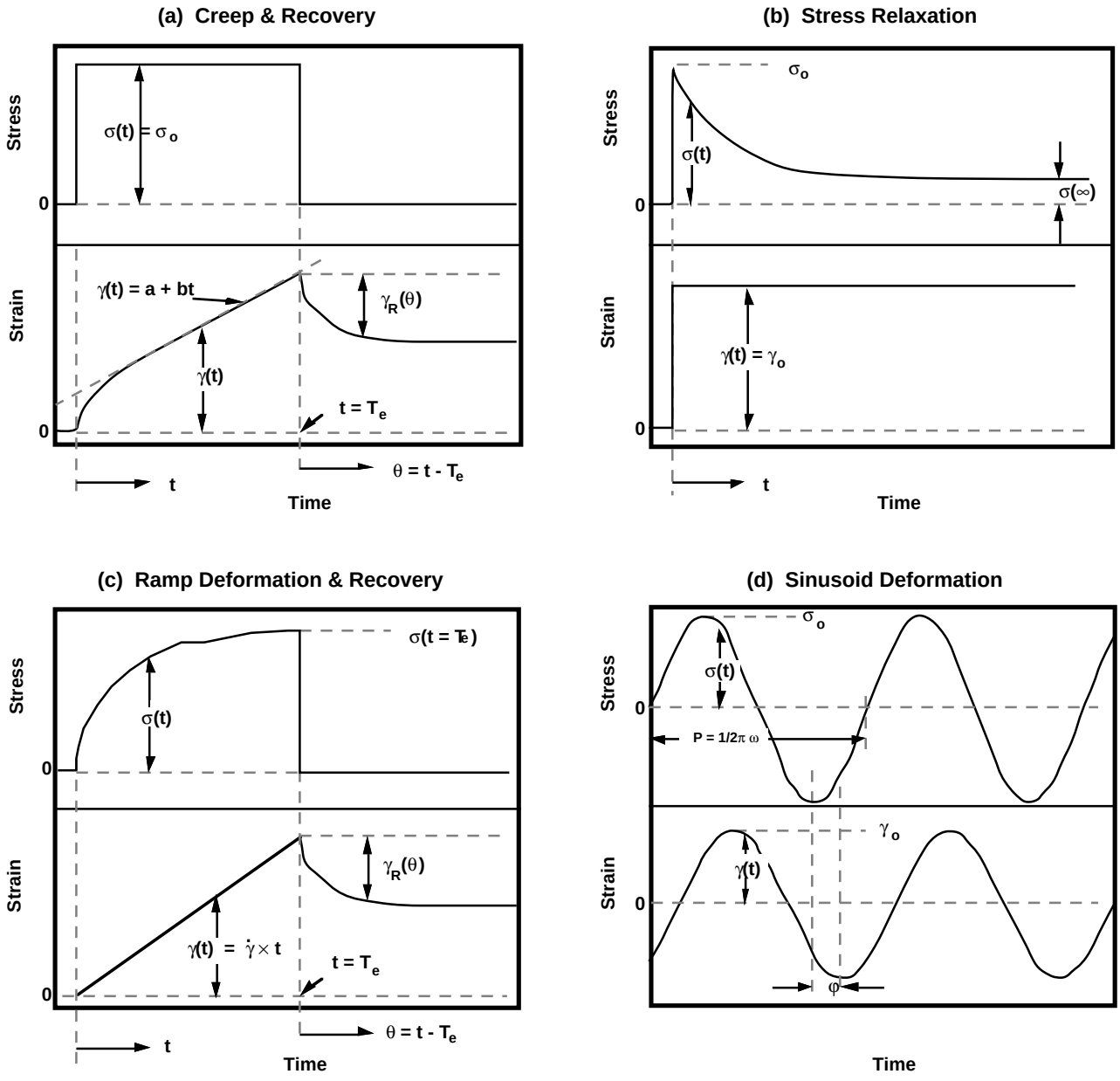
(a) Creep & Recovery
Stress
σ(t) = σ o
0
Strain
γ(t) = a + bt
γR(θ)
γ(t)
t = Te
0
t
θ = t - Te
Time
(b) Stress Relaxation
σo
Stress
σ(t)
σ(∞)
0
Strain
γ(t) = γo
0
t
Time
(c) Ramp Deformation & Recovery
σ(t = Te)
Stress
σ(t)
0
γR(θ)
Strain
γ(t) = γ̇ × t
t = Te
0
t
θ = t - Te
Time
(d) Sinusoid Deformation
σo
Stress
σ(t)
0
P = 1/2π ω
γo
Strain
γ(t)
0
φ
Time

Figure 7

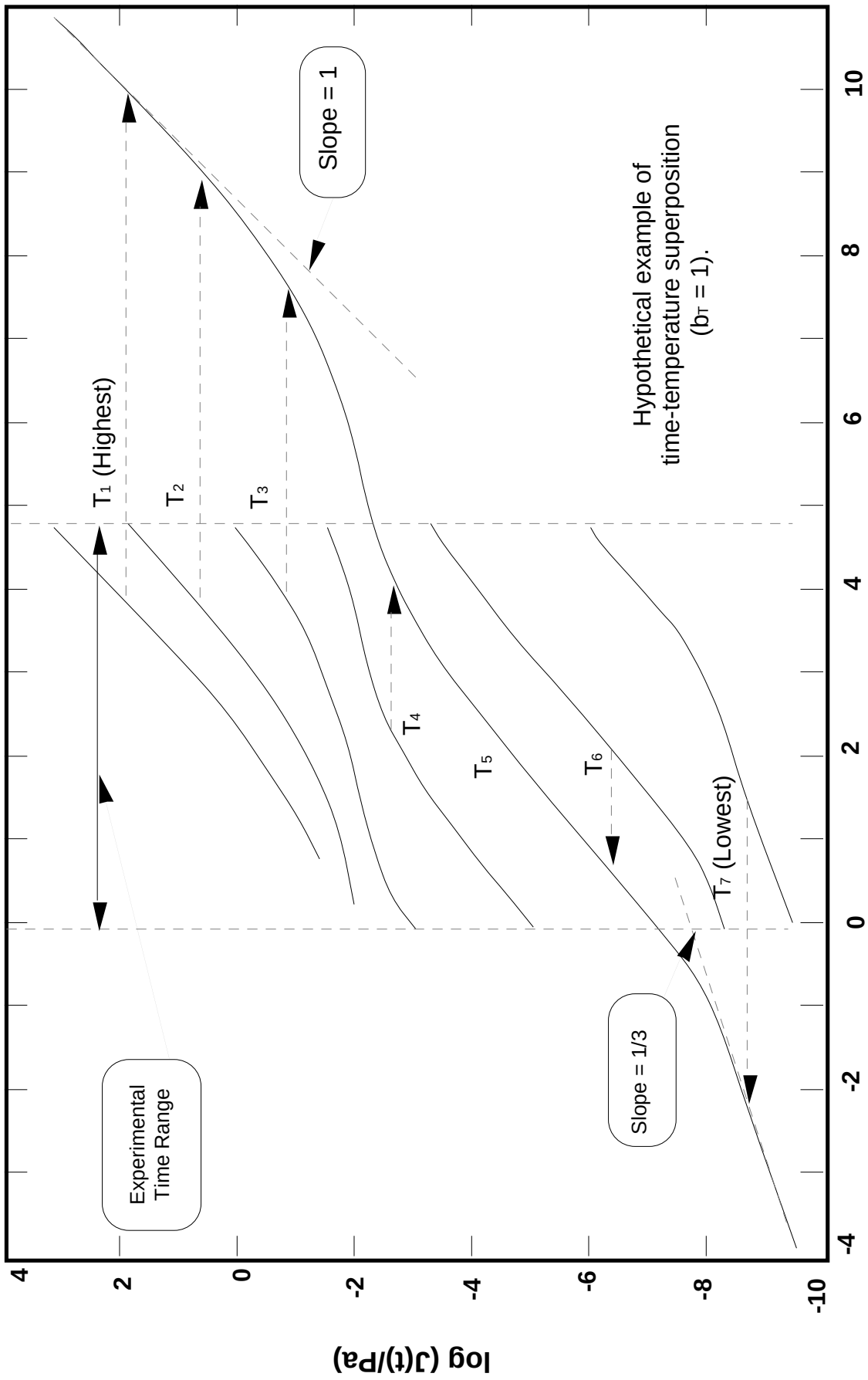
Hypothetical example of
time-temperature superposition
(b_T = 1).
Slope = 1
Slope = 1/3
Experimental
Time Range
T_1 (Highest)
T_2
T_3
T_4
T_5
T_6
T_7 (Lowest)
log (J(t)/Pa)
log (t/s) or log (a_T^{-1}t/s)
4
2
0
-2
-4
-6
-8
-10
-4
-2
0
2
4
6
8
10

Figure 8

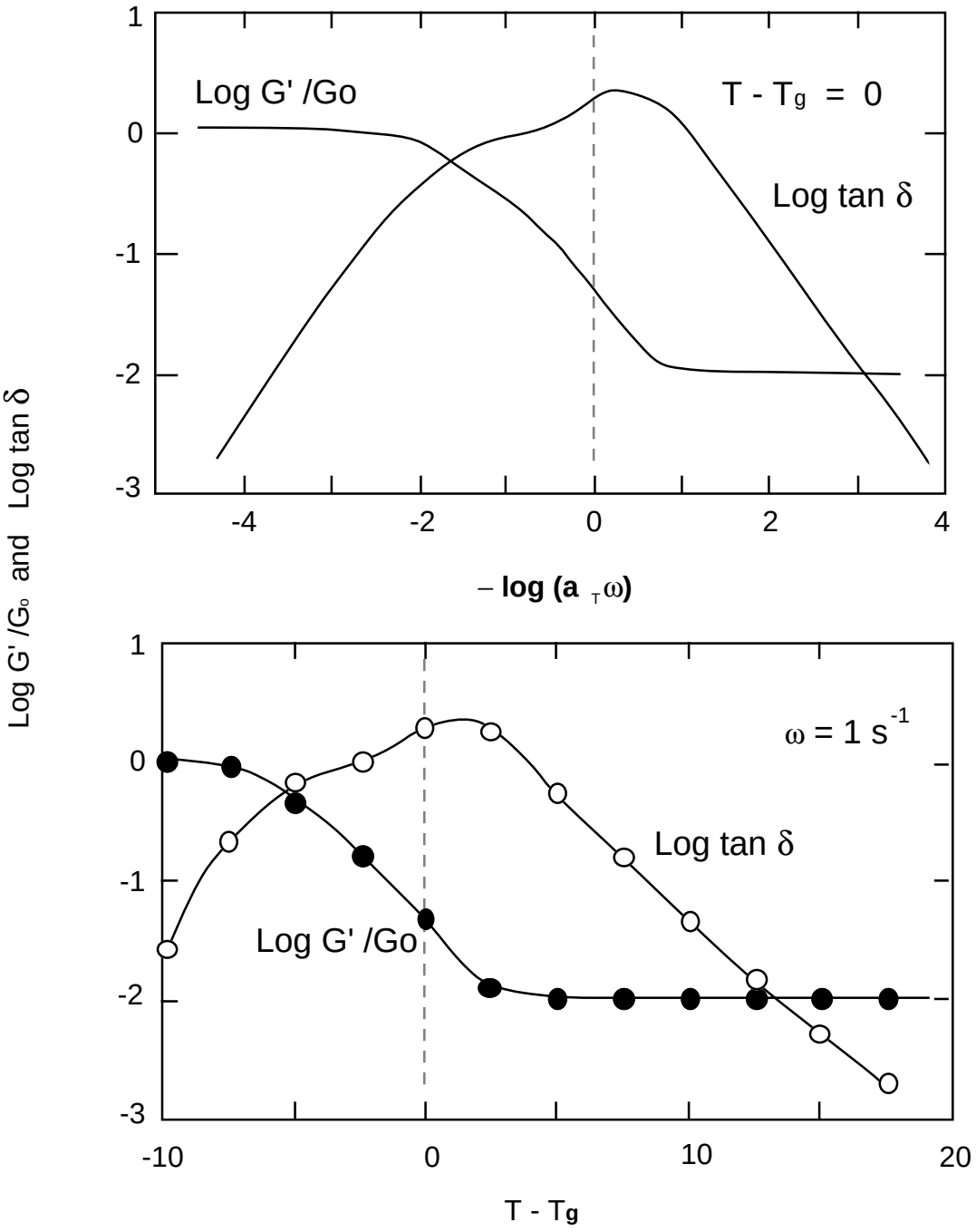
Log G' /Go
T - Tg = 0
Log tan δ
Log G' /Go and Log tan δ
– log (a T ω)
ω = 1 s-1
Log tan δ
Log G' /Go
T - Tg

Figure 9

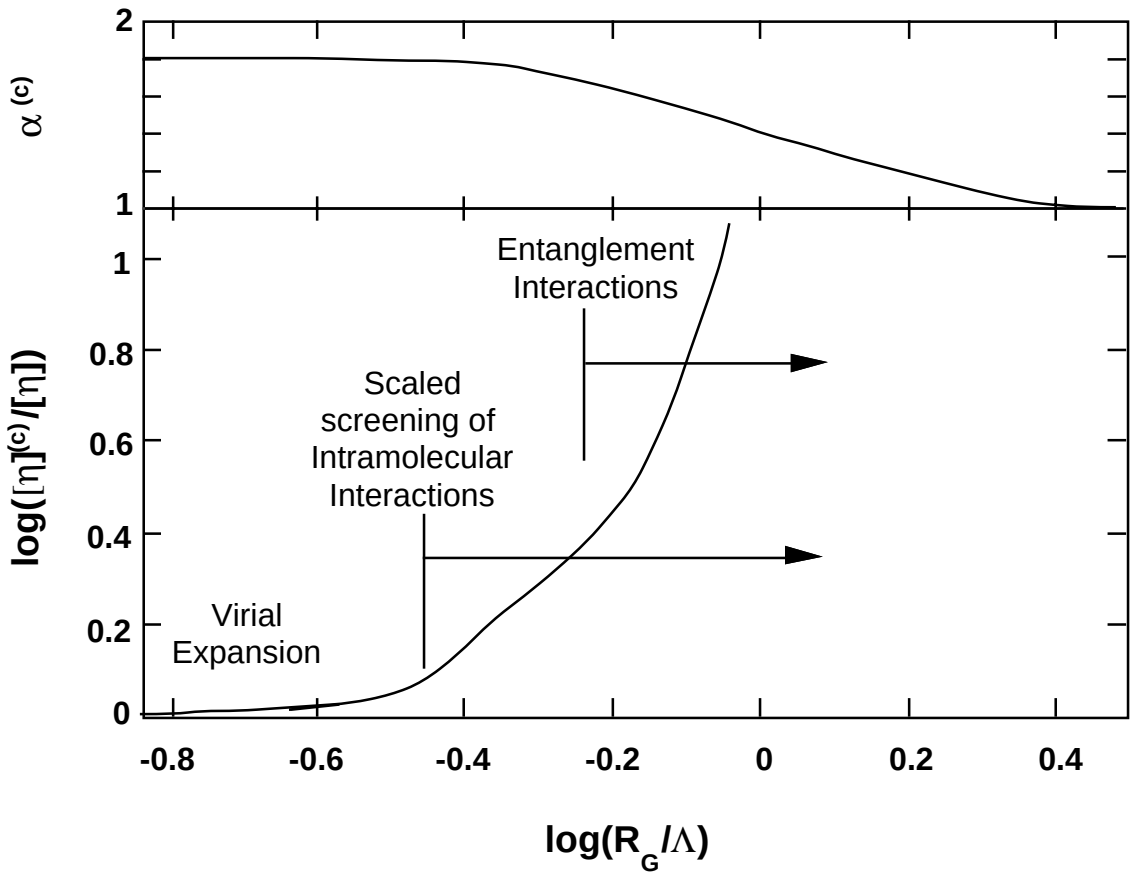
2
1
α (c)
1
0.8
0.6
0.4
0.2
0
log([η](c)/[η])
Entanglement
Interactions
Scaled
screening of
Intramolecular
Interactions
Virial
Expansion
-0.8
-0.6
-0.4
-0.2
0
0.2
0.4
log(RG/Λ)

Figure 10

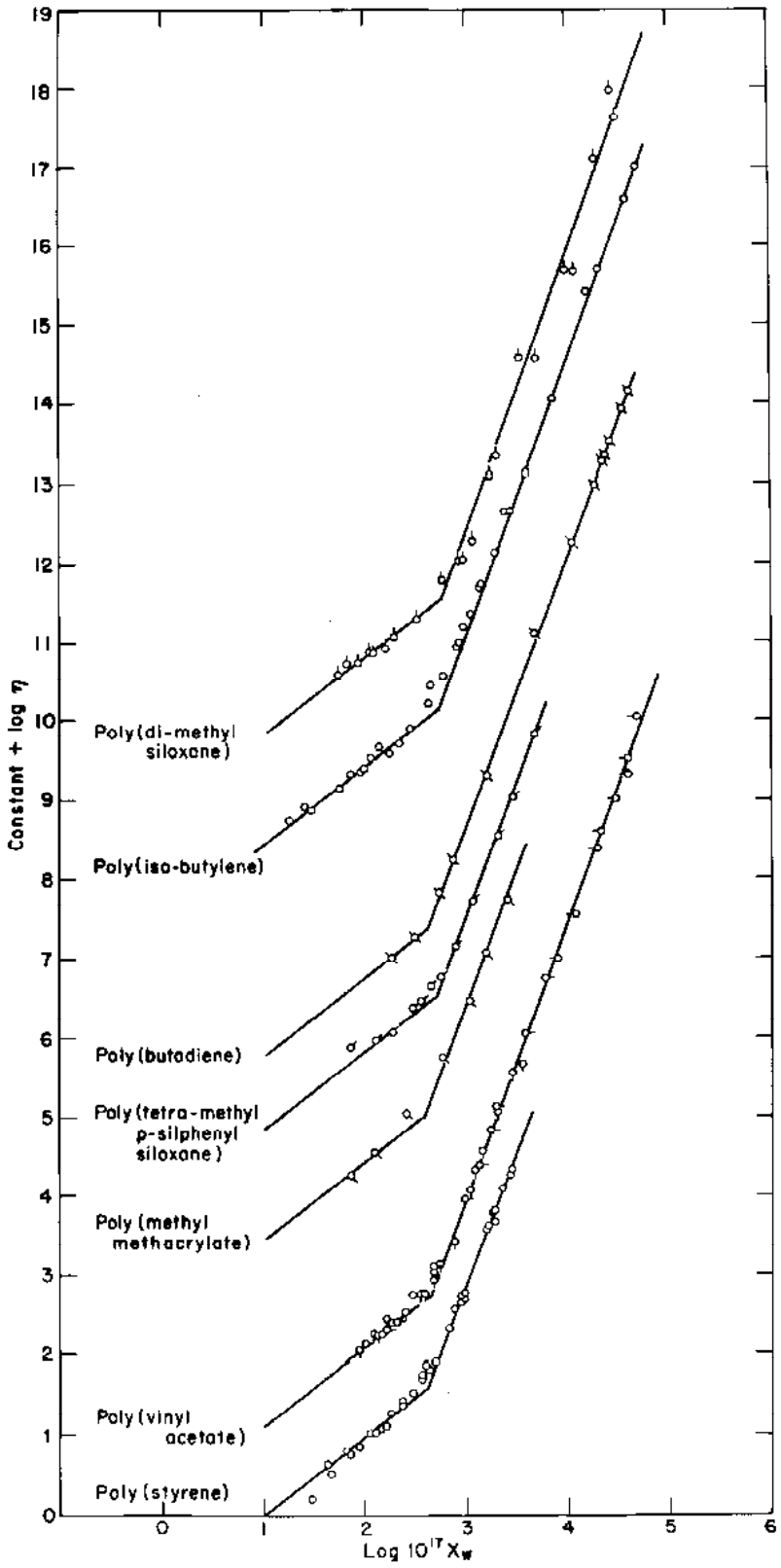
Constant + log η
Log 10^17 Xw
Poly (di-methyl siloxane)
Poly (iso-butylene)
Poly (butadiene)
Poly (tetra-methyl p-silphenyl siloxane)
Poly (methyl methacrylate)
Poly (vinyl acetate)
Poly (styrene)

Figure 11

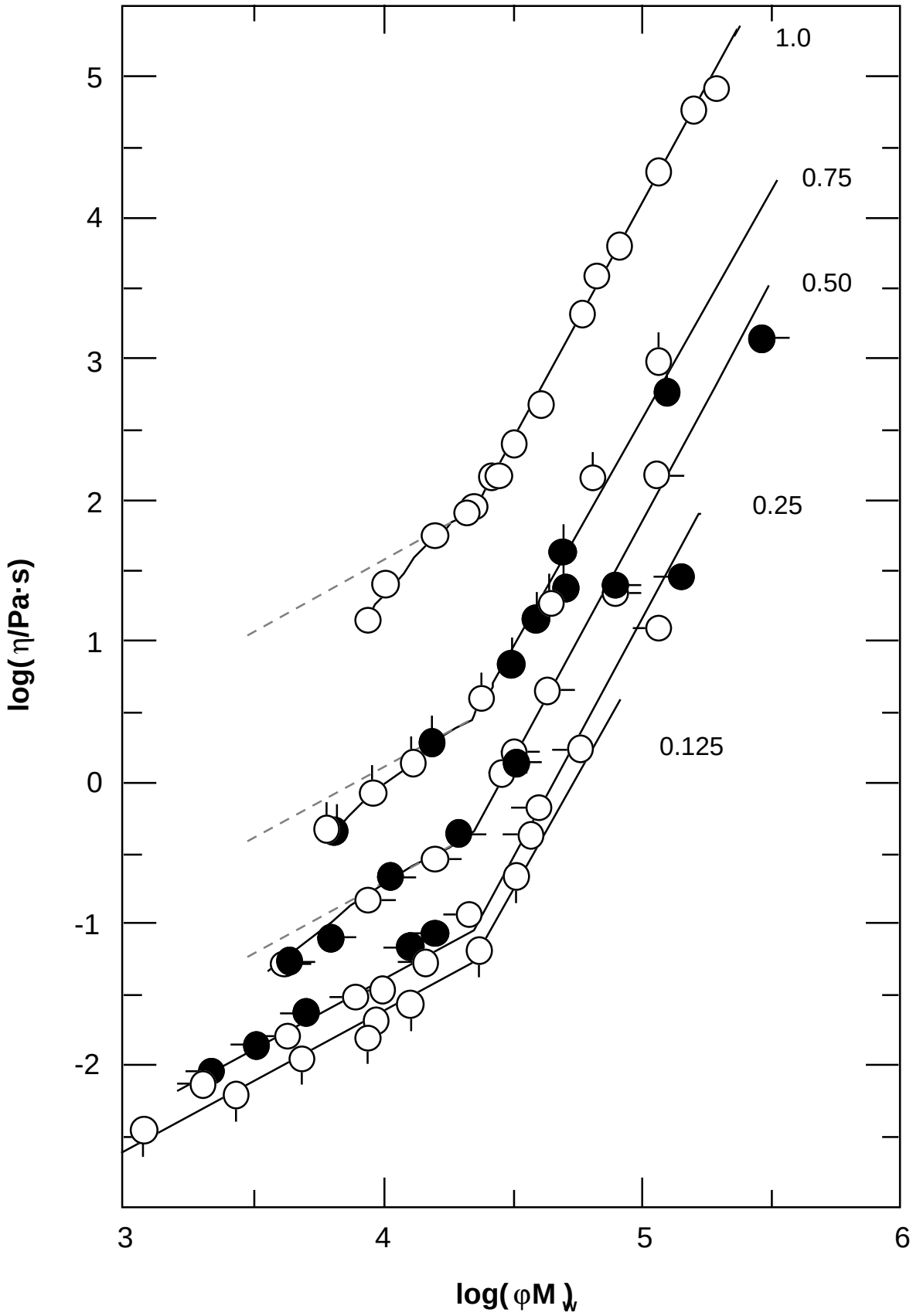

Figure 12

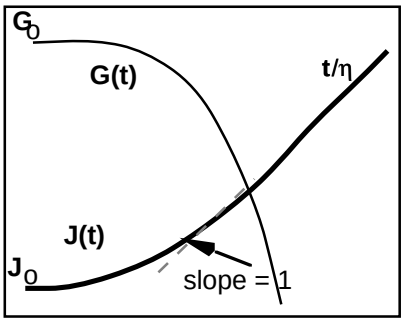

log t

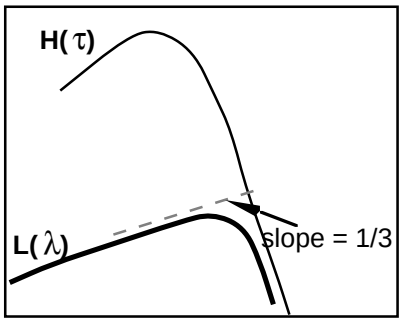

log λ or log τ

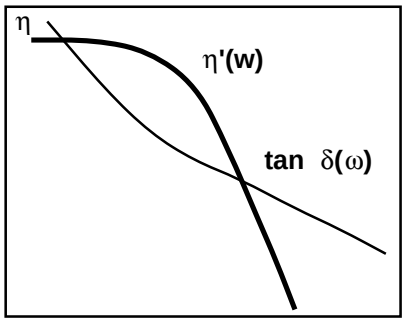

log ω

Low Molecular Weight Glass Former

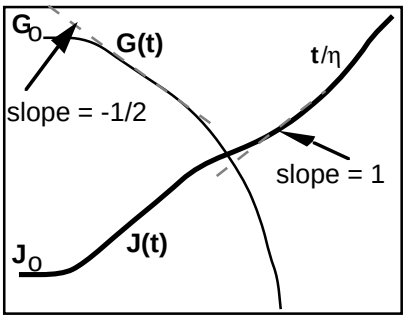

log t

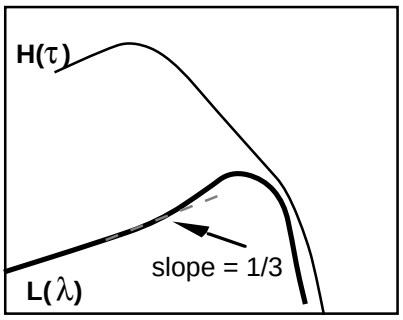

log λ or log τ

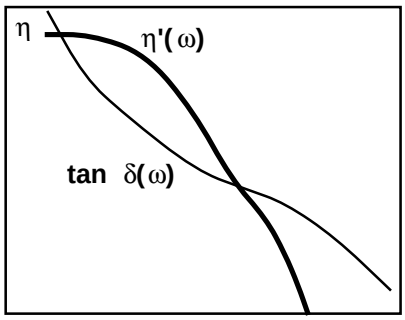

log ω

Polymeric Fluid with M < M_e

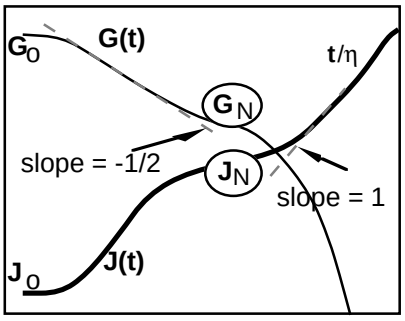

log t

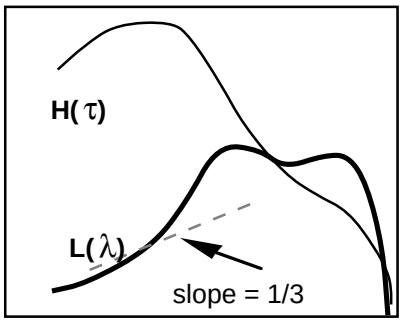

log λ or log τ

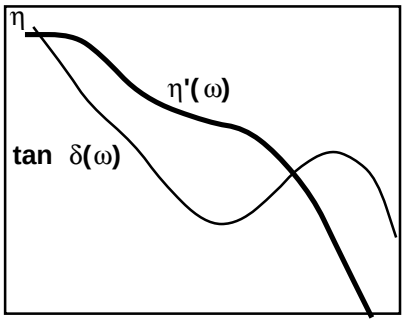

log ω

Polymeric Fluid with M >> M_e

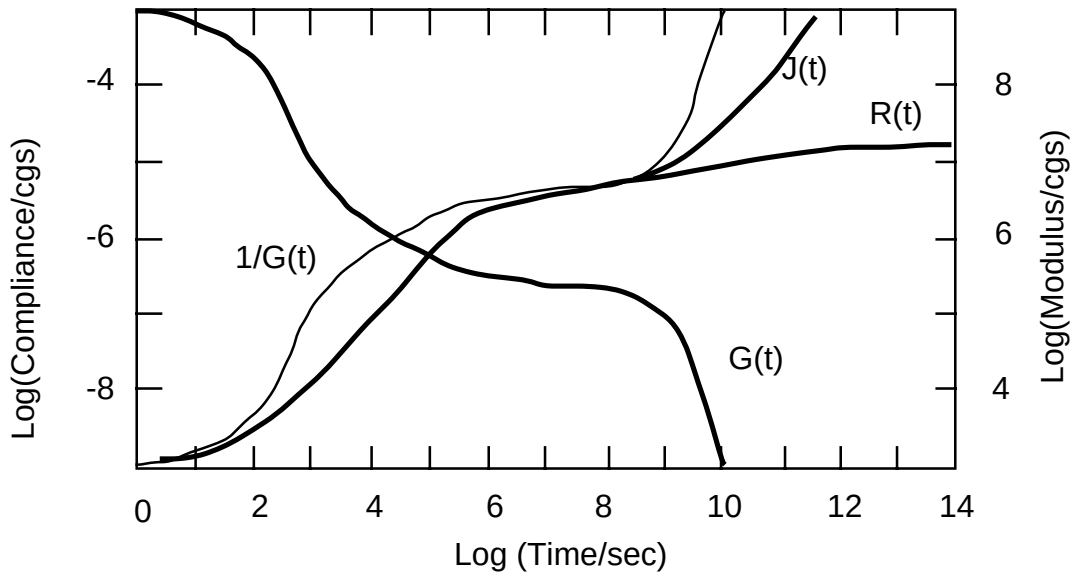
Log(Compliance/cgs)
-4
-6
-8
Log(Modulus/cgs)
8
6
4
J(t)
R(t)
1/G(t)
G(t)
0
2
4
6
8
10
12
14
Log (Time/sec)

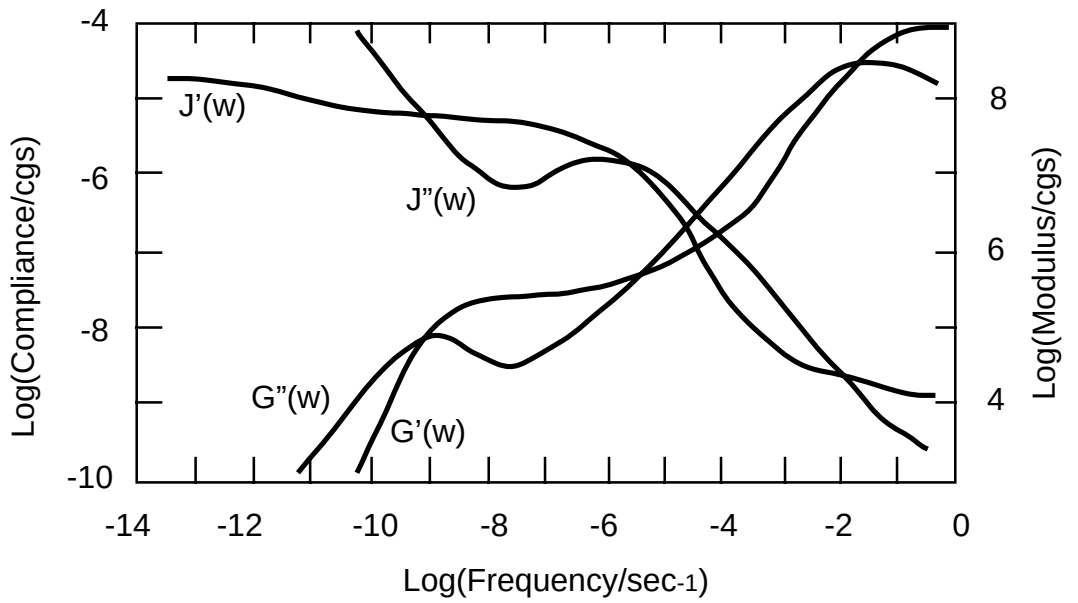
Log(Compliance/cgs)
-4
-6
-8
-10
Log(Modulus/cgs)
8
6
4
J'(w)
J"(w)
G"(w)
G'(w)
-14
-12
-10
-8
-6
-4
-2
0
Log(Frequency/sec-1)

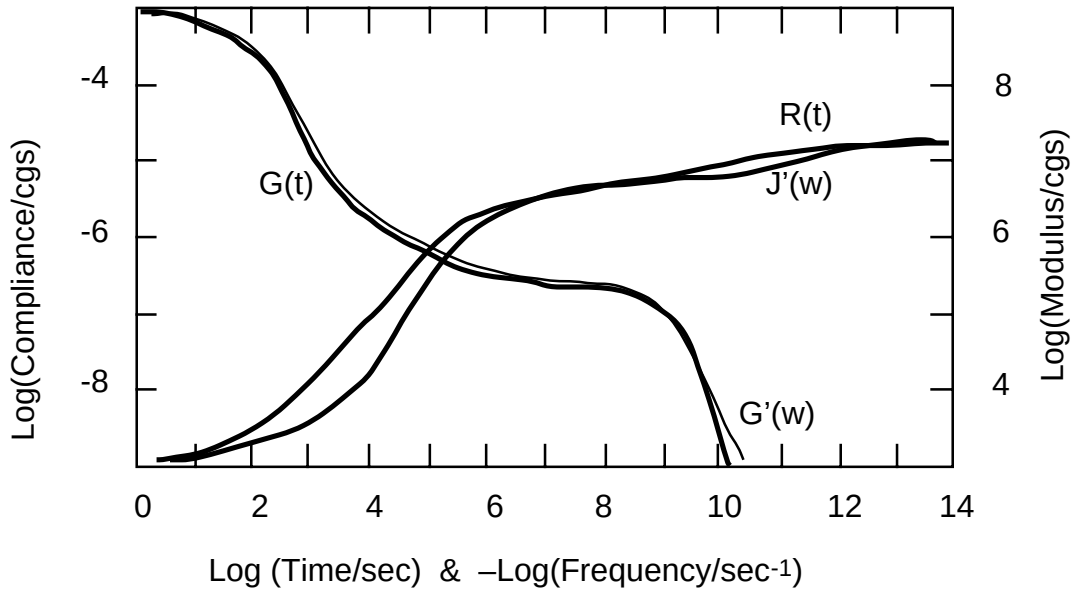
Log(Compliance/cgs)
-4
-6
-8
Log(Modulus/cgs)
8
6
4
R(t)
G(t)
J'(w)
G'(w)
0
2
4
6
8
10
12
14
Log (Time/sec) & –Log(Frequency/sec-1)

Figure 14

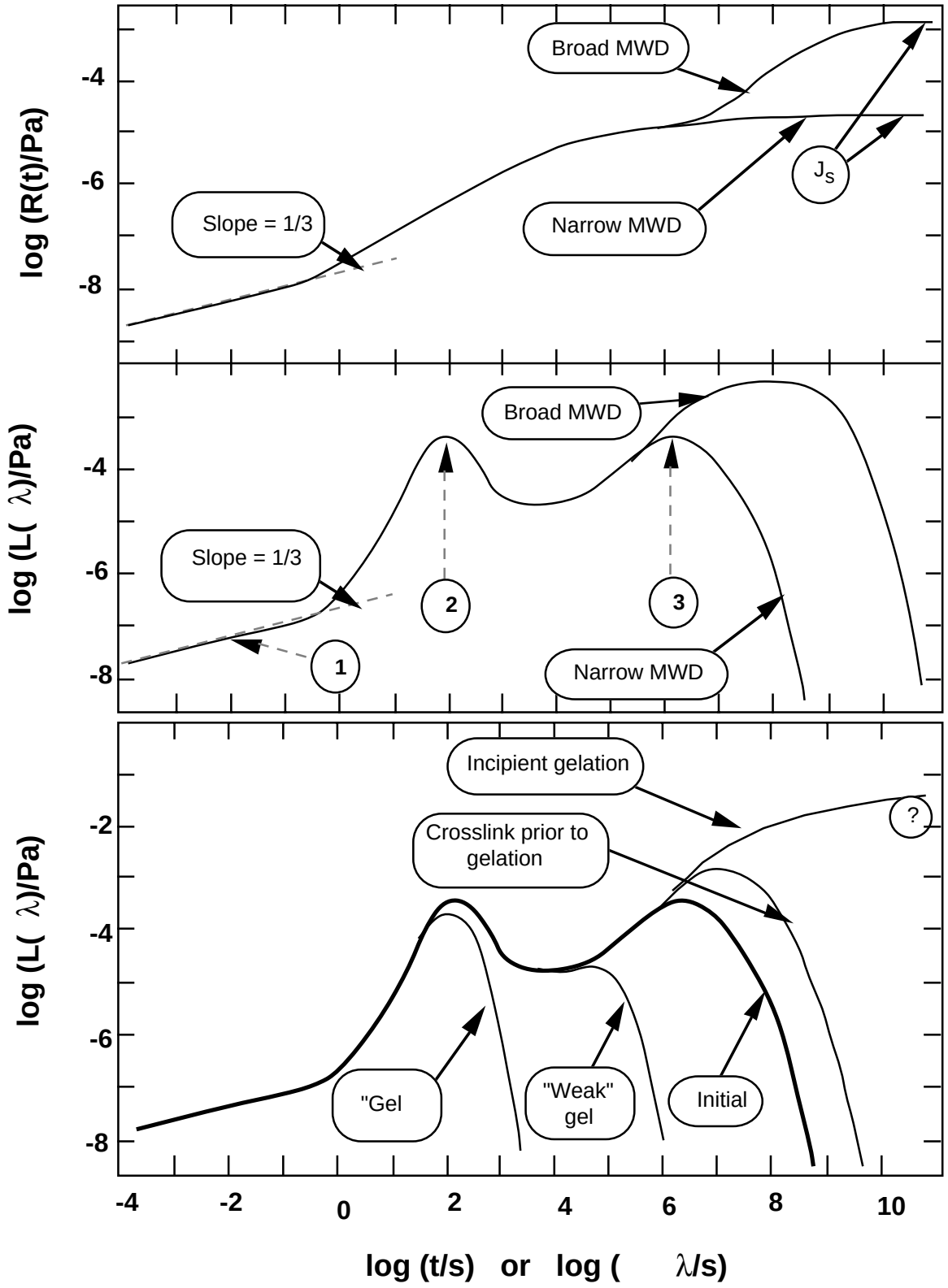
log (R(t)/Pa)
-4
-6
-8
Broad MWD
Slope = 1/3
Narrow MWD
J_s
log (L(λ)/Pa)
-4
-6
-8
Broad MWD
Slope = 1/3
2
3
1
Narrow MWD
log (L(λ)/Pa)
-2
-4
-6
-8
Incipient gelation
Crosslink prior to gelation
?
"Gel
"Weak" gel
Initial
-4
-2
0
2
4
6
8
10
log (t/s) or log (λ/s)

Figure 15

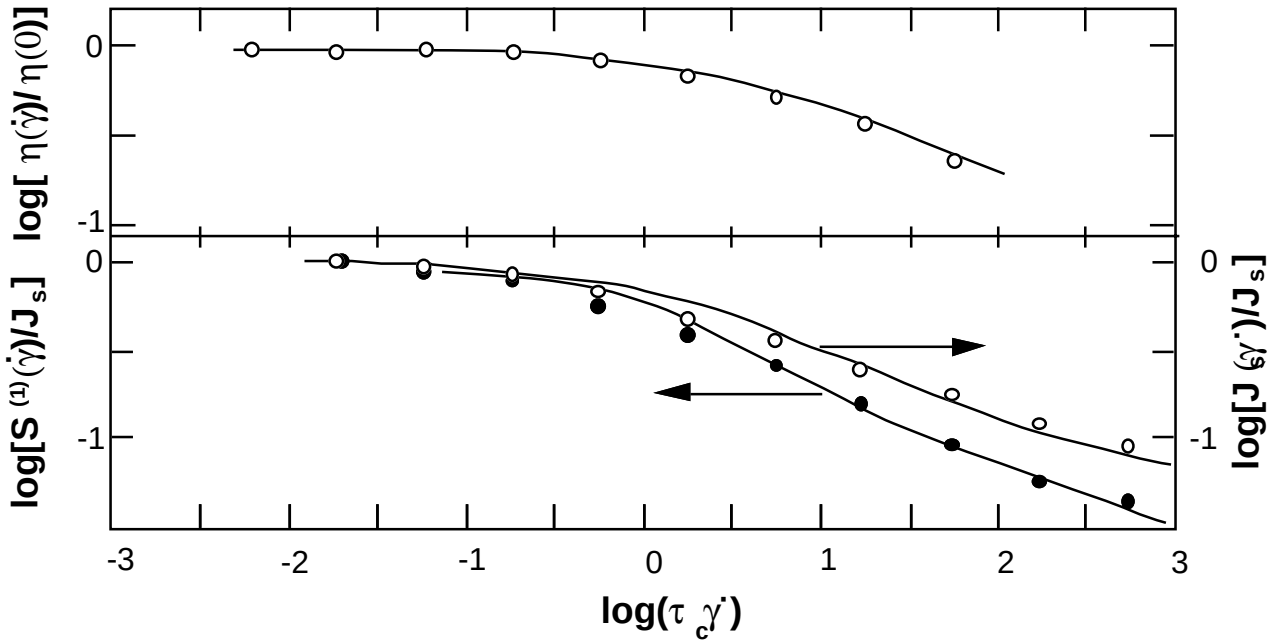

Figure 16

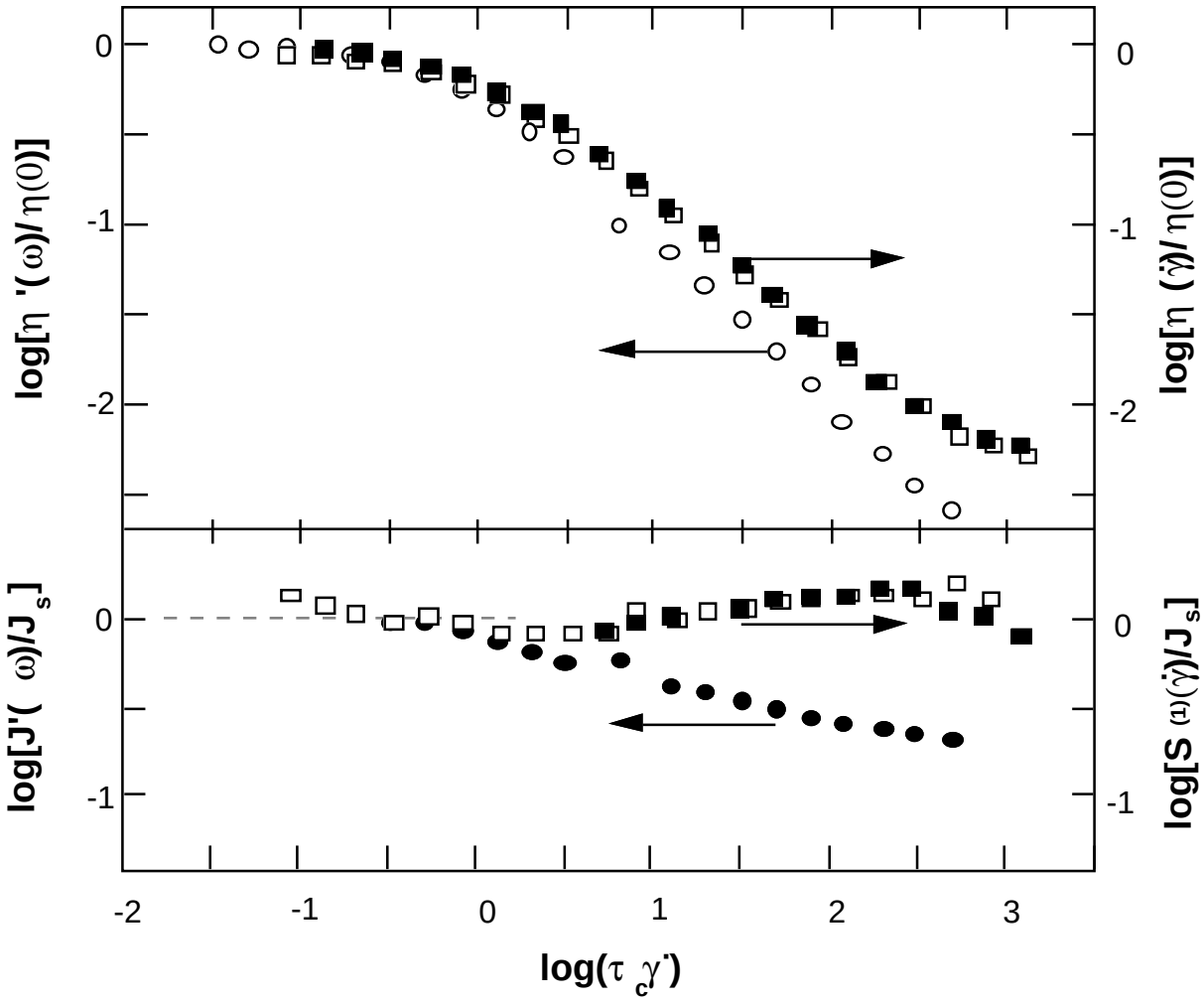

Figure 17

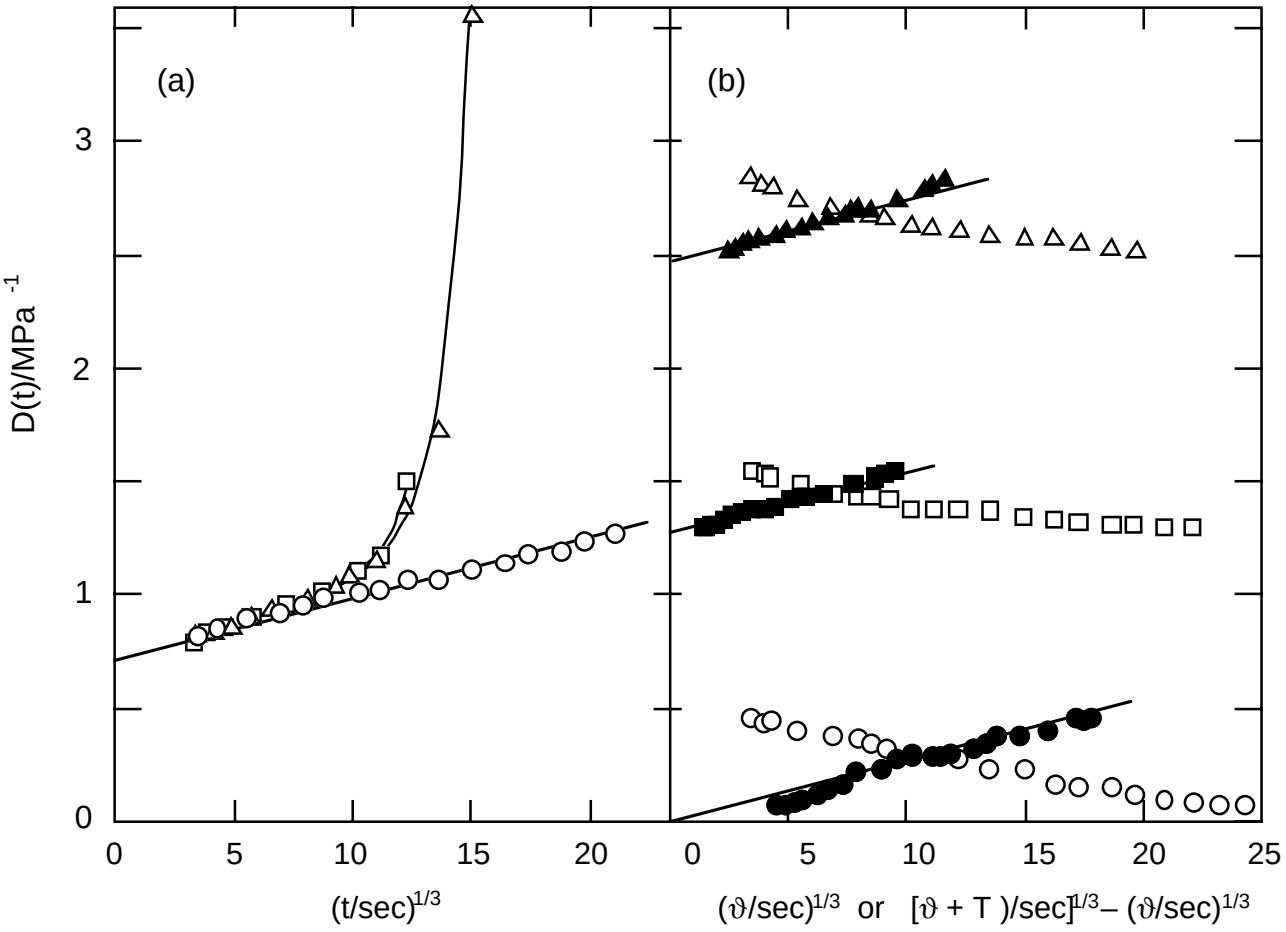

Figure 18

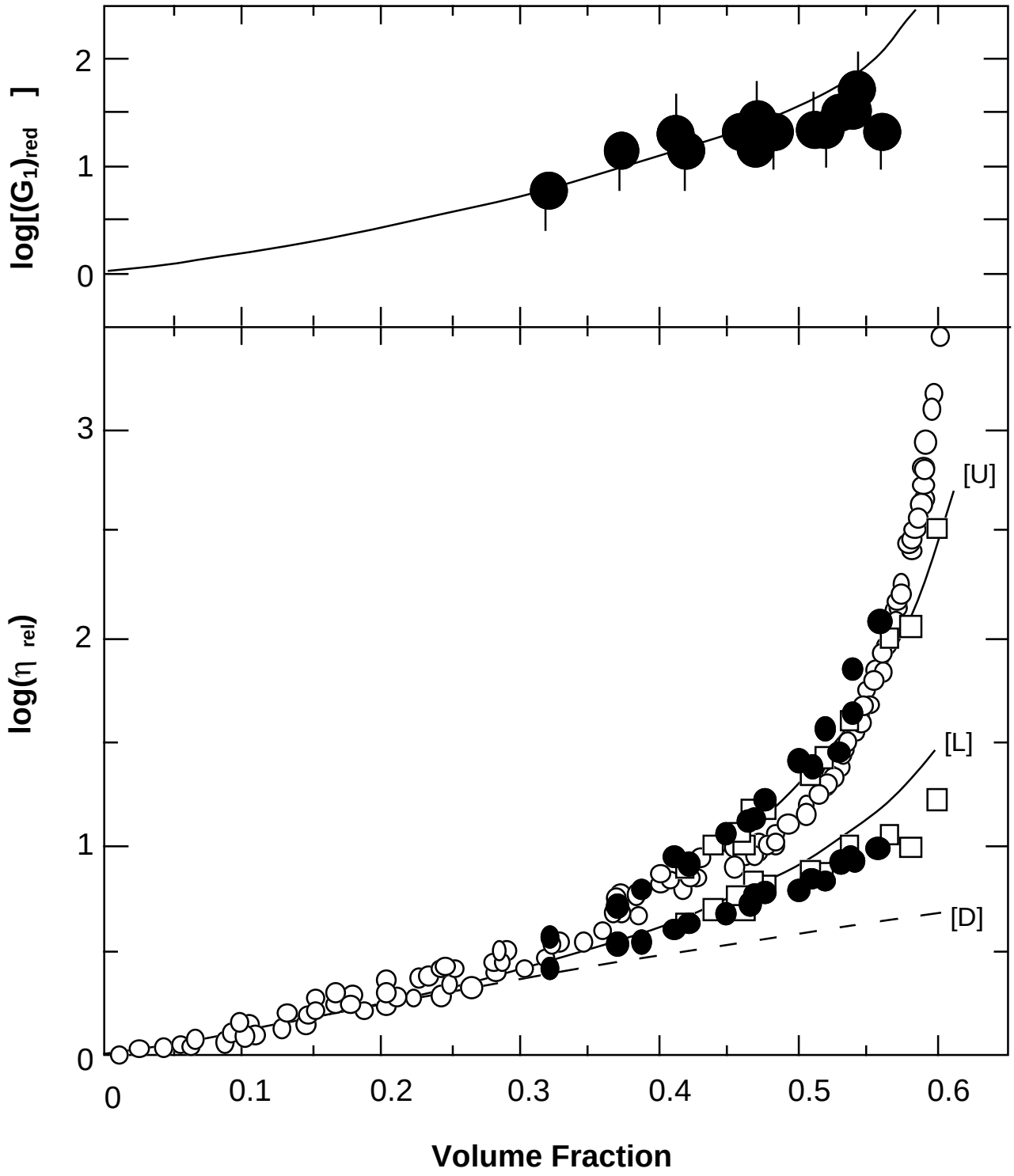
log[(G1)red]
2
1
0
log(η rel)
3
2
1
0
[U]
[L]
[D]
0
0.1
0.2
0.3
0.4
0.5
0.6
Volume Fraction

Figure 19

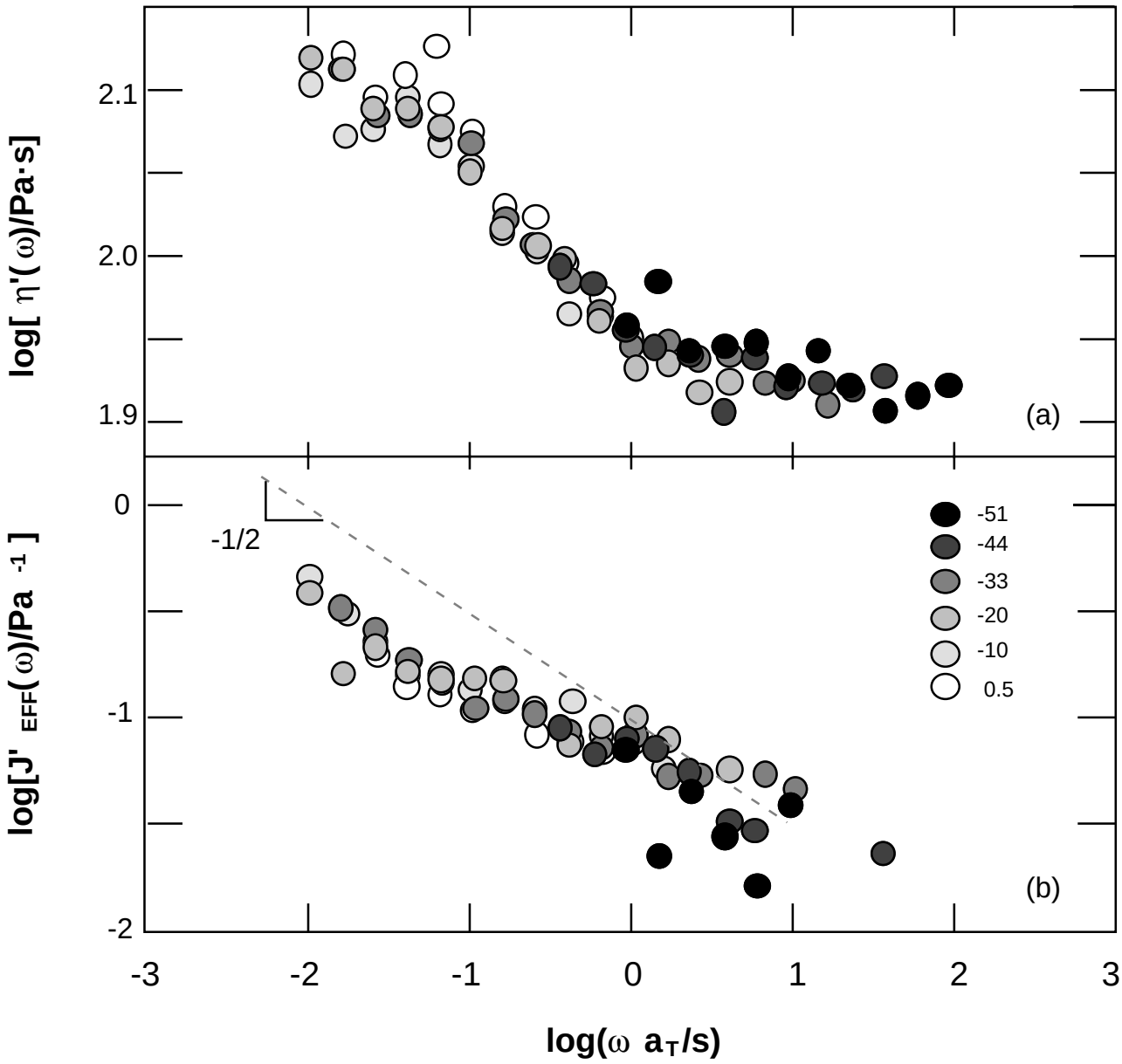
log[η'(ω)/Pa·s]
2.1
2.0
1.9
(a)
log[J' EFF(ω)/Pa -1]
0
-1
-2
-1/2
-51
-44
-33
-20
-10
0.5
(b)
-3
-2
-1
0
1
2
3
log(ω aT/s)

Figure 20

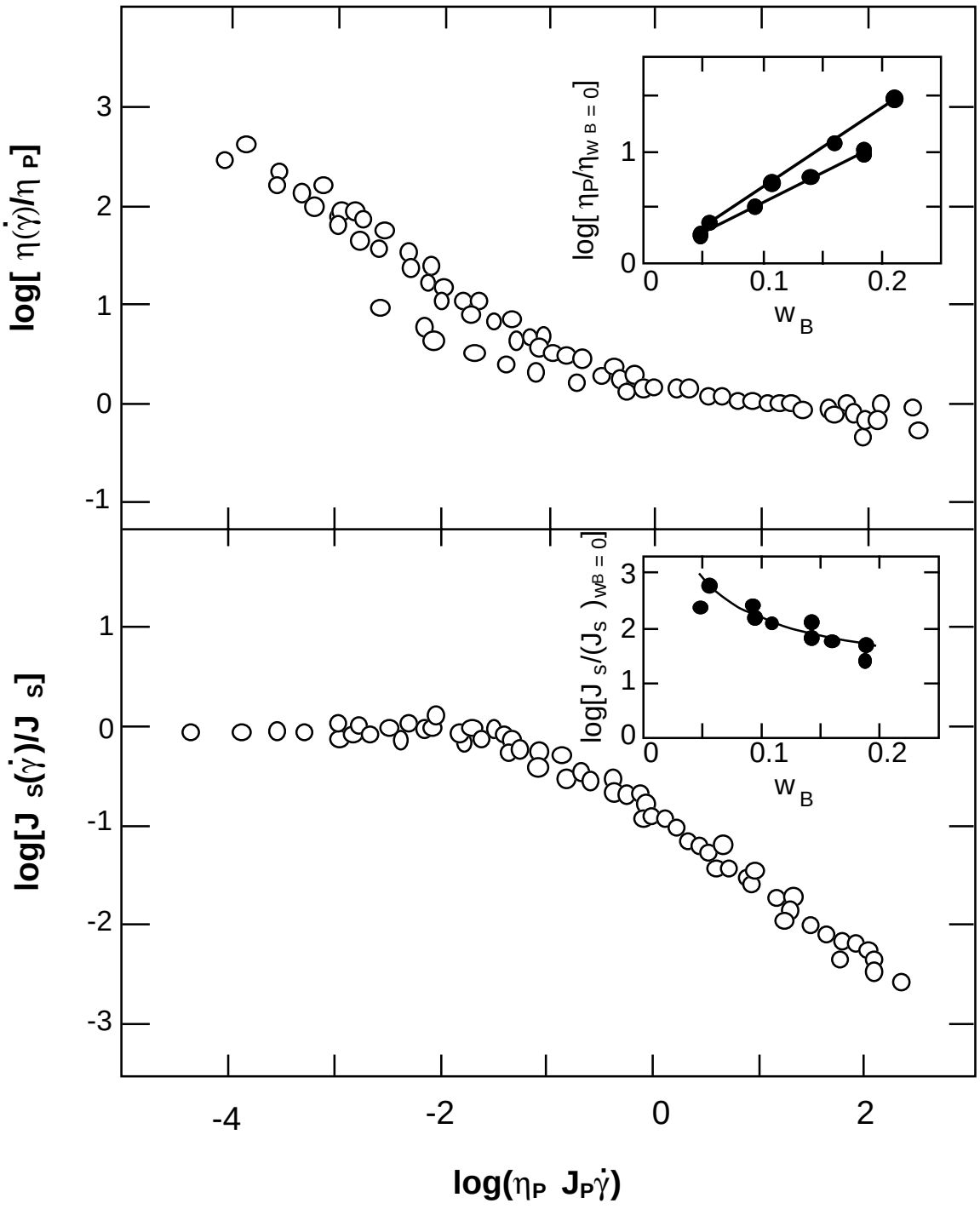

Figure 21